Electronic Supplementary Material (ESI) for Physical Chemistry Chemical Physics.

Supporting information

Title

Probing the functional conformations of an atypical proline-rich fusion peptide

Author Names

Nivedita Dutta, Saikat Dutta Chowdhury, Ansuman Lahiri

Author Affiliation

Department of Biophysics, Molecular Biology and Bioinformatics, University of Calcutta, 92, Acharya Prafulla Chandra Road, Kolkata 700009, West Bengal, India

Corresponding Author's email

albmbg@caluniv.ac.in

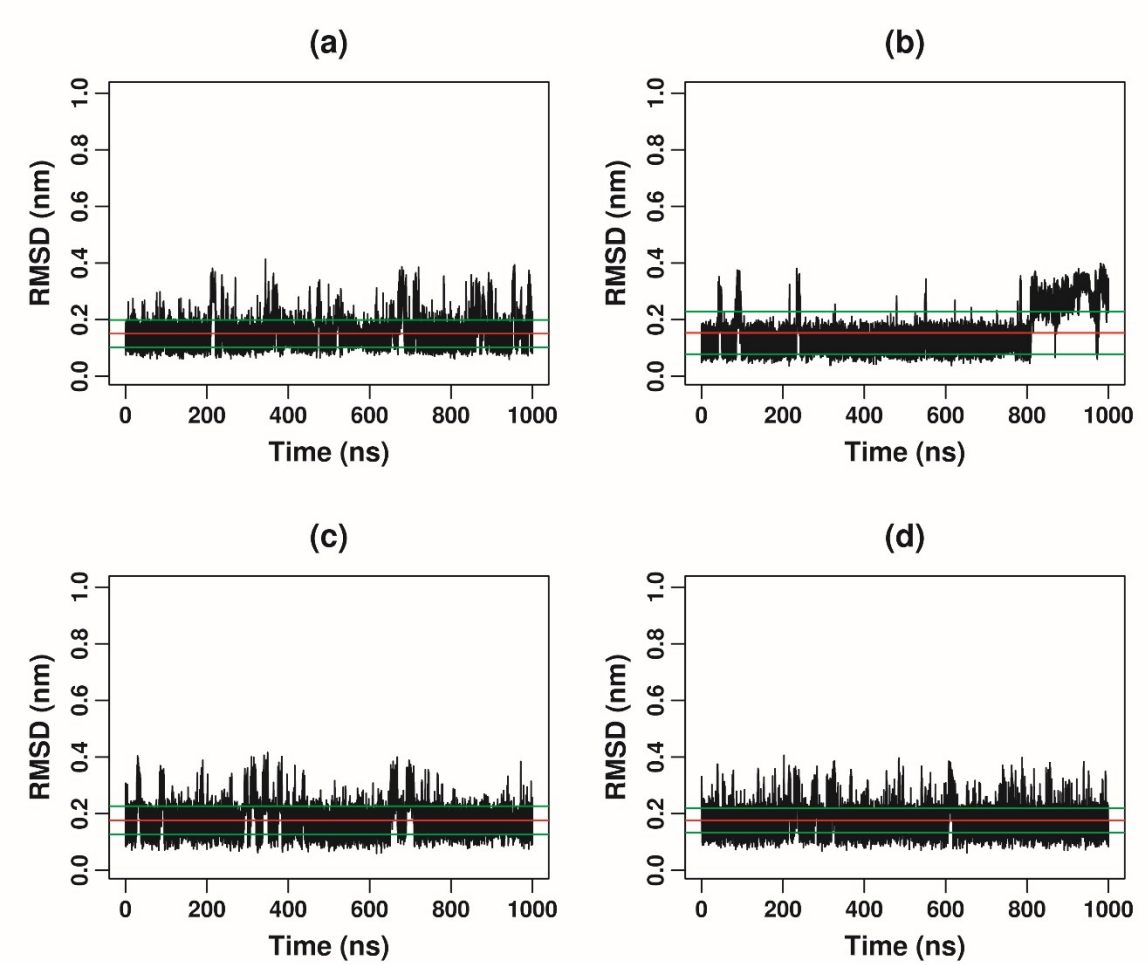

Figure S1. Time evolution of the root mean square deviation (RMSD) (in nm) of p15 FAST peptide with respect to residues Q9-P15 for the second replicate for corresponding to the force-fields (a) AMBER ff99SB*-ILDNP; (b) OPLS-AA; (c) AMBER ff03ws; and (d) CHARMM36m. The red line indicates the mean RMSD and the upper and lower green lines indicate the mean+standard deviation and mean-standard deviation of the RMSDs.

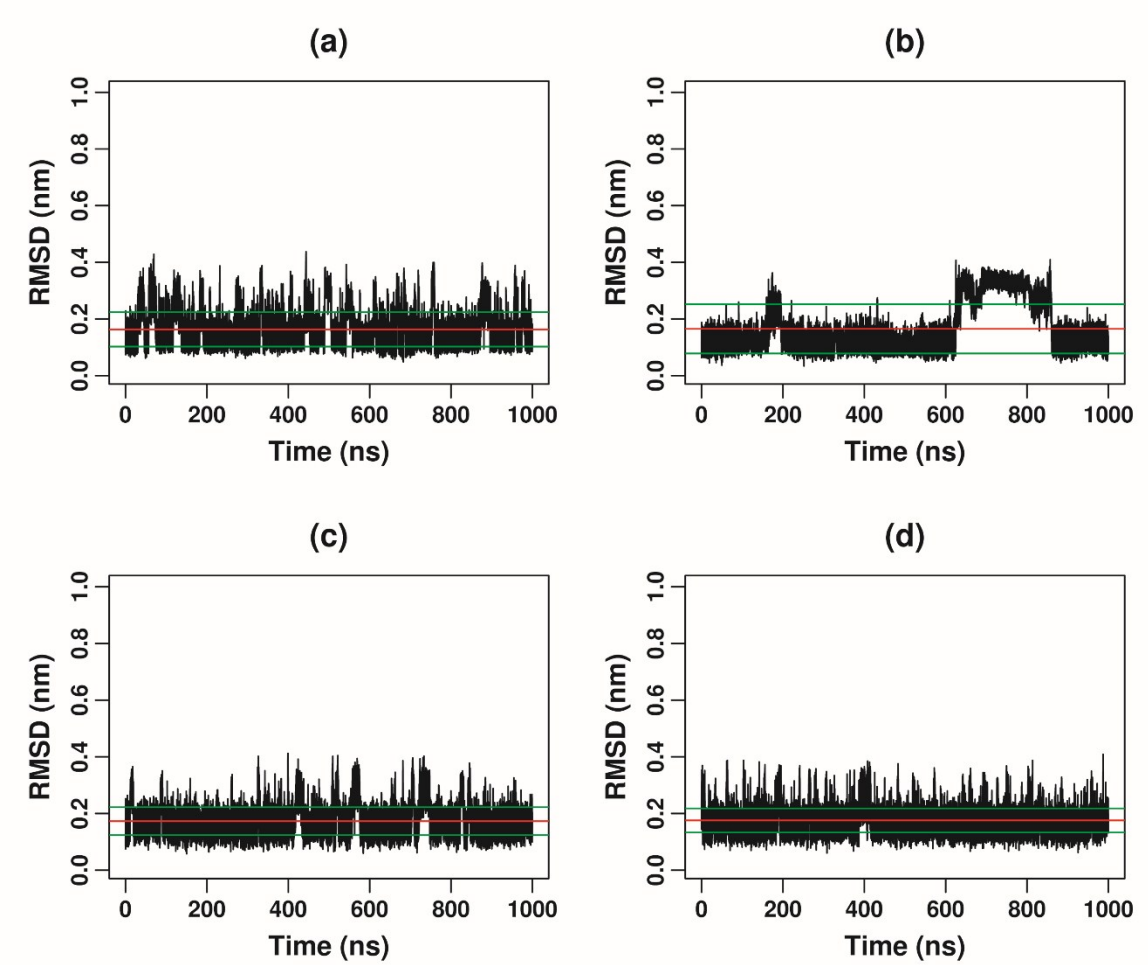

Figure S2. Time evolution of the root mean square deviation (RMSD) (in nm) of p15 FAST peptide with respect to residues Q9-P15 for the third replicate for corresponding to the force-fields (a) AMBER ff99SB*-ILDNP; (b) OPLS-AA; (c) AMBER ff03ws; and (d) CHARMM36m. The red line indicates the mean RMSD and the upper and lower green lines indicate the mean+standard deviation and mean-standard deviation of the RMSDs.

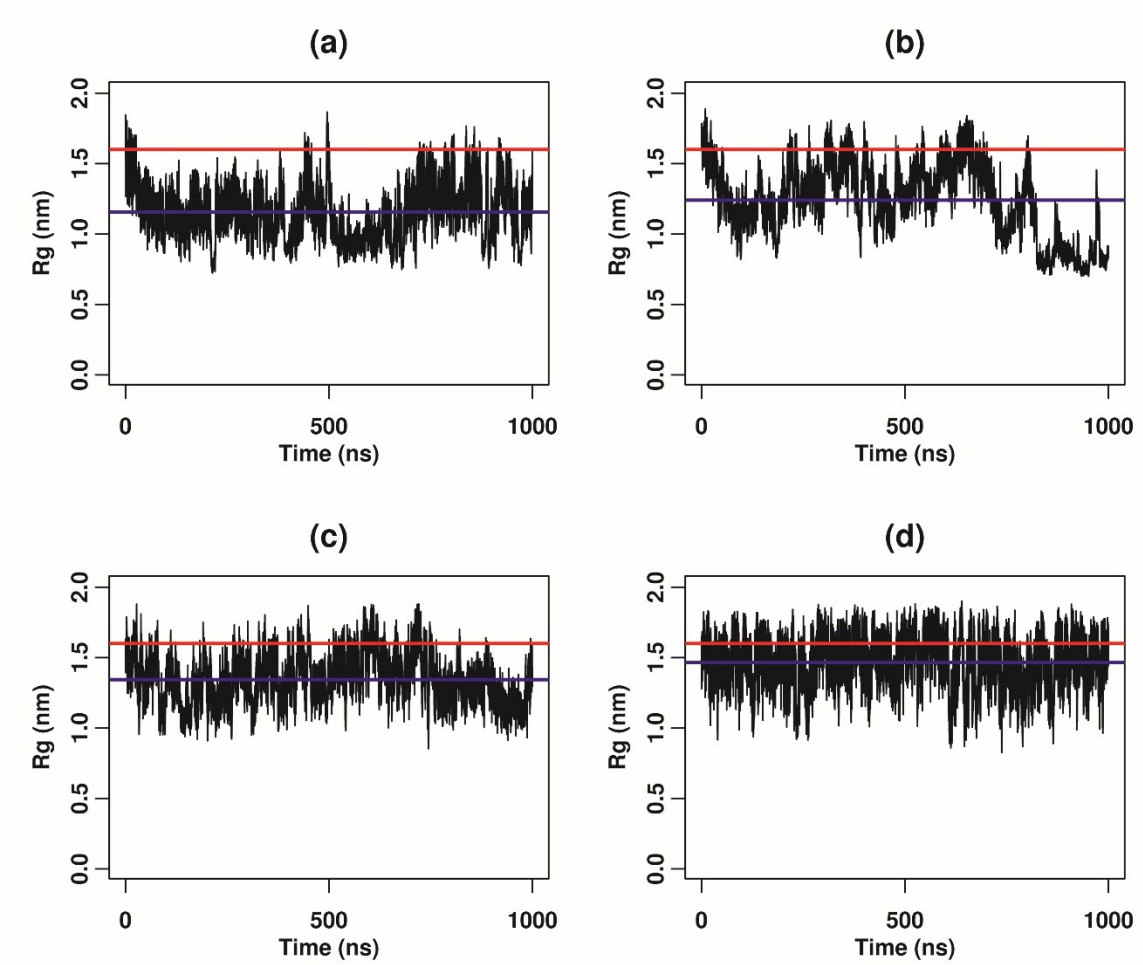

Figure S3. Time evolution of the radius of gyration (R_g) (in nm) of p15 FAST peptide for the second replicate corresponding to the force-fields respectively (a) AMBER ff99SB*-ILDNP; (b) OPLS-AA; (c) AMBER ff03ws; and (d) CHARMM36m. The red line indicates the experimental R_g and the blue lines indicate the average R_g of the simulated trajectory.

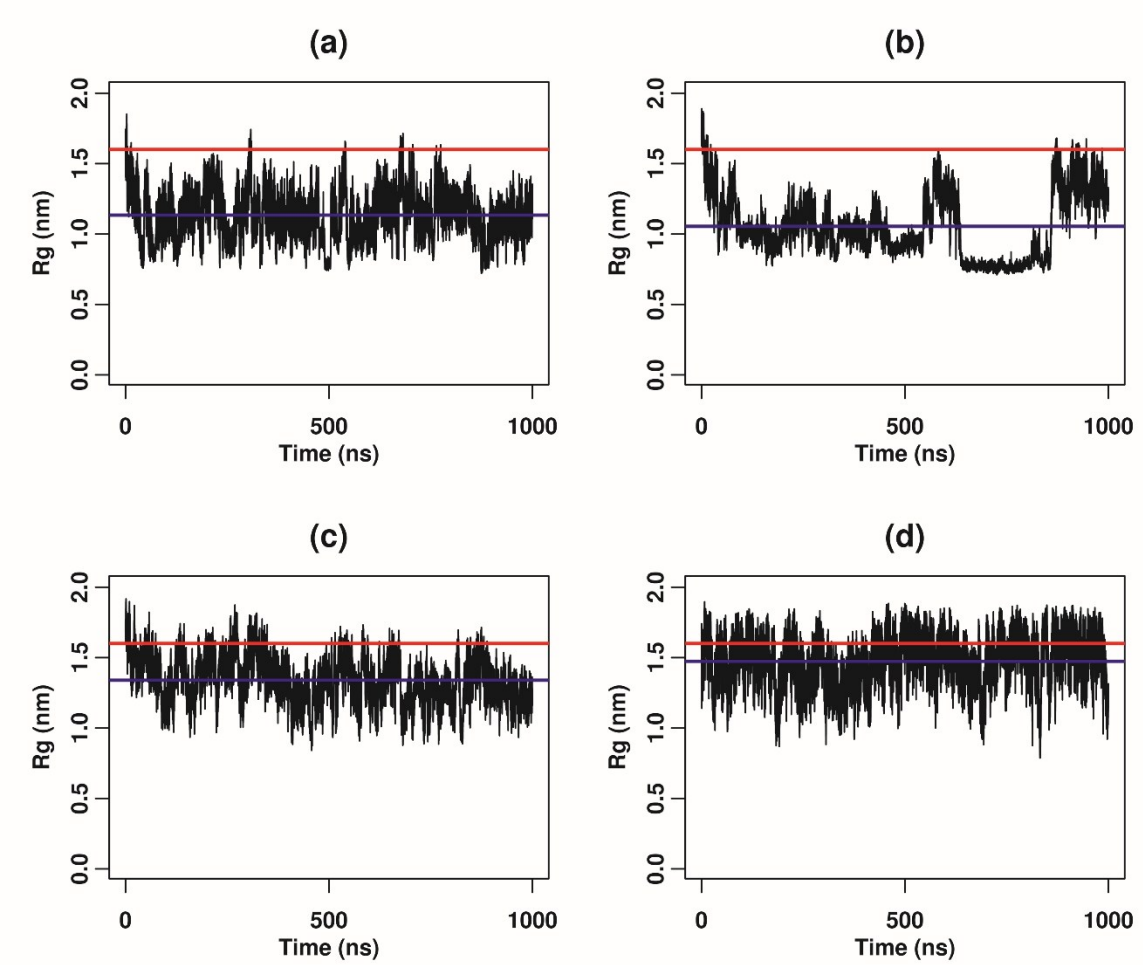

Figure S4. Time evolution of the radius of gyration (R_g) (in nm) of p15 FAST peptide for the third replicate corresponding to the force-fields respectively (a) AMBER ff99SB*-ILDNP; (b) OPLS-AA; (c) AMBER ff03ws; and (d) CHARMM36m. The red line indicates the experimental R_g and the blue lines indicate the average R_g of the simulated trajectory.

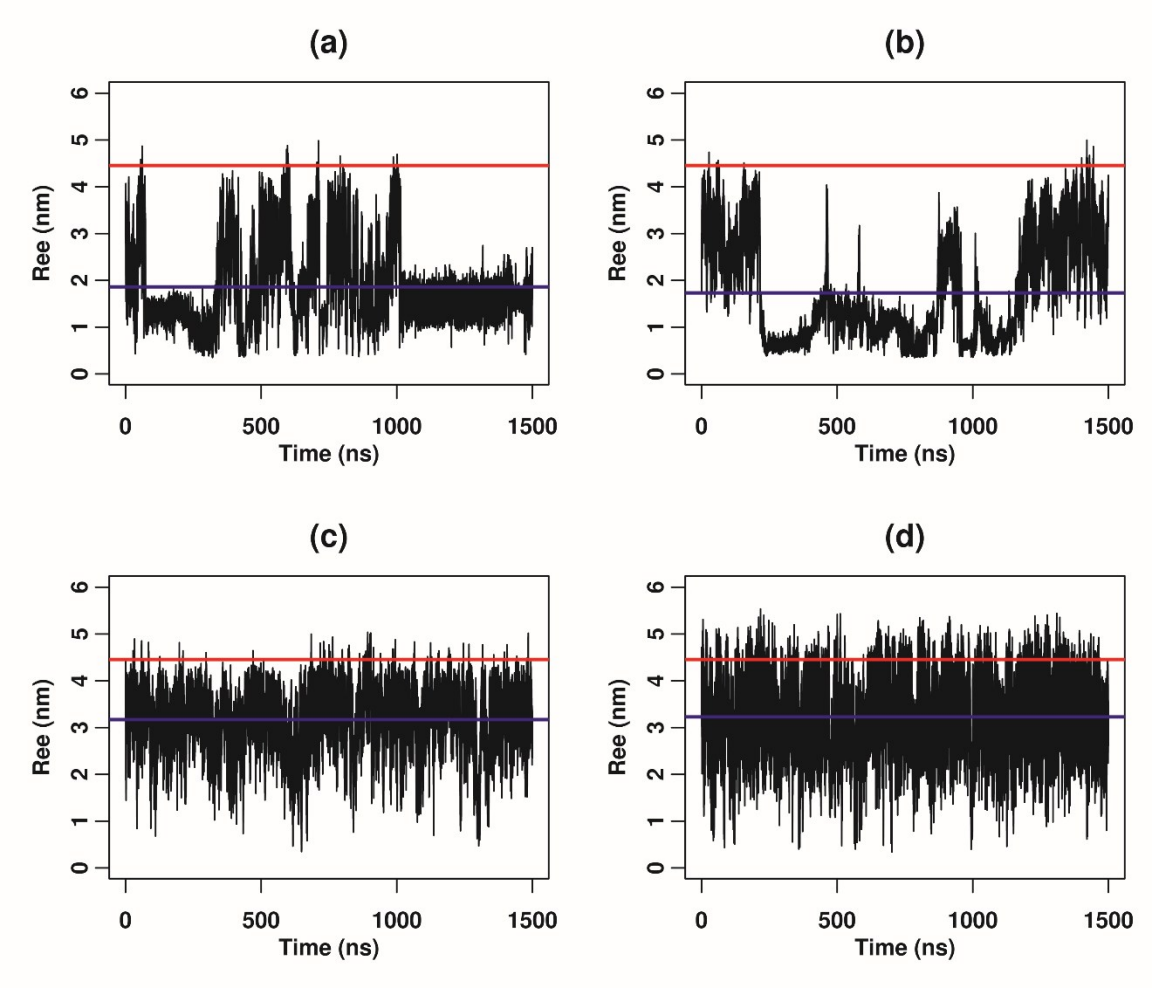

Figure S5. Time evolution of the end to end distance (R_{ee}) (in nm) of p15 FAST peptide for the first replicate corresponding to the force-fields respectively (a) AMBER ff99SB*-ILDNP; (b) OPLS-AA; (c)AMBER ff03ws; and (d) CHARMM36m. The red line indicates the experimental R_{ee} and the blue lines indicate the average R_{ee} of the simulated trajectory.

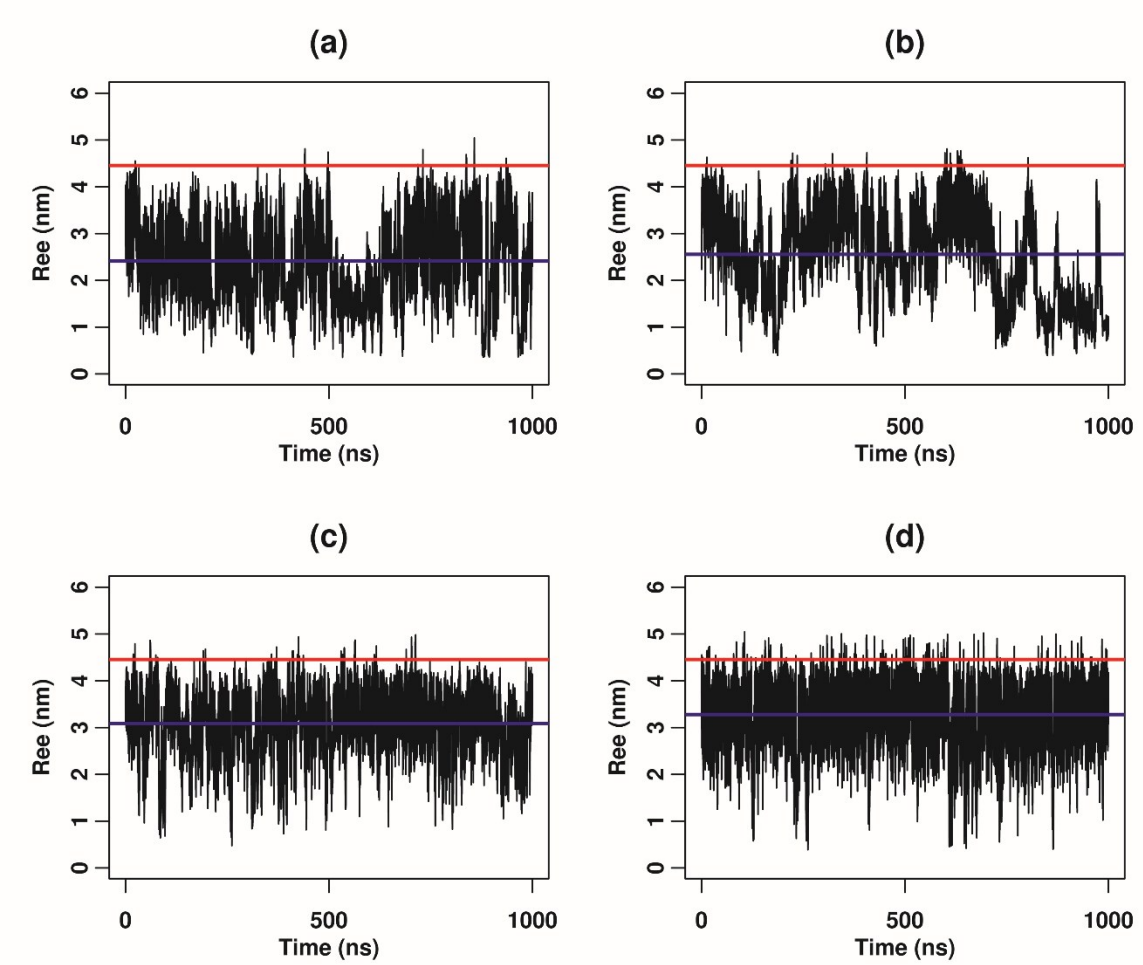

Figure S6. Time evolution of the end to end distance (R_{ee}) (in nm) of p15 FAST peptide for the second replicate corresponding to the force-fields respectively (a) AMBER ff99SB*-ILDNP; (b) OPLS-AA; (c)AMBER ff03ws; and (d) CHARMM36m. The red line indicates the experimental R_{ee} and the blue lines indicate the average R_{ee} of the simulated trajectory.

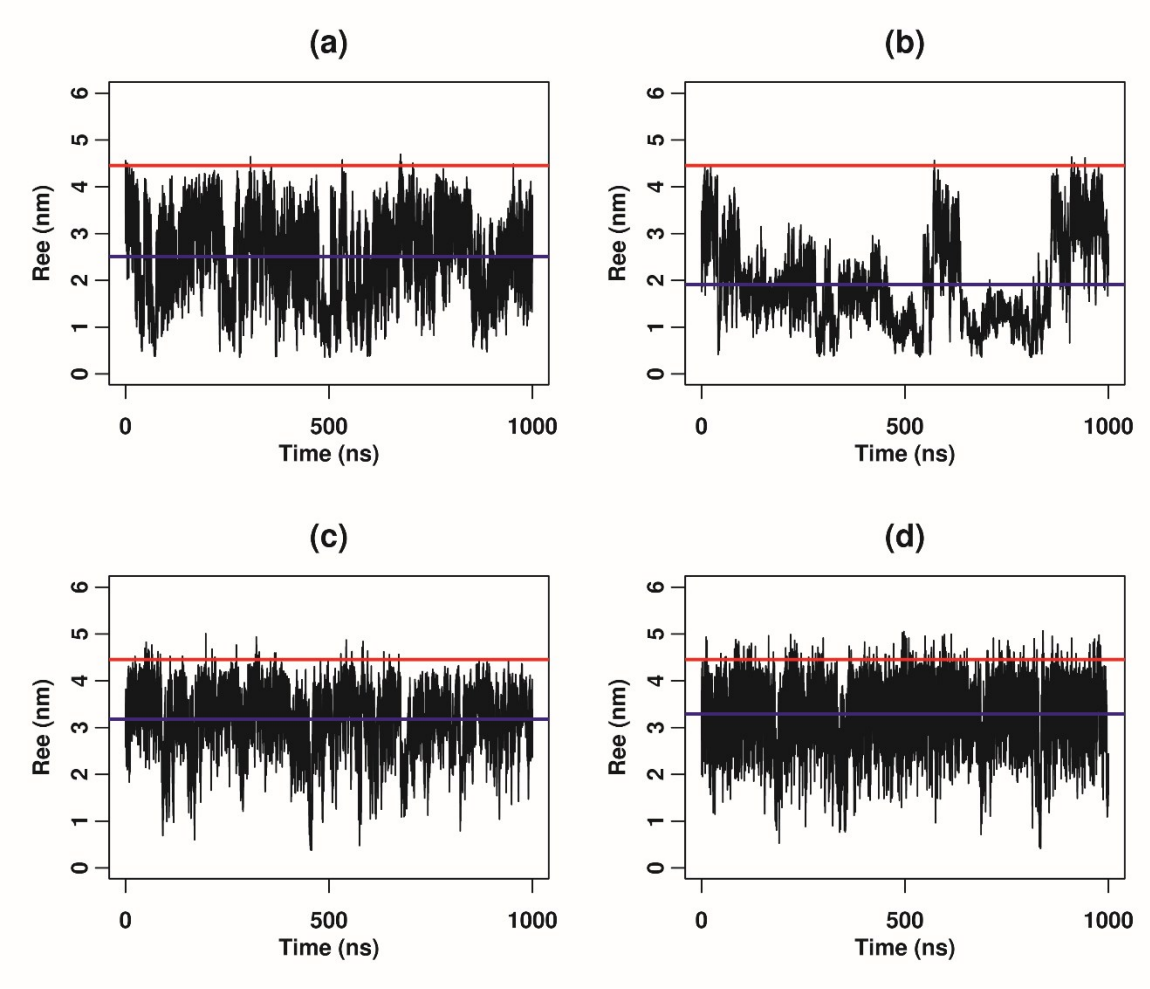

Figure S7. Time evolution of the end to end distance (R_{ee}) (in nm) of p15 FAST peptide for the third replicate corresponding to the force-fields respectively (a) AMBER ff99SB*-ILDNP; (b) OPLS-AA; (c)AMBER ff03ws; and (d) CHARMM36m. The red line indicates the experimental R_{ee} and the blue lines indicate the average R_{ee} of the simulated trajectory.

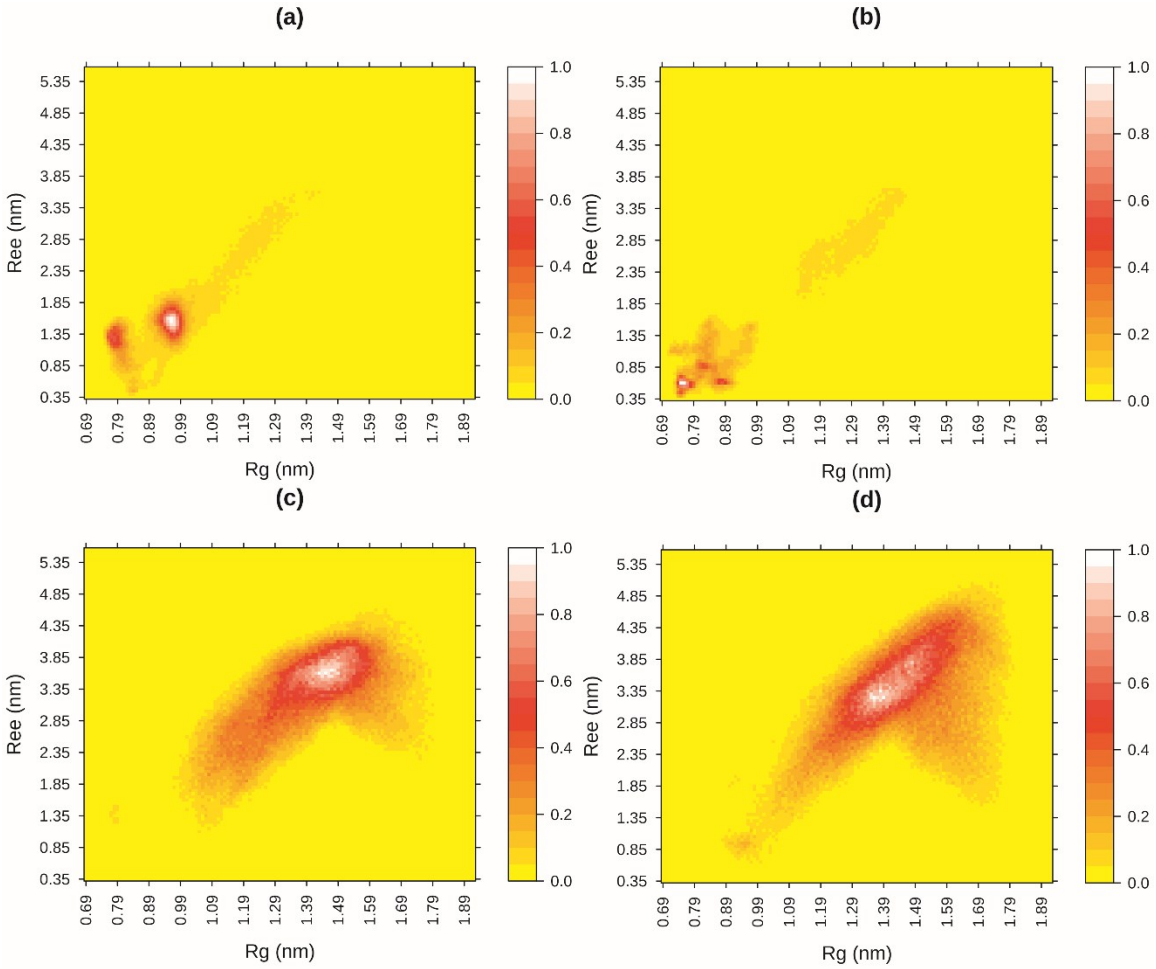

Figure S8. Probability distribution in the radius of gyration (R_g) and end to end distance (R_{ee}) space of p15 FAST peptide for the first replicate corresponding to the force-fields respectively (a) AMBER ff99SB*-ILDNP; (b) OPLS-AA; (c) AMBER ff03ws; and (d) CHARMM36m.

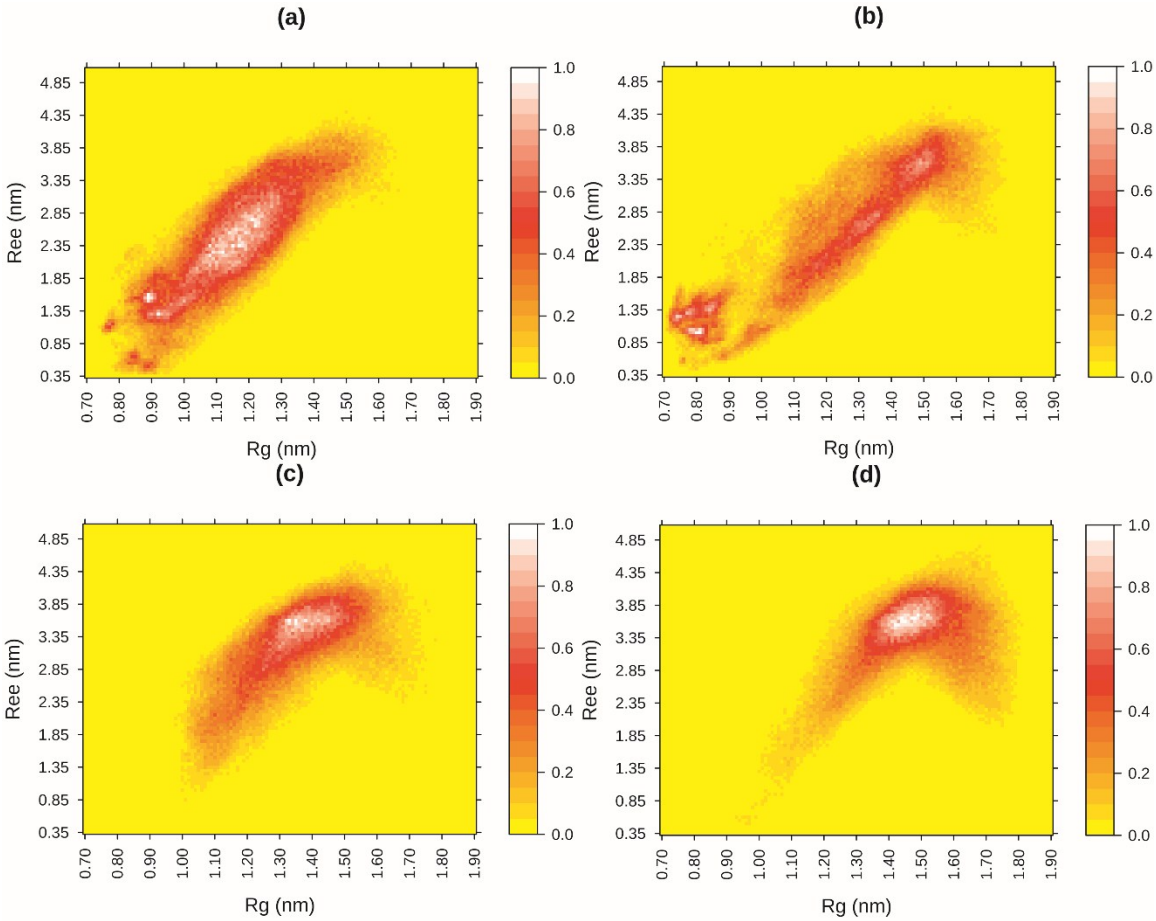

Figure S9. Probability distribution in the radius of gyration (R_g) and end to end distance (R_{ee}) space of p15 FAST peptide for the second replicate corresponding to the force-fields respectively (a) AMBER ff99SB*-ILDNP; (b) OPLS-AA; (c) AMBER ff03ws; and (d) CHARMM36m.

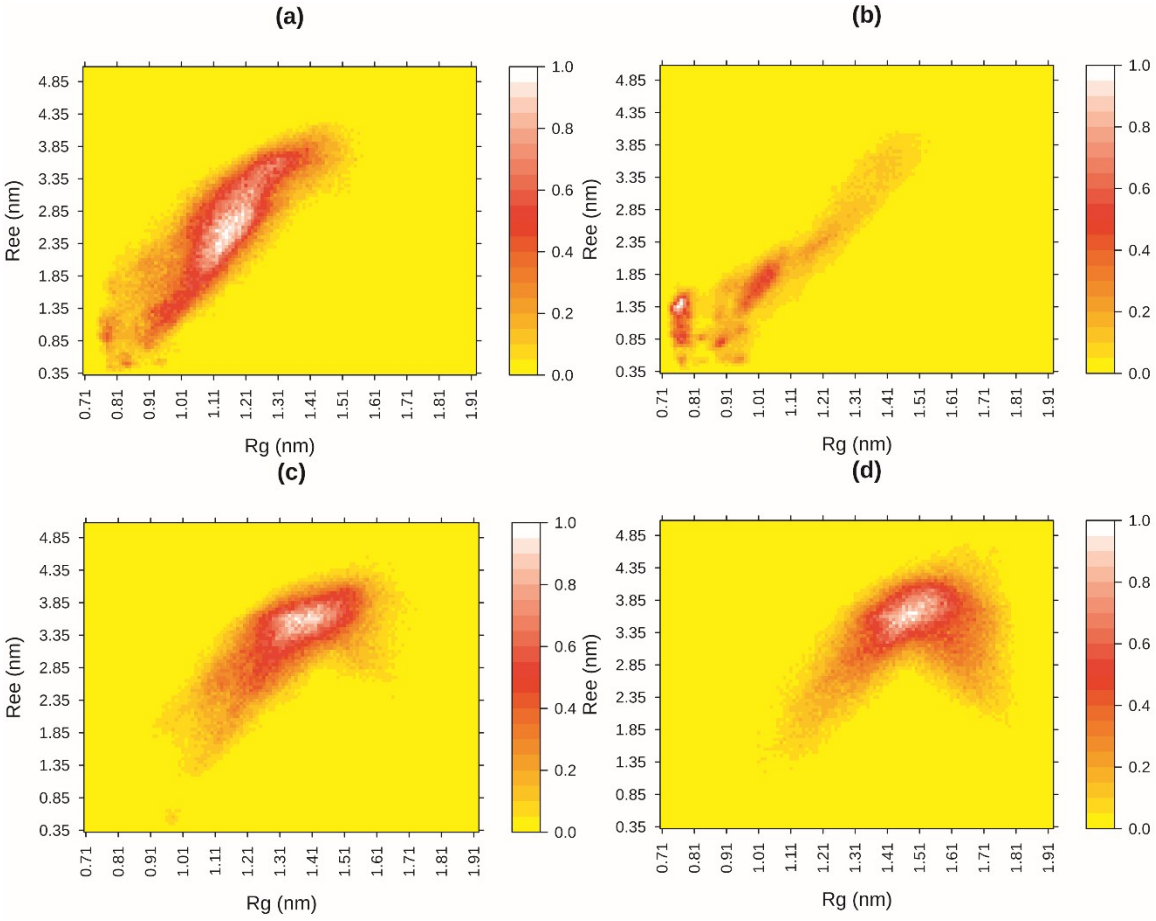

Figure S10. Probability distribution in the radius of gyration (R_g) and end to end distance (R_{ee}) space of p15 FAST peptide for the third replicate corresponding to the force-fields respectively (a) AMBER ff99SB*-ILDNP; (b) OPLS-AA; (c) AMBER ff03ws; and (d) CHARMM36m.

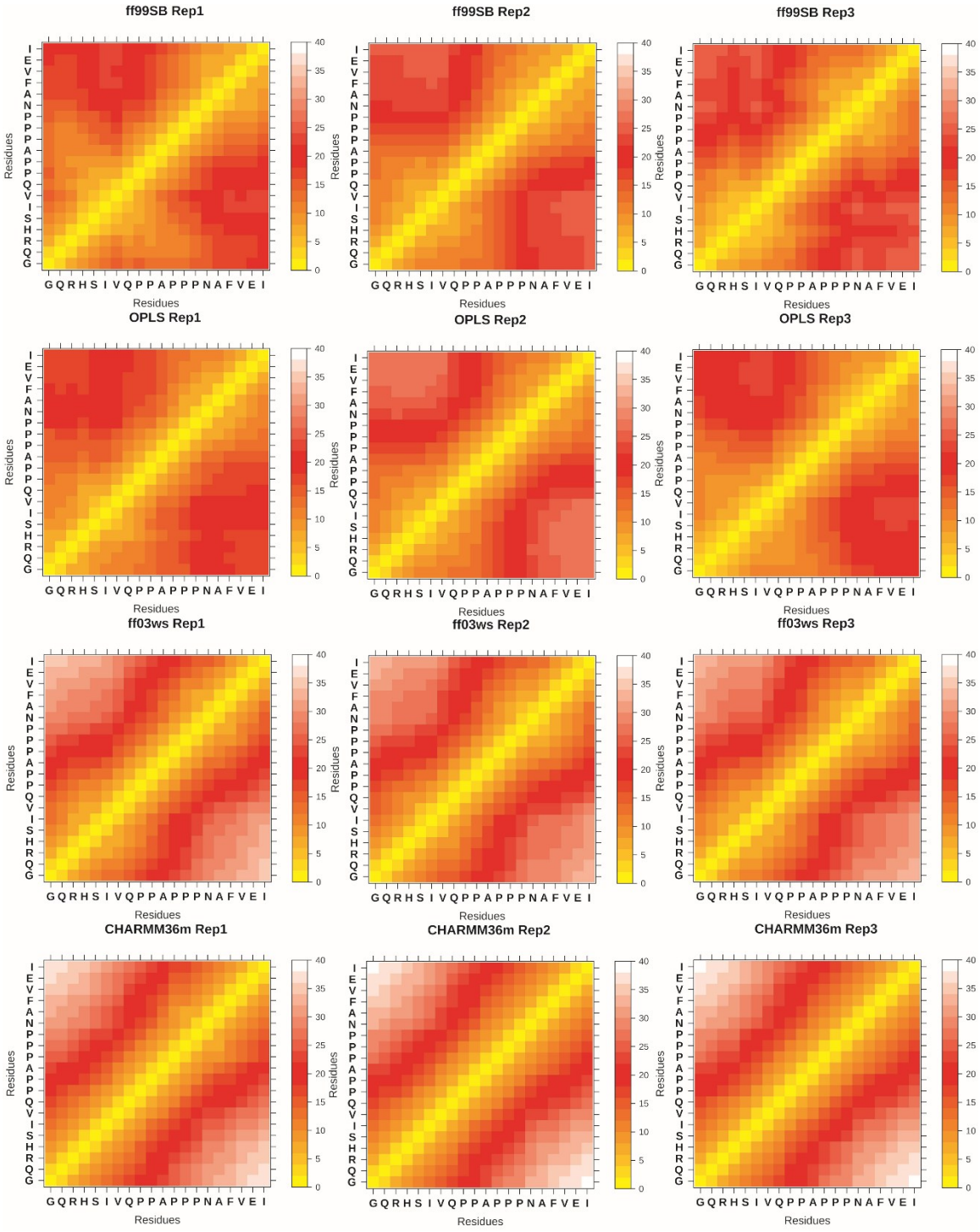

Figure S11. Heat map of average inter-residue distances of the p15 FAST peptide for all the three replicates corresponding to the force-fields respectively from top to bottom AMBER ff99SB*-ILDNP, OPLS-AA, AMBER ff03ws and CHARMM36m.

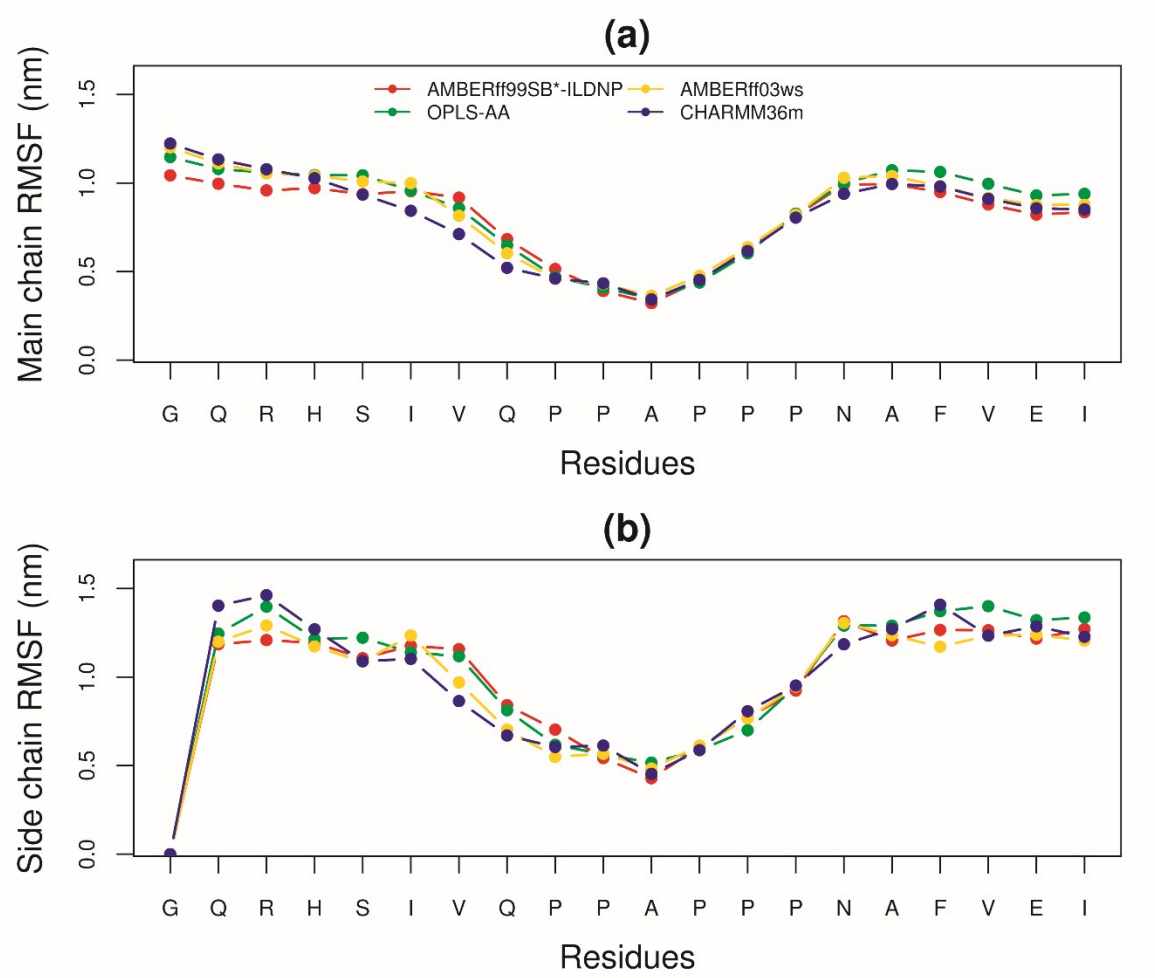

Figure S12. Residue-wise root mean square fluctuations (RMSFs) (in nm) for the second replicate all force fields considering (a) main chain atoms (N, CA, C, O) and (b) side chain atoms.

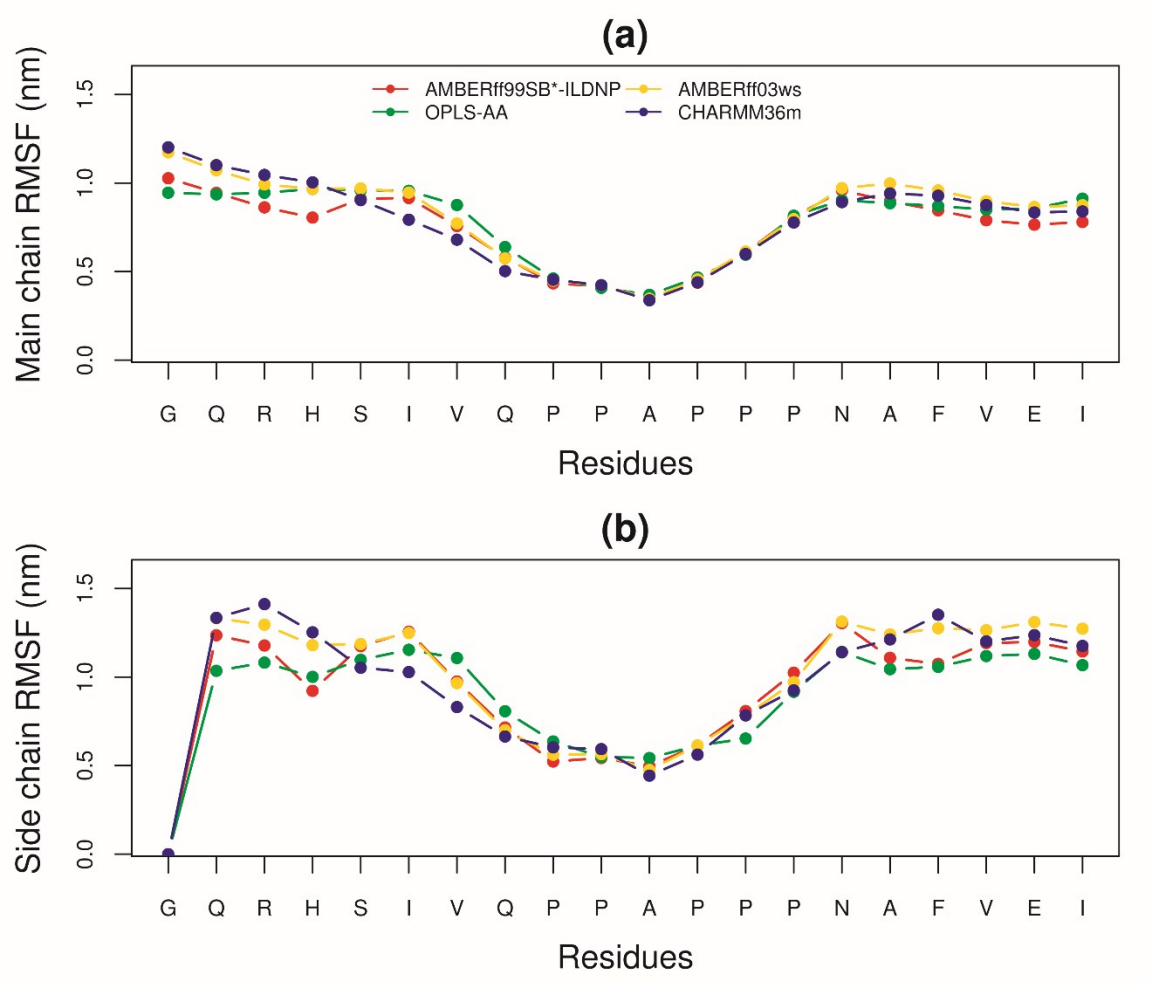

Figure S13. Residue-wise root mean square fluctuations (RMSFs) (in nm) for the third replicate for all force fields considering (a) main chain atoms (N, CA, C, O) and (b) side chain atoms.

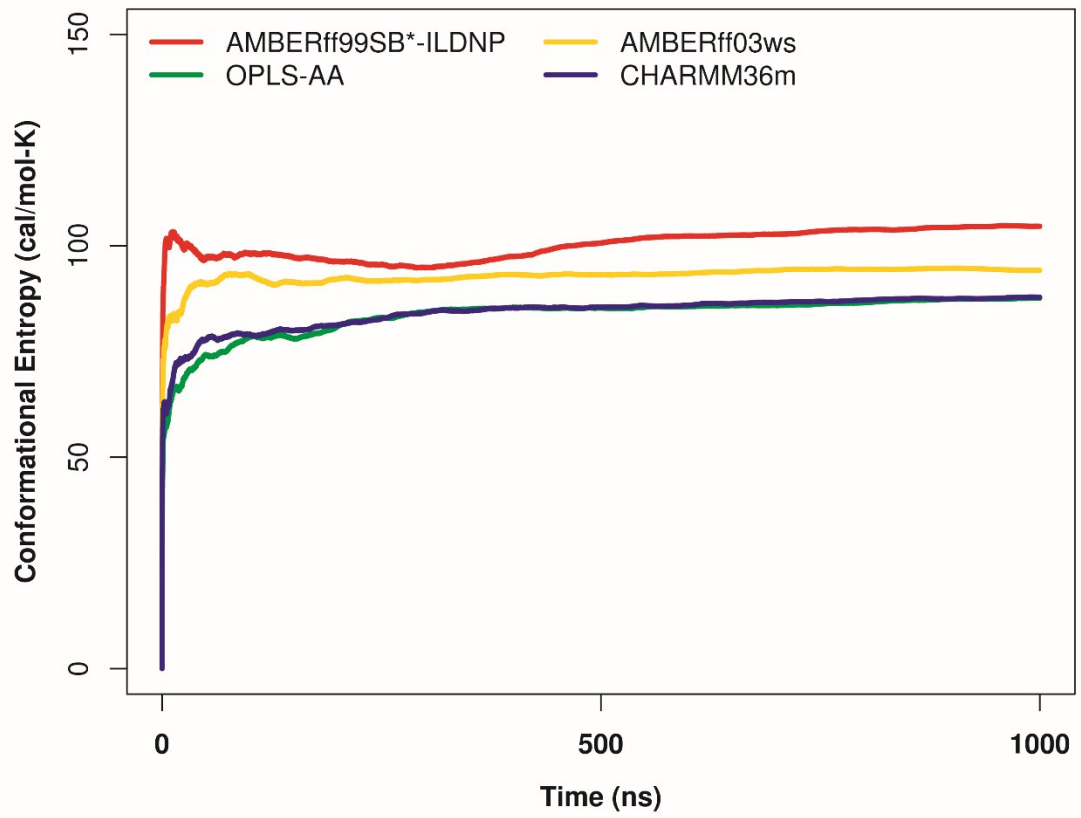

Figure S14. Time evolution plot of conformational entropy for the residues G2-I21 (in cal/mol-K) (using CC-MLA method) for the second replicate corresponding to the four different force-fields AMBER ff99SB*-ILDNP, OPLS-AA, AMBER ff03ws and CHARMM36m.

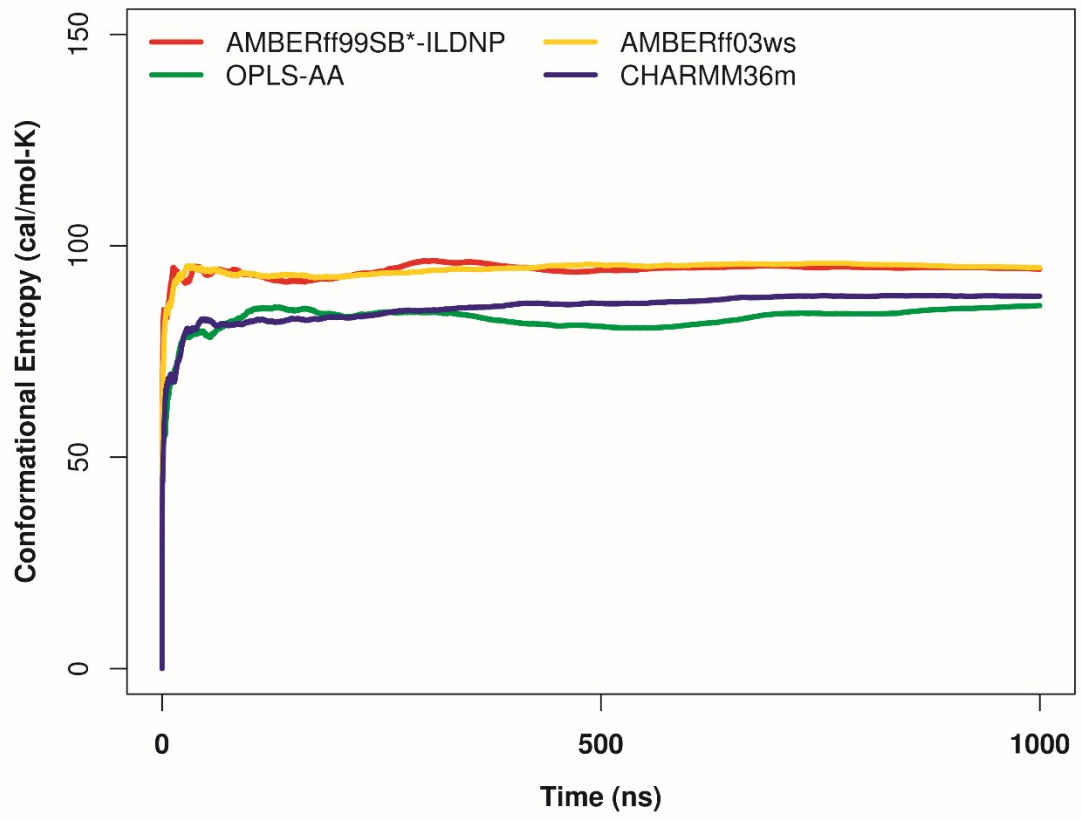

Figure S15. Time evolution plot of conformational entropy for the residues G2-I21 (in cal/mol-K) (using CC-MLA method) for the third replicate corresponding to the four different force-fields AMBER ff99SB*-ILDNP, OPLS-AA, AMBER ff03ws and CHARMM36m.

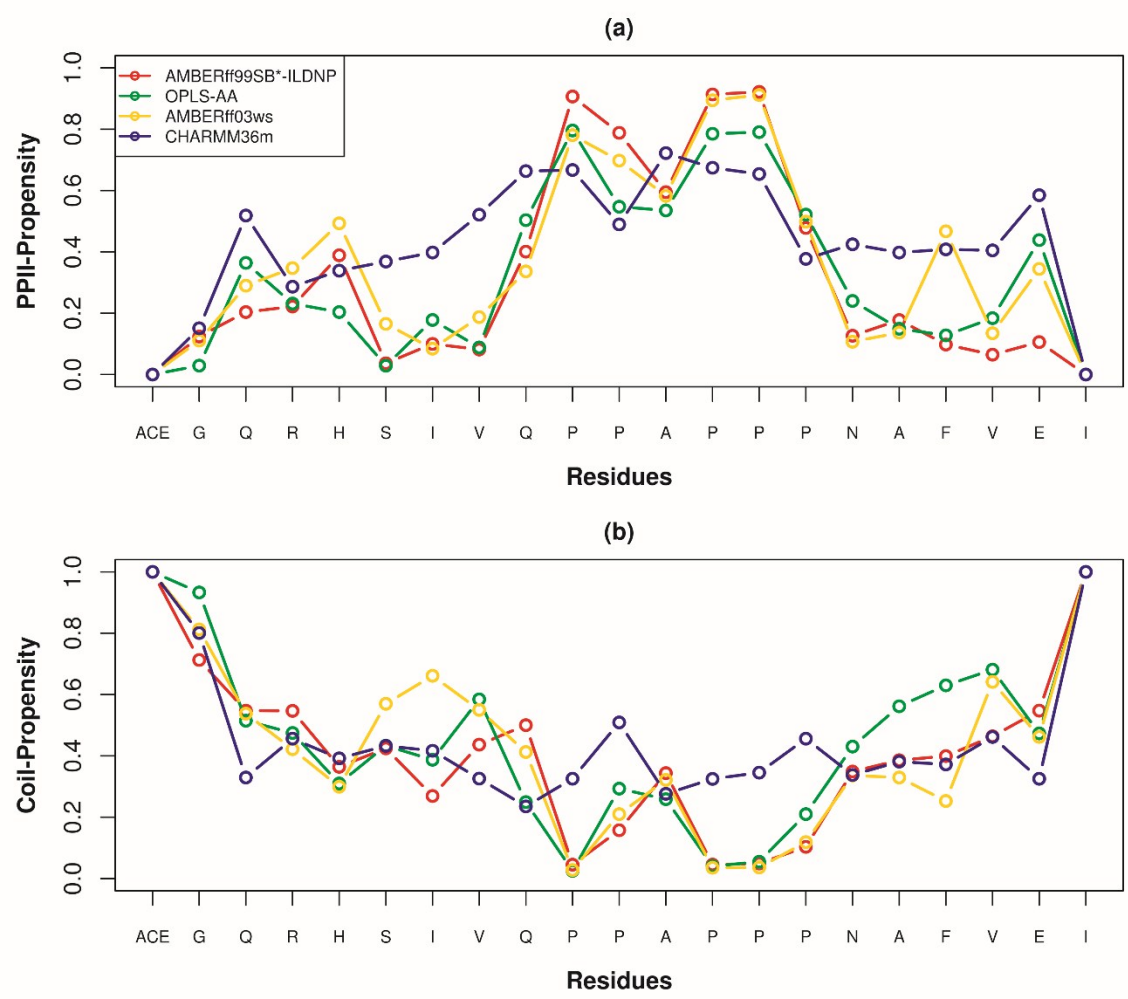

Figure S16. Residue-wise plot of the (a) PP-II and (b) coil propensities of the p15 FAST peptide for the second replicate corresponding to the force-fields AMBER ff99SB*-ILDNP, OPLS-AA, AMBER ff03ws and CHARMM36m.

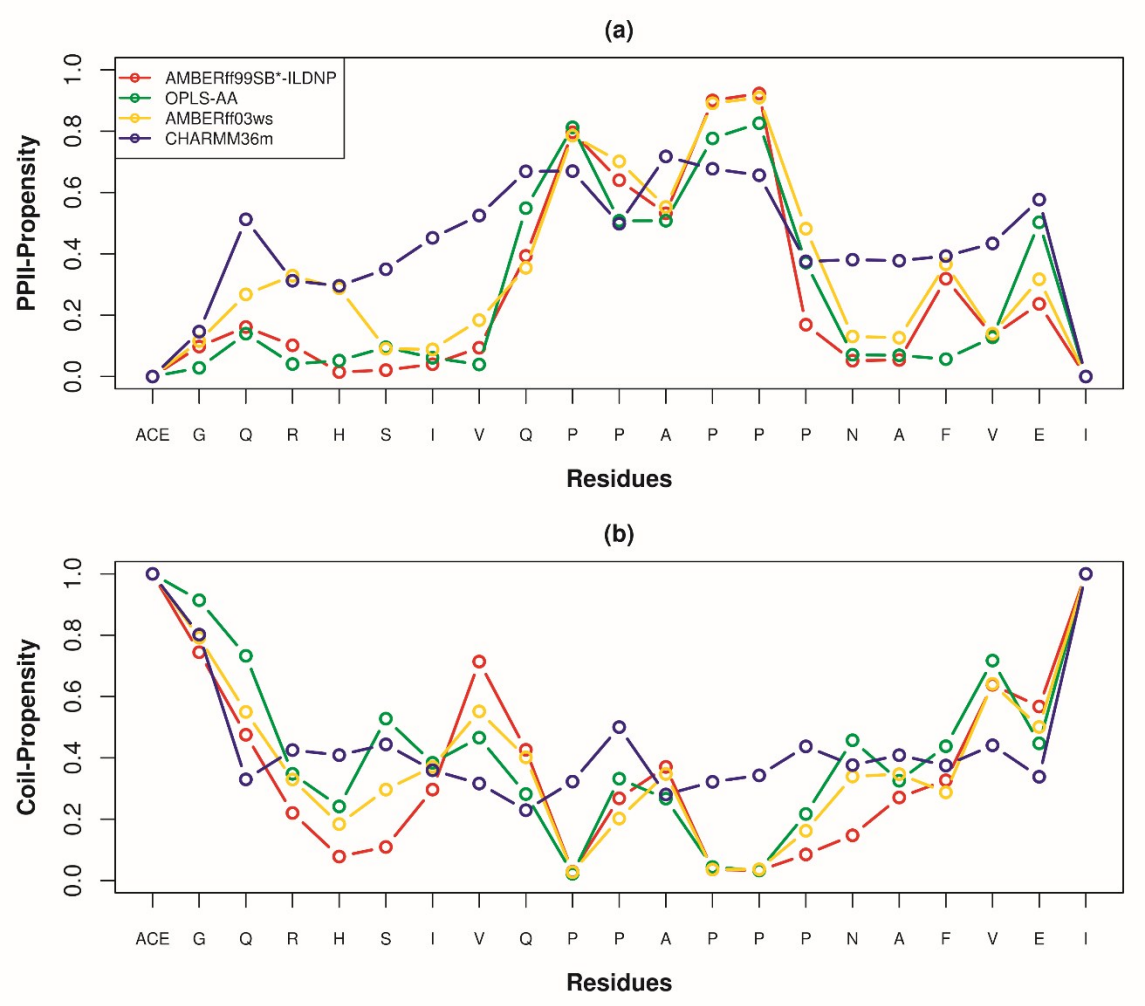

Figure S17. Residue-wise plot of the (a) PP-II and (b) coil propensities of the p15 FAST peptide for the third replicate corresponding to the force-fields AMBER ff99SB*-ILDNP, OPLS-AA, AMBER ff03ws and CHARMM36m.

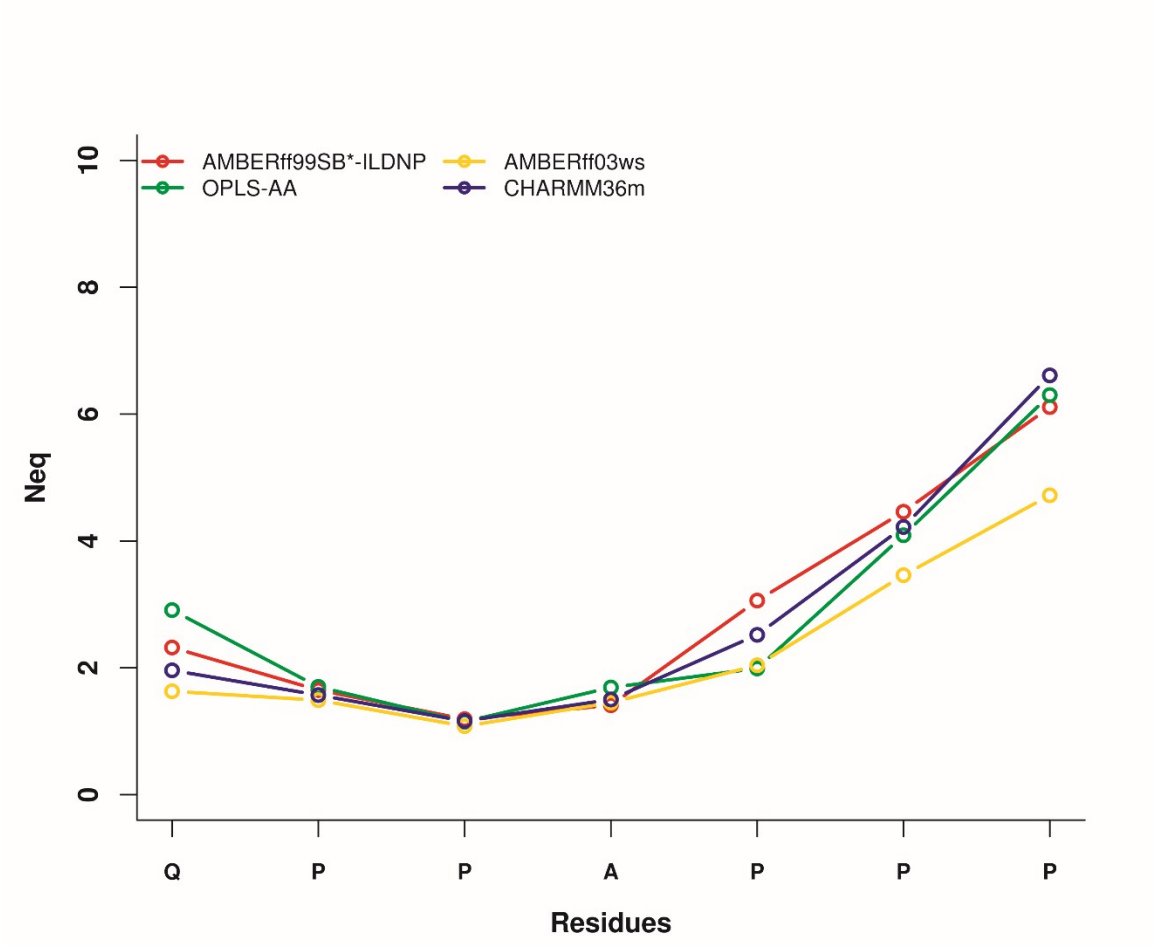

Figure S18. Residue-wise plot of the equivalent number of protein blocks sampled by the residues Q9 to P15 for the second replicate corresponding to the four different force-fields AMBER ff99SB*-ILDNP, OPLS-AA, AMBER ff03ws and CHARMM36m.

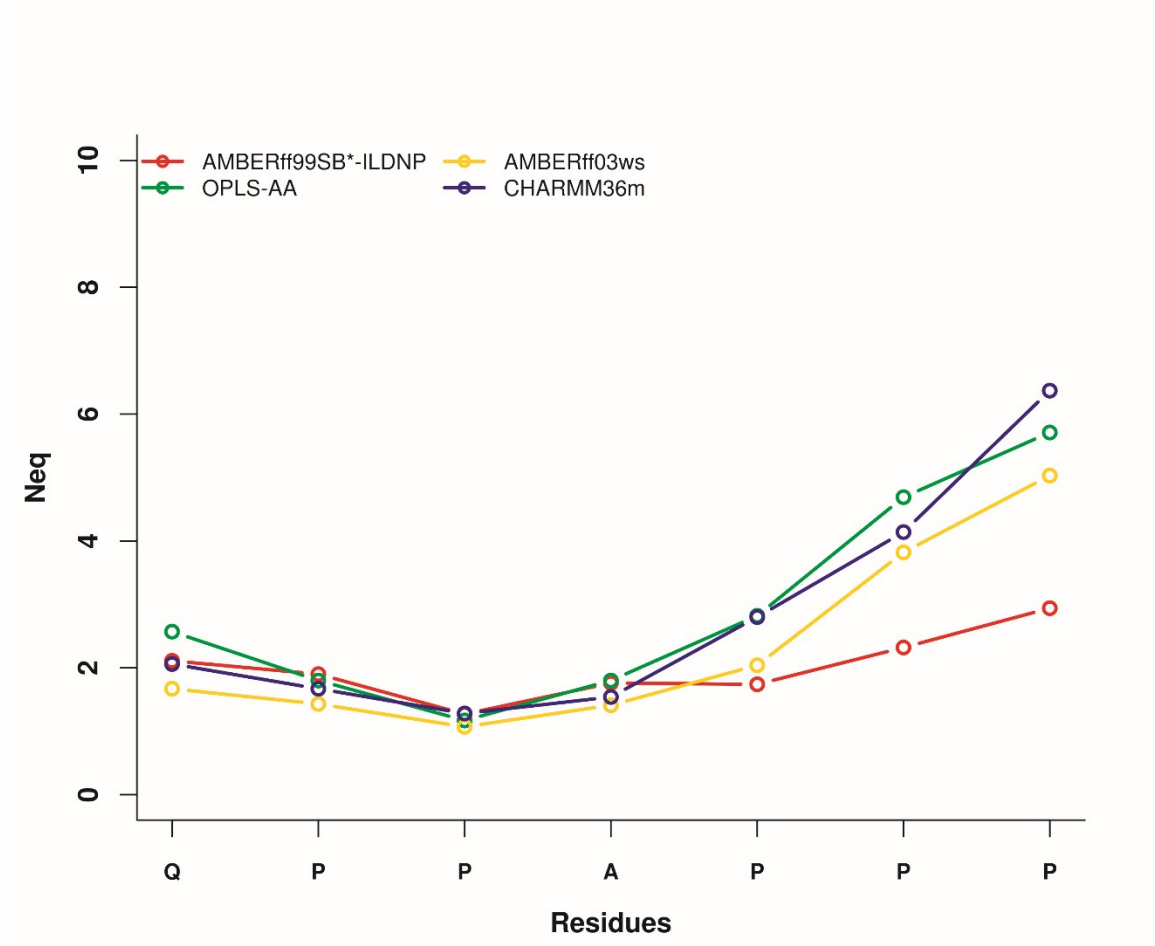

Figure S19. Residue-wise plot of the equivalent number of protein blocks sampled by the residues Q9 to P15 for the third replicate corresponding to the four different force-fields AMBER ff99SB*-ILDNP, OPLS-AA, AMBER ff03ws and CHARMM36m.

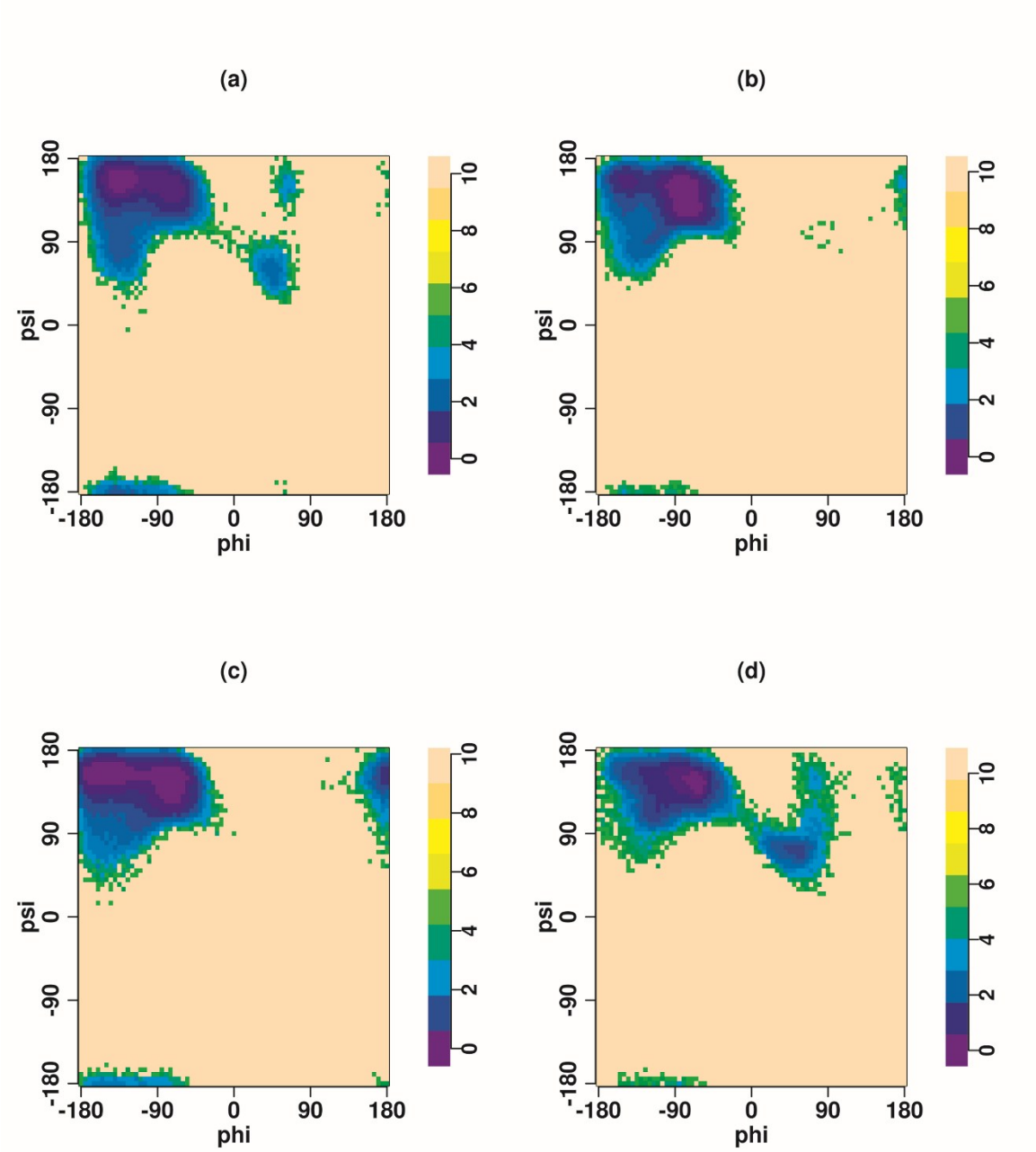

Figure S20. Free energy landscape (in kcal/mole) in ϕ, ψ dihedral space for glutamine at position 9 for the first replicate. (a) AMBER ff99SB*-ILDNP; (b) OPLS-AA; (c) AMBER ff03ws; and (d) CHARMM36m.

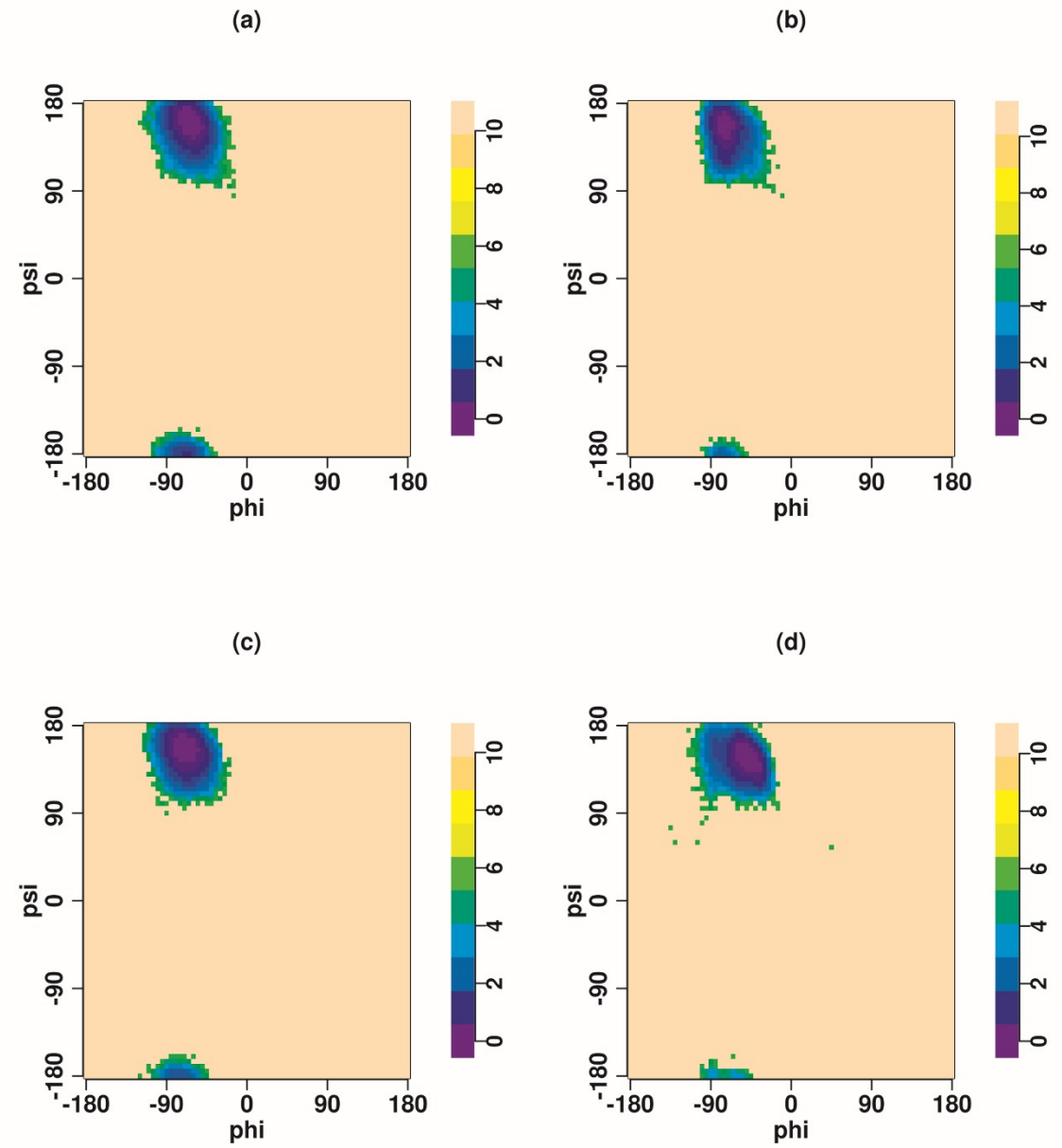

Figure S21. Free energy landscape (in kcal/mole) in ϕ, ψ dihedral space for proline at position 10 for the first replicate. (a) AMBER ff99SB*-ILDNP; (b) OPLS-AA; (c) AMBER-ff03ws; and (d) CHARMM36m.

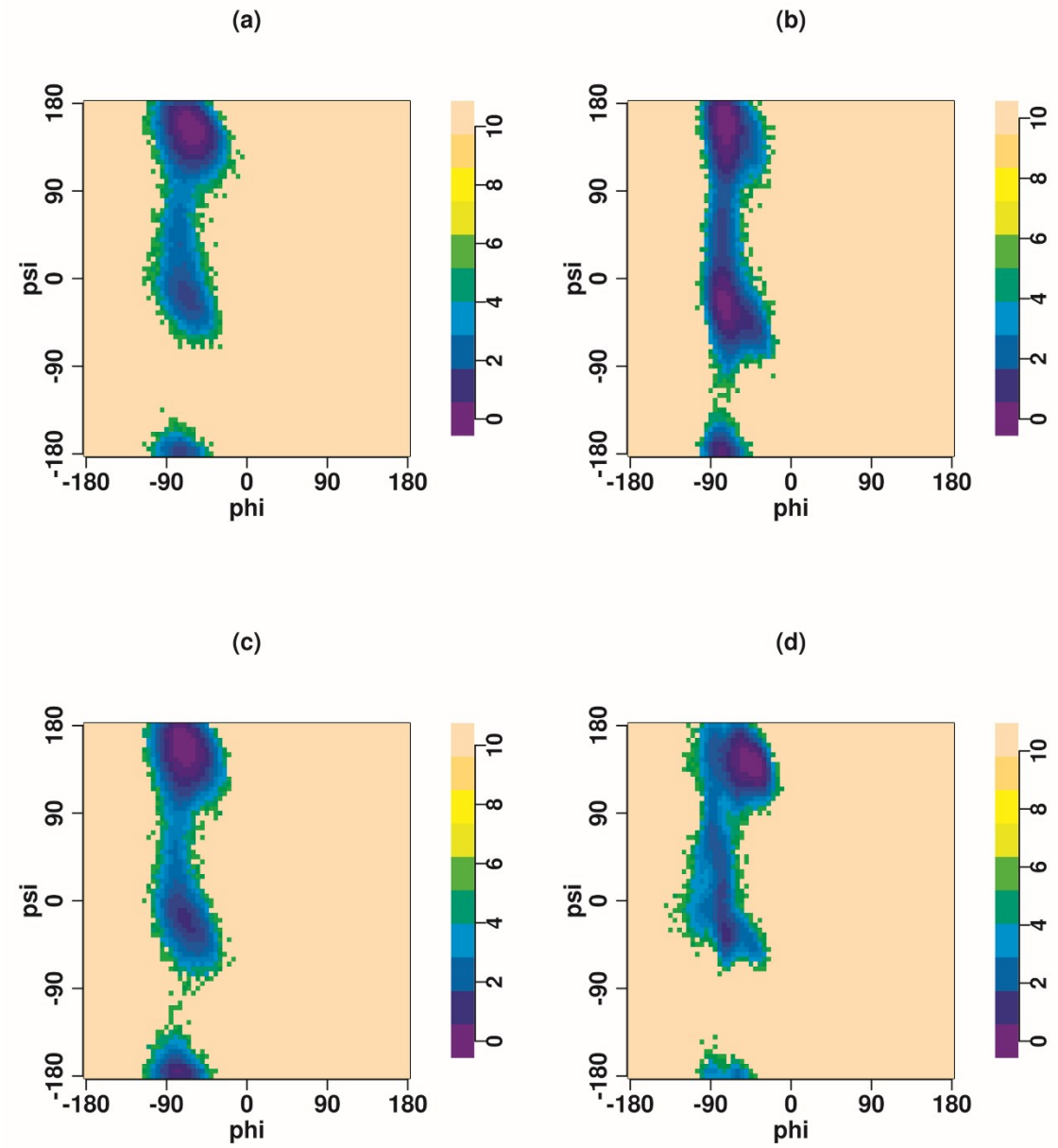

Figure S22. Free energy landscape (in kcal/mole) in ϕ, ψ dihedral space for proline at position 11 for the first replicate. (a) AMBER ff99SB*-ILDNP; (b) OPLS-AA; (c) AMBER ff03ws; and (d) CHARMM36m.

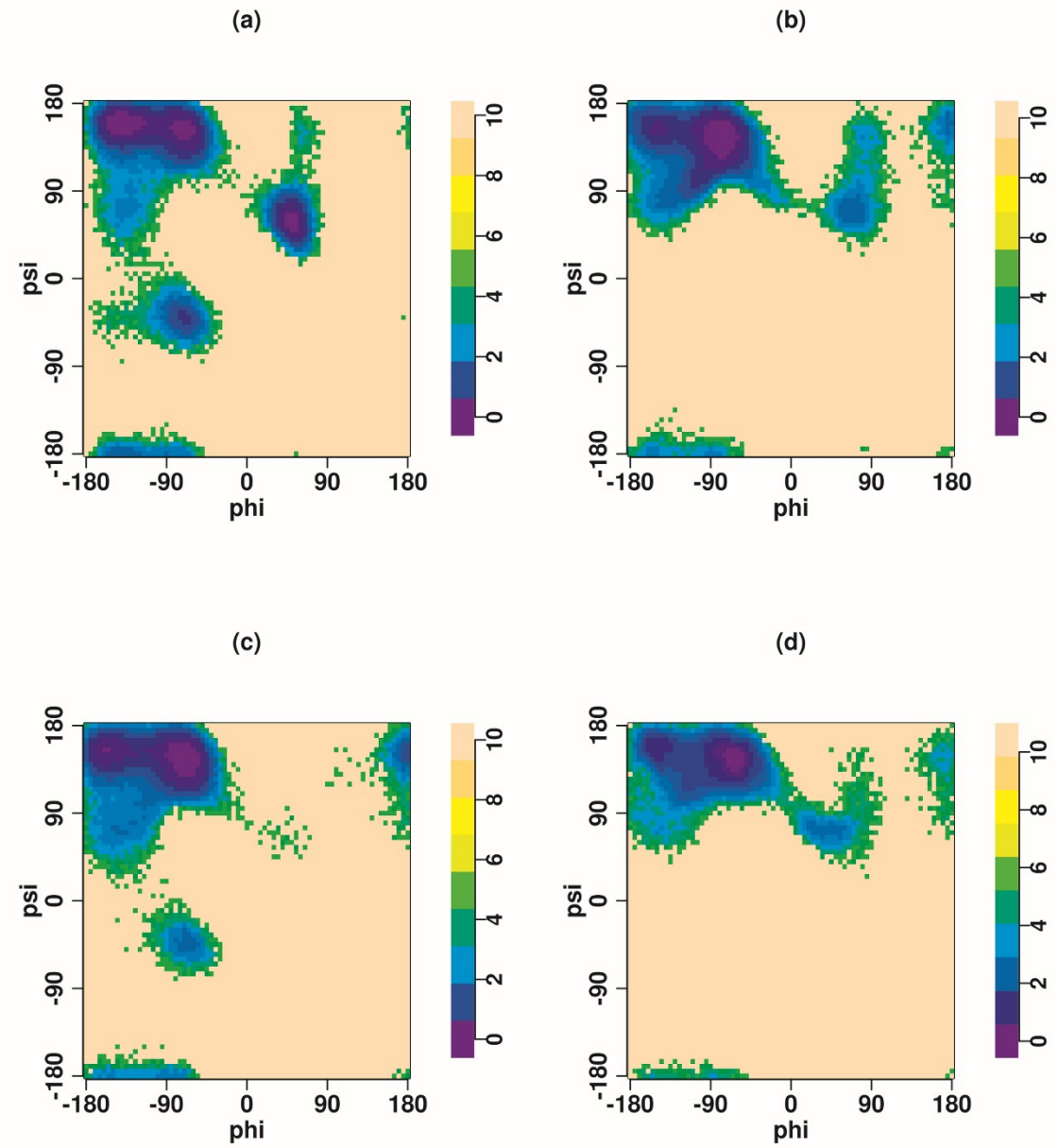

Figure S23. Free energy landscape (in kcal/mole) in ϕ, ψ dihedral space for alanine at position 12 for the first replicate. (a) AMBER ff99SB*-ILDNP; (b) OPLS-AA; (c) AMBER ff03ws; and (d) CHARMM36m.

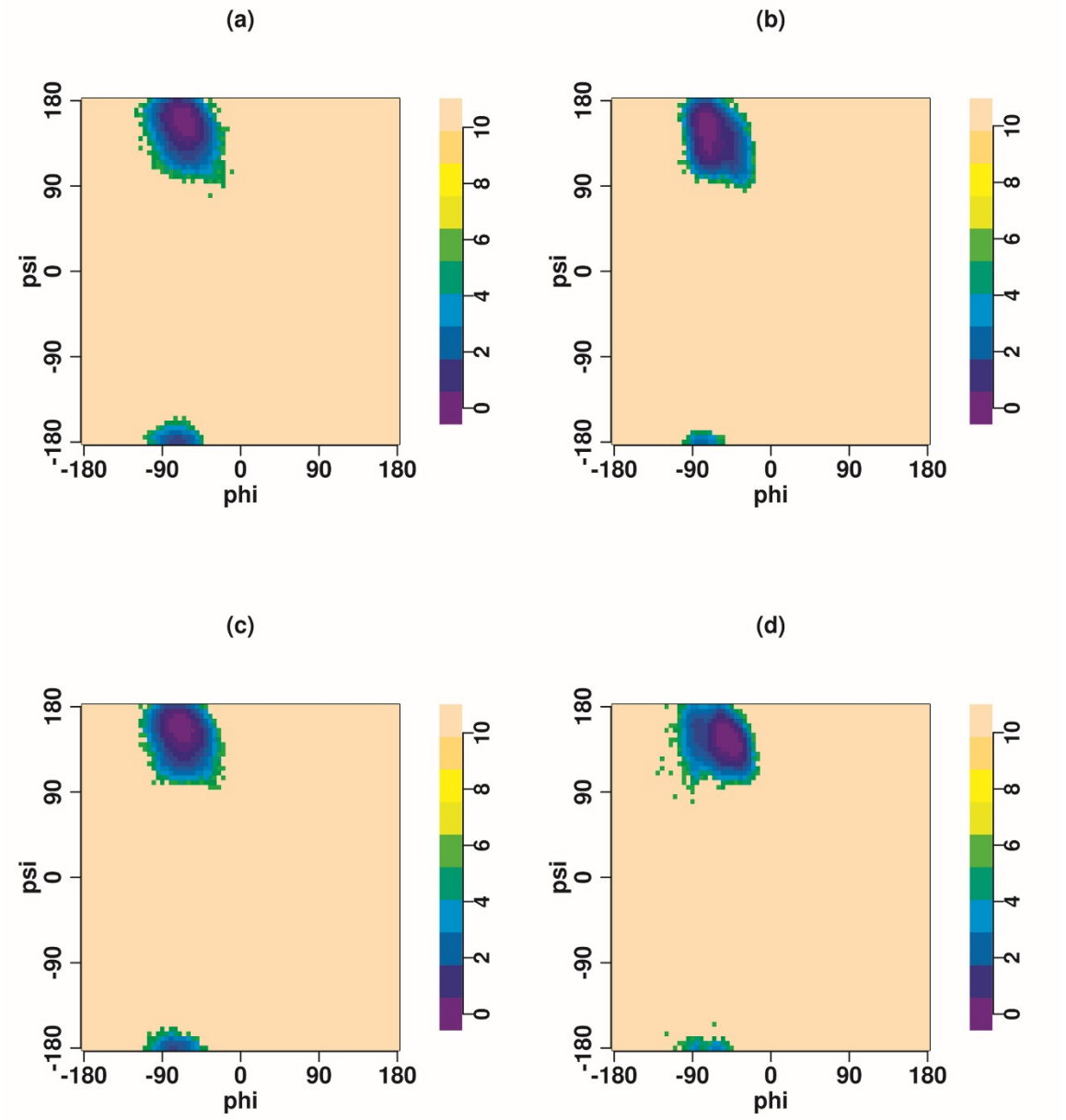

Figure S24. Free energy landscape (in kcal/mole) in ϕ, ψ dihedral space for proline at position 13 for the first replicate. (a) AMBER ff99SB*-ILDNP; (b) OPLS-AA; (c) AMBER ff03ws; and (d) CHARMM36m.

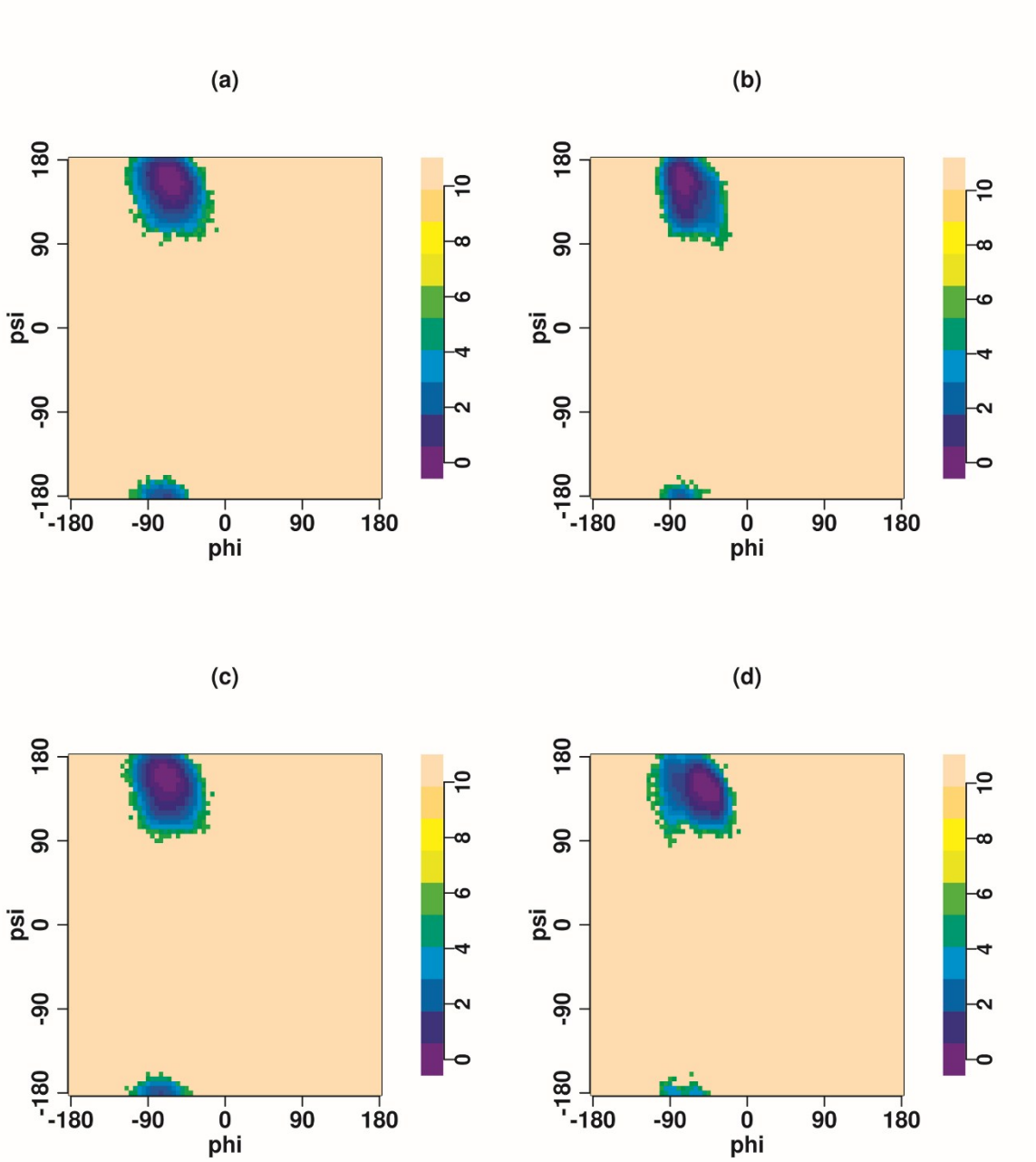

Figure S25. Free energy landscape (in kcal/mole) in ϕ, ψ dihedral space for proline at position 14 for the first replicate. (a) AMBER ff99SB*ILDNP; (b) OPLS-AA; (c) AMBER ff03ws; and (d) CHARMM36m.

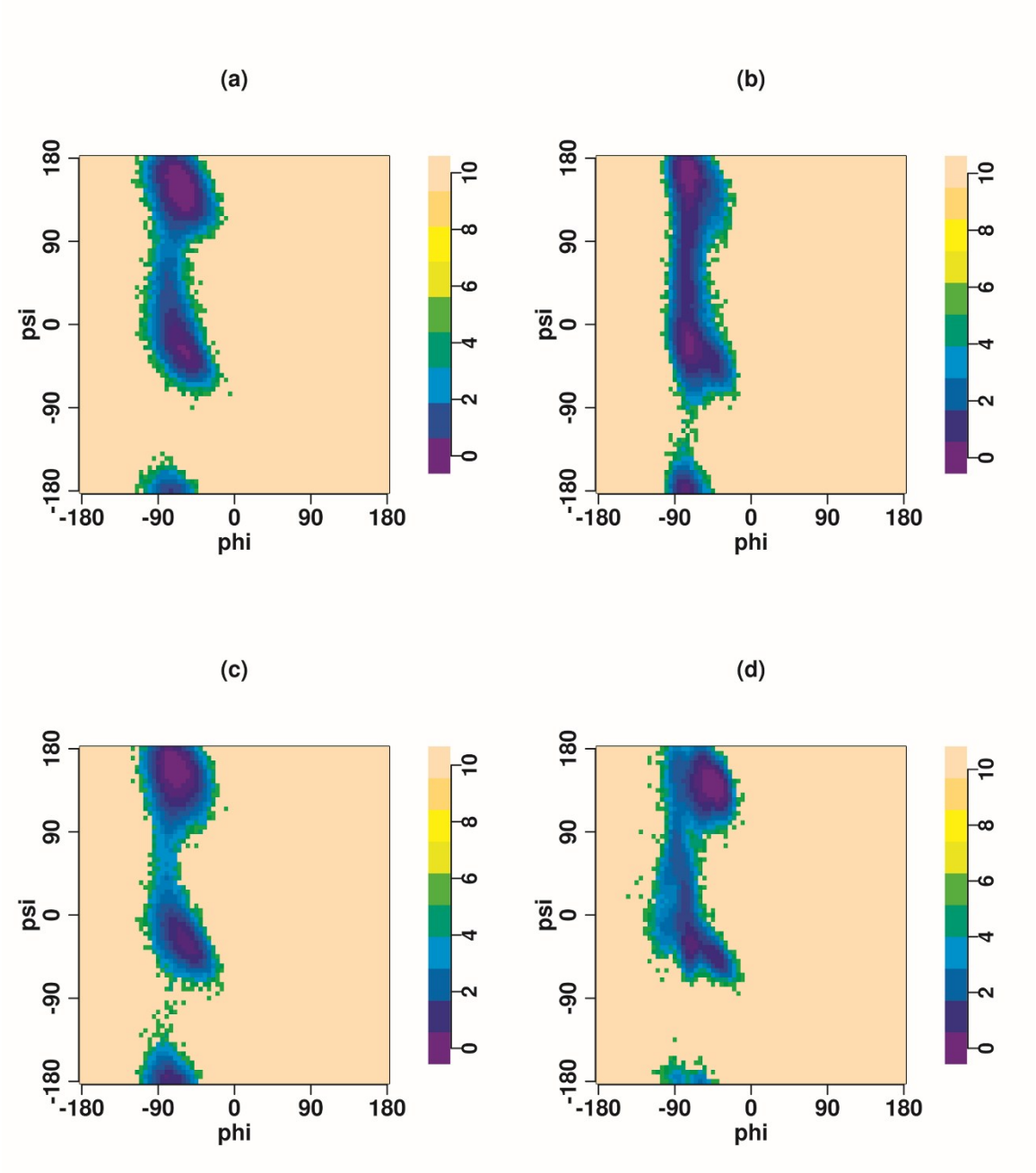

Figure S26. Free energy landscape (in kcal/mole) in ϕ, ψ dihedral space for proline at position 15 for the first replicate. (a) AMBER ff99SB*-ILDNP; (b) OPLS-AA; (c) AMBER ff03ws; and (d) CHARMM36m.

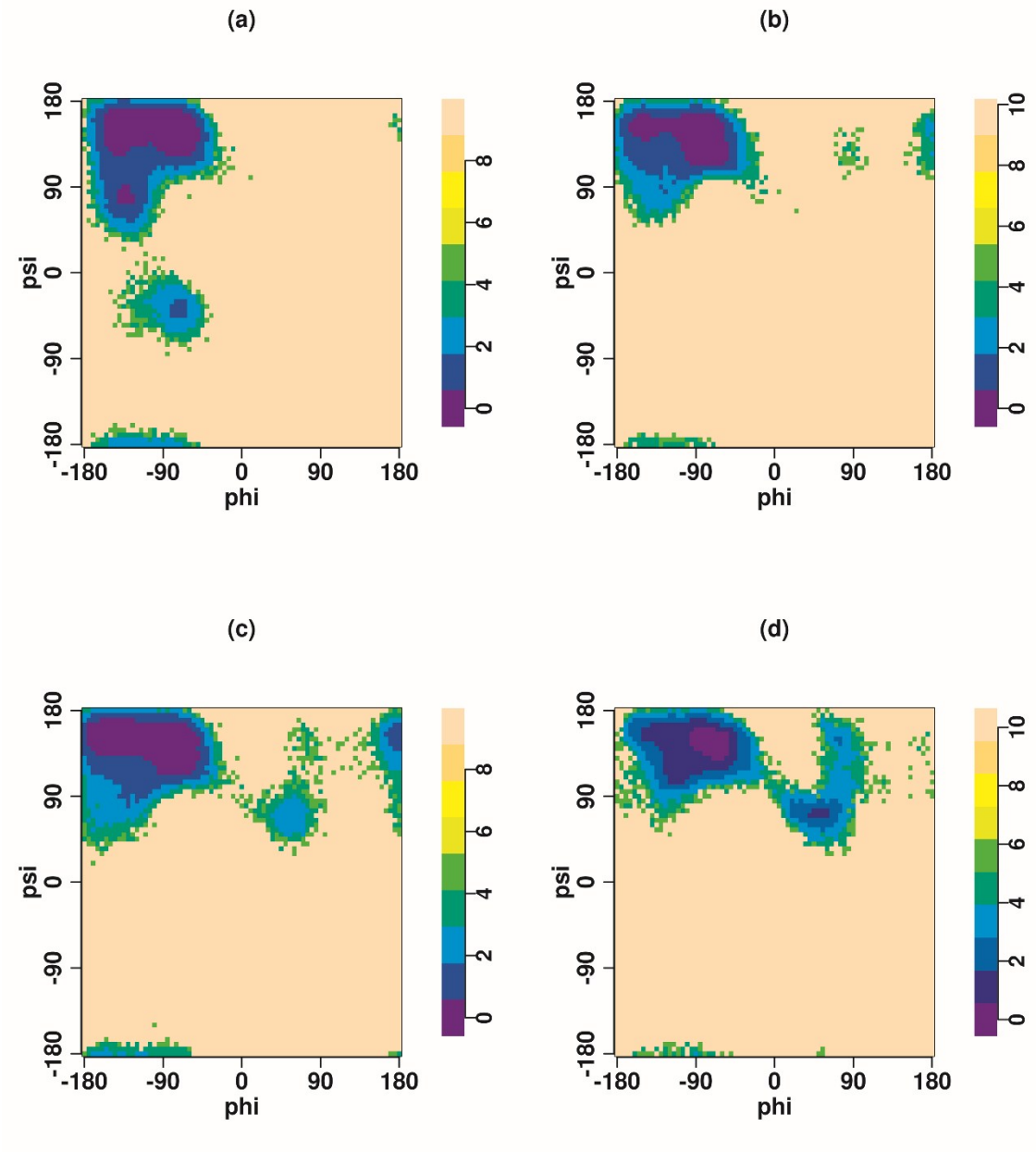

Figure S27. Free energy landscape (in kcal/mole) in ϕ, ψ dihedral space for glutamine at position 9 for the second replicate. (a) AMBER ff99SB*-ILDNP; (b) OPLS-AA; (c) AMBER ff03ws; and (d) CHARMM36m.

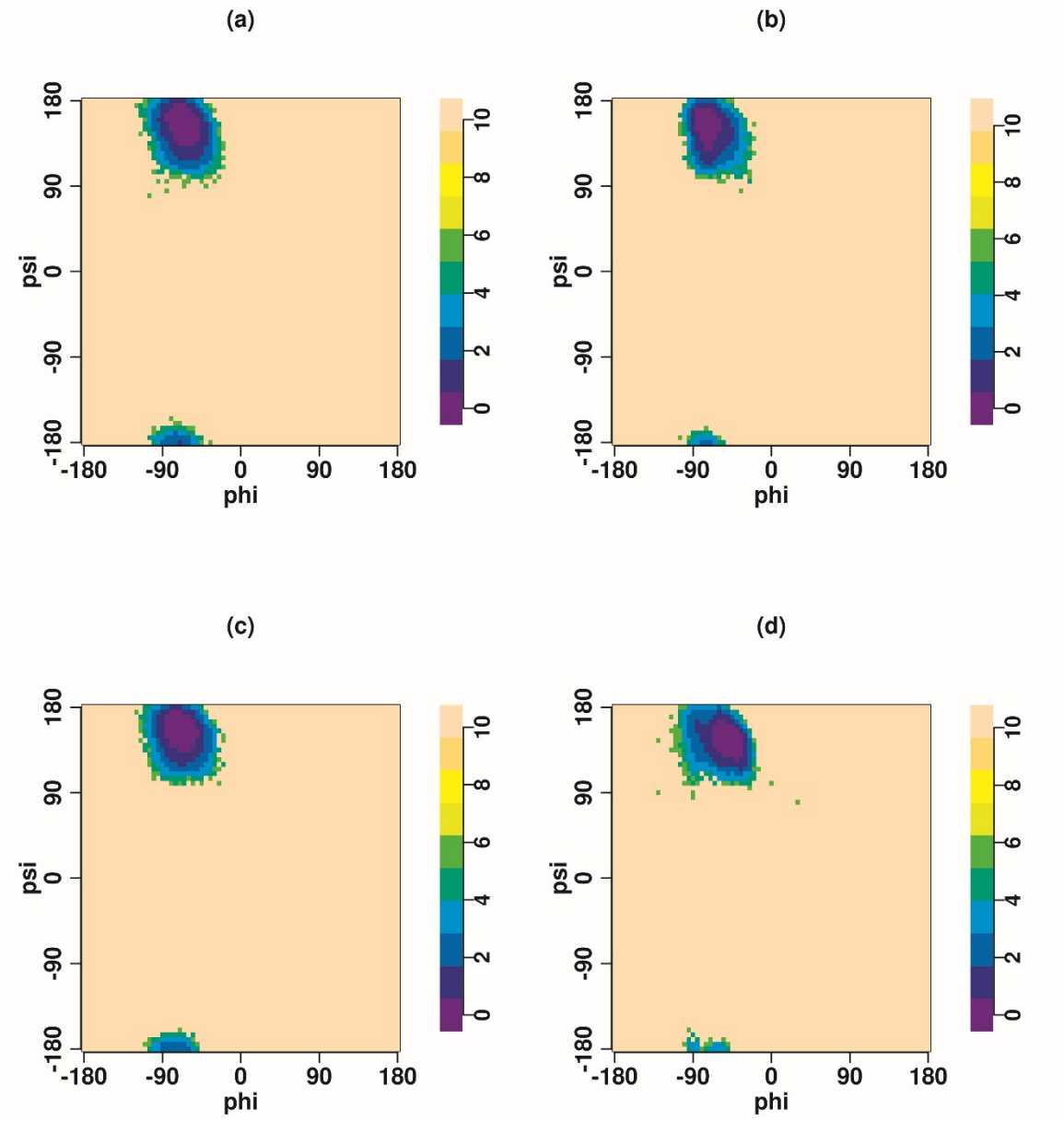

Figure S28. Free energy landscape (in kcal/mole) in ϕ, Ψ dihedral space for proline at position 10 for the second replicate. (a) AMBER ff99SB*-ILDNP; (b) OPLS-AA; (c) AMBER-ff03ws; and (d) CHARMM36m.

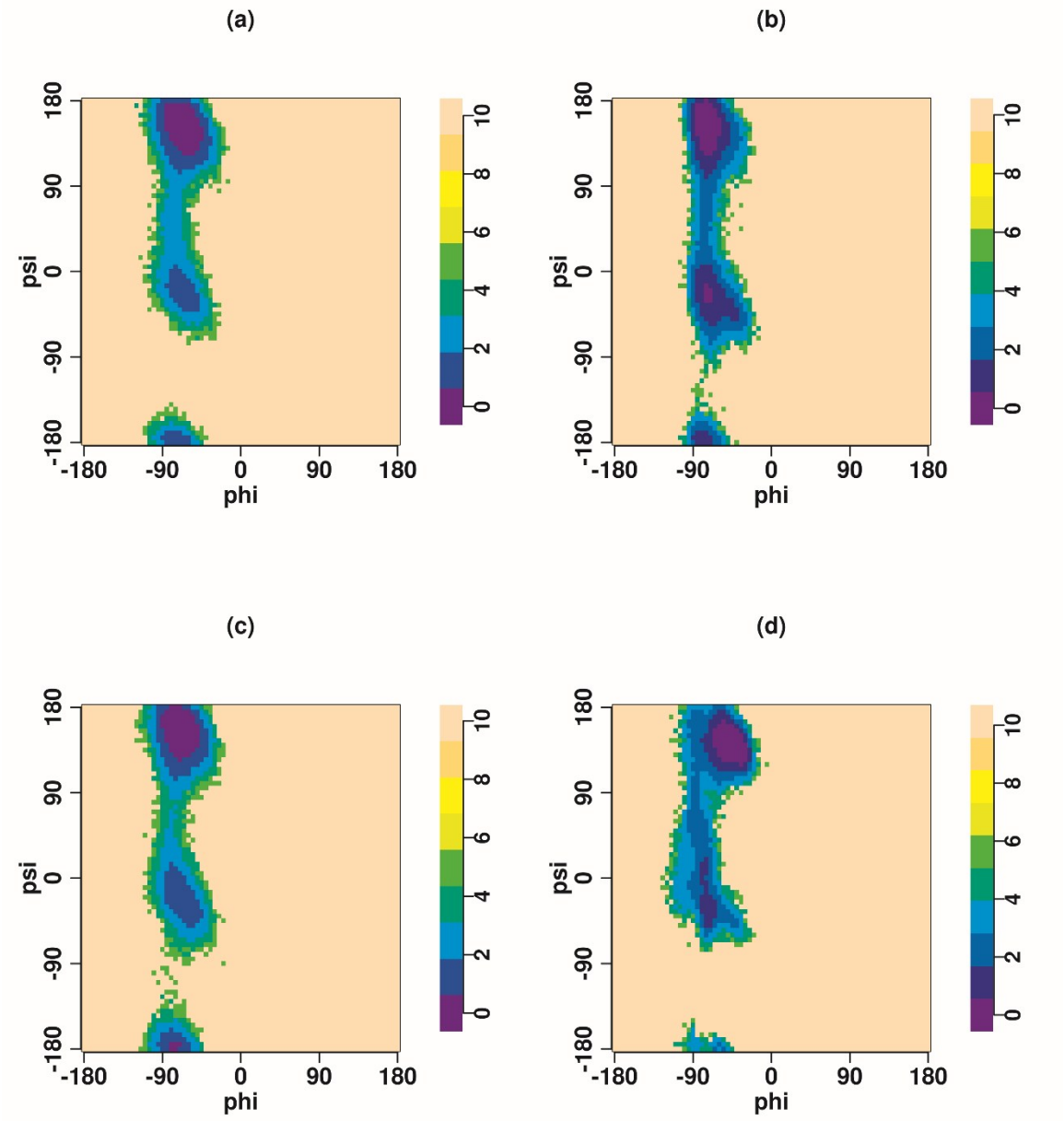

Figure S29. Free energy landscape (in kcal/mole) in ϕ, Ψ dihedral space for proline at position 11 for the second replicate. (a) AMBER ff99SB*-ILDNP; (b) OPLS-AA; (c) AMBER ff03ws; and (d) CHARMM36m.

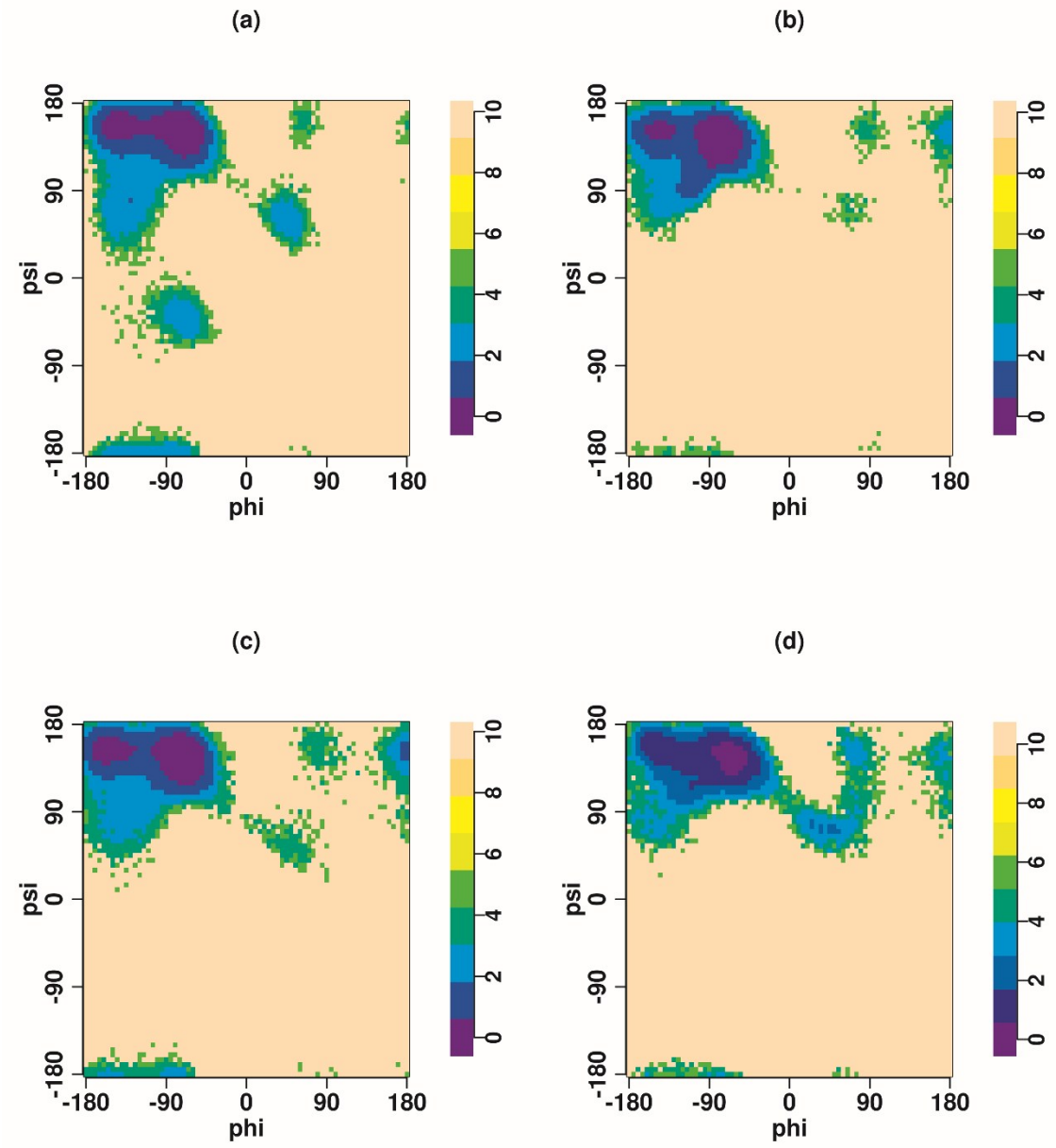

Figure S30. Free energy landscape (in kcal/mole) in ϕ, Ψ dihedral space for alanine at position 12 for the second replicate. (a) AMBER ff99SB*-ILDNP; (b) OPLS-AA; (c) AMBER ff03ws; and (d) CHARMM36m.

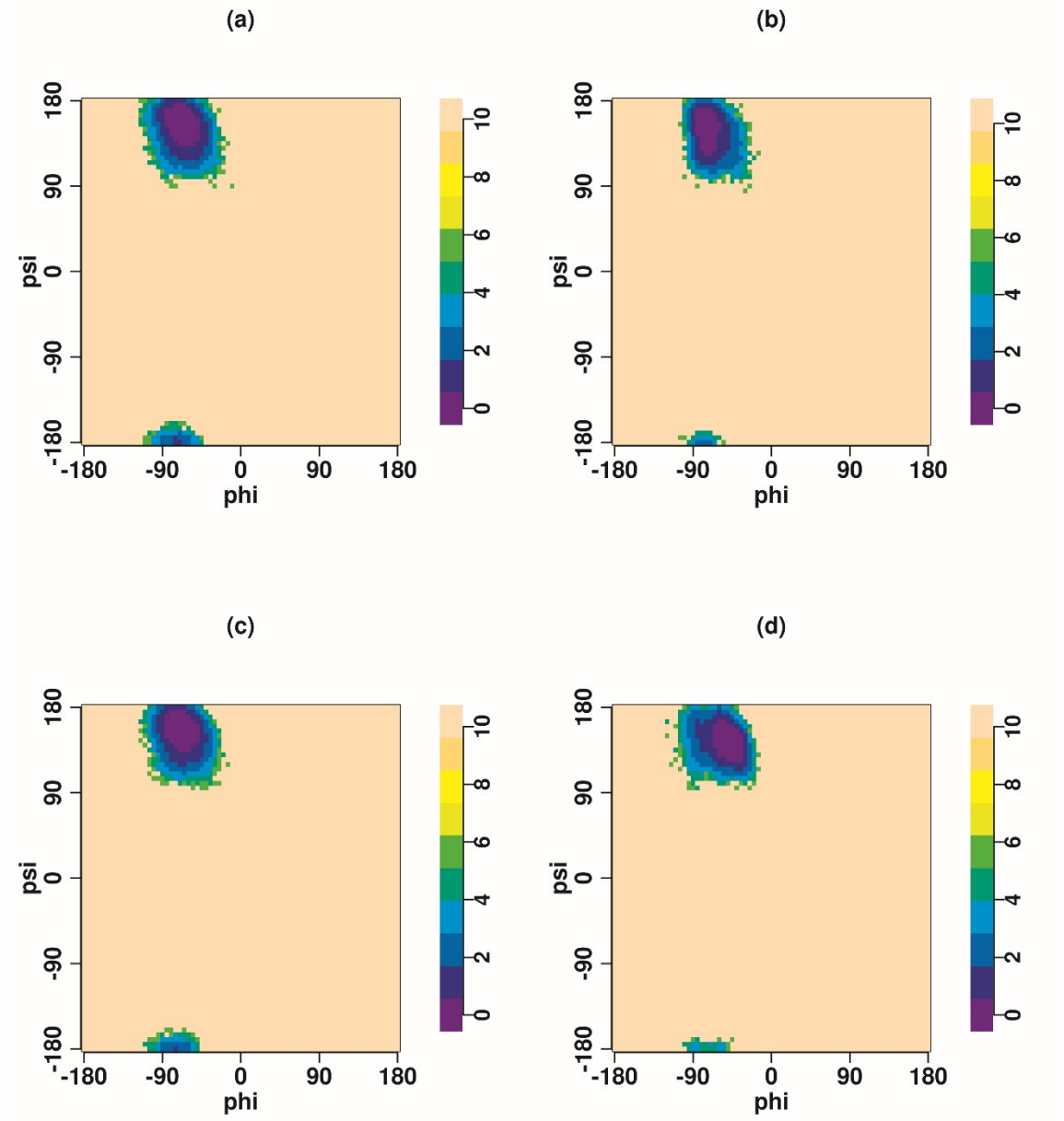

Figure S31. Free energy landscape (in kcal/mole) in ϕ, Ψ dihedral space for proline at position 13 for the second replicate. (a) AMBER ff99SB*-ILDNP; (b) OPLS-AA; (c) AMBER ff03ws; and (d) CHARMM36m.

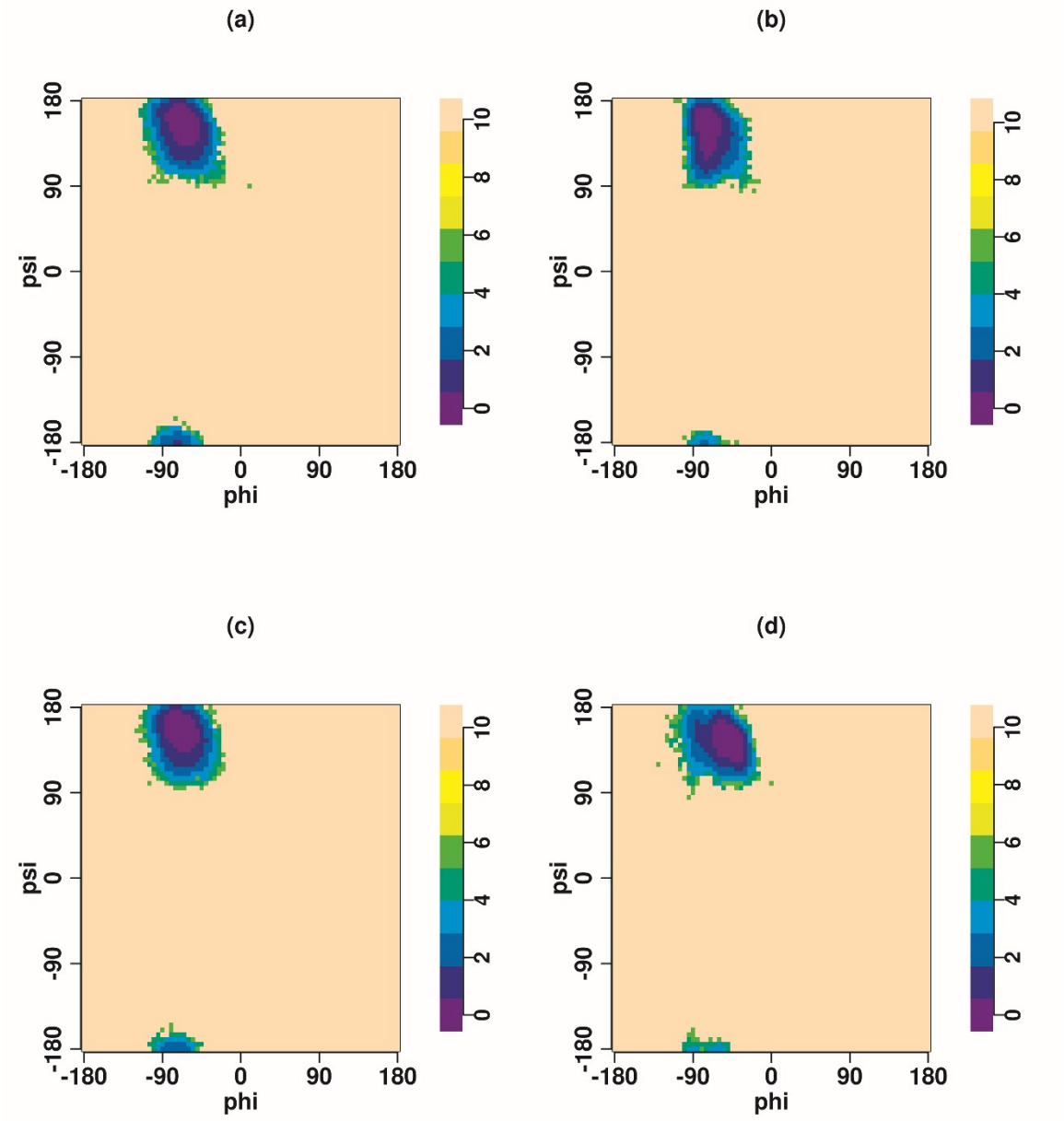

Figure S32. Free energy landscape (in kcal/mole) in ϕ, Ψ dihedral space for proline at position 14 for the second replicate. (a) AMBER ff99SB*ILDNP; (b) OPLS-AA; (c) AMBER ff03ws; and (d) CHARMM36m.

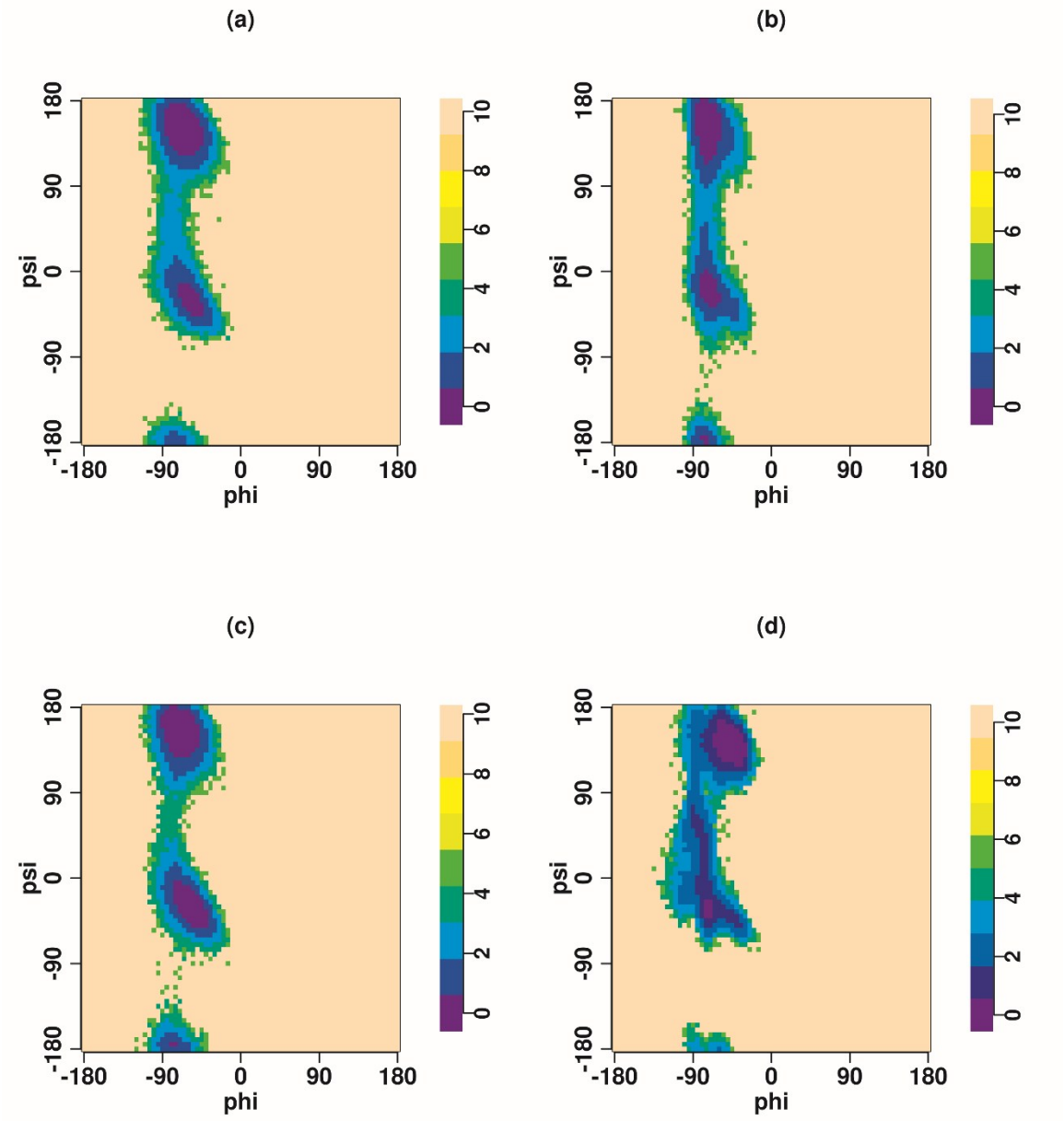

Figure S33. Free energy landscape (in kcal/mole) in ϕ, Ψ dihedral space for proline at position 15 for the second replicate. (a) AMBER ff99SB*-ILDNP; (b) OPLS-AA; (c) AMBER ff03ws; and (d) CHARMM36m.

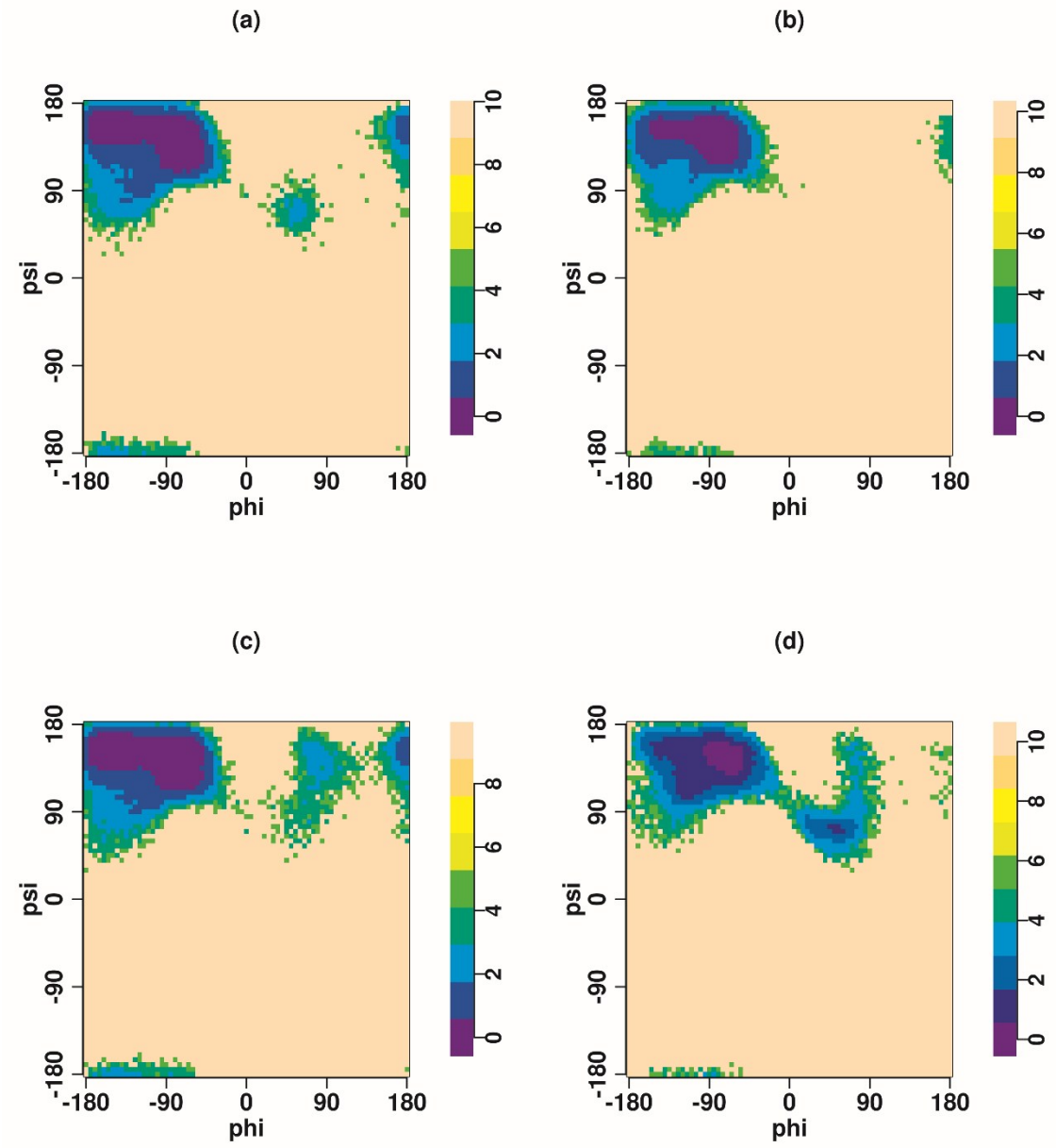

Figure S34. Free energy landscape (in kcal/mole) in ϕ, ψ dihedral space for glutamine at position 9 for the third replicate. (a) AMBER ff99SB*-ILDNP; (b) OPLS-AA; (c) AMBER ff03ws; and (d) CHARMM36m.

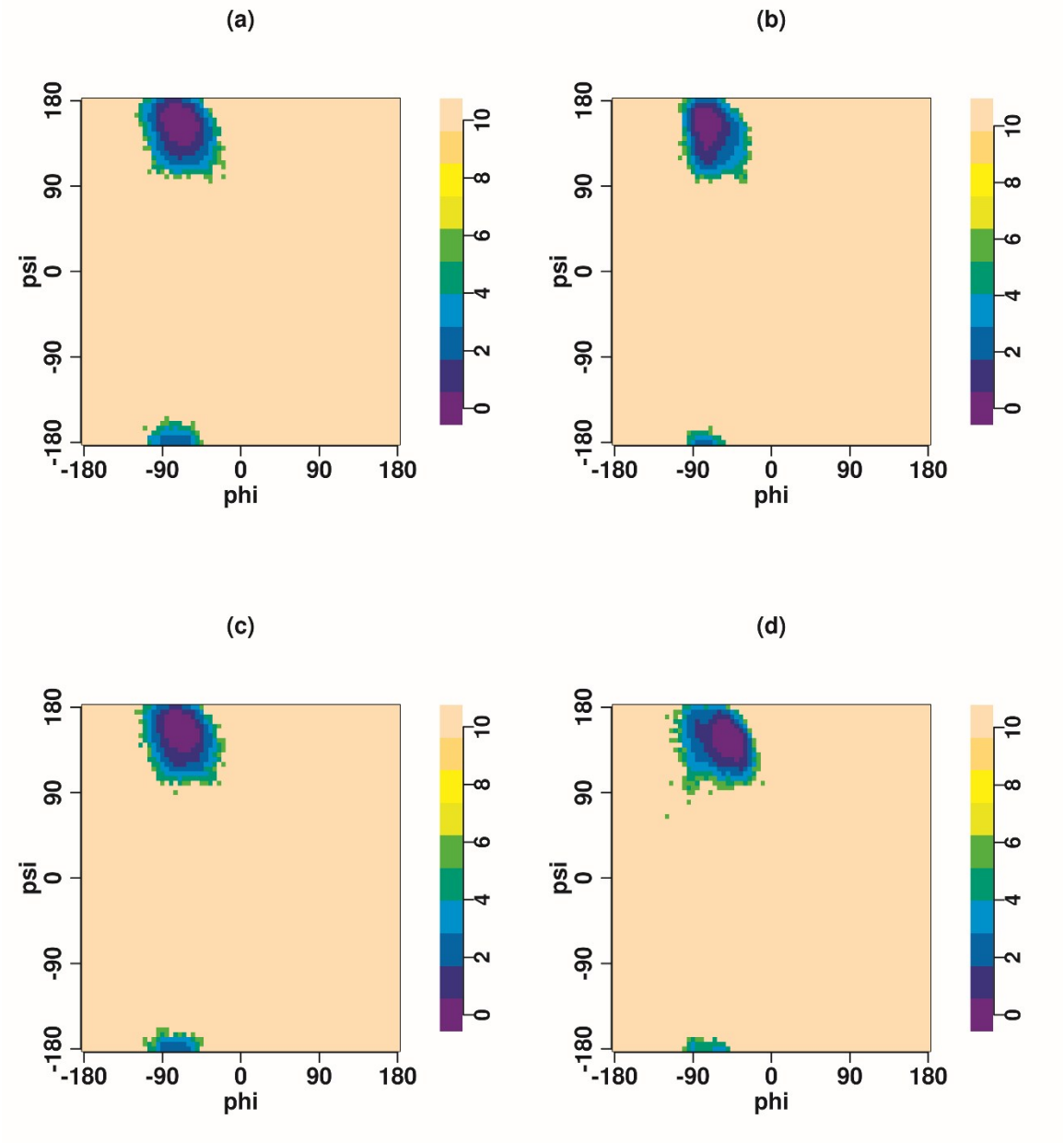

Figure S35. Free energy landscape (in kcal/mole) in ϕ, Ψ dihedral space for proline at position 10 for the third replicate. (a) AMBER ff99SB*-ILDNP; (b) OPLS-AA; (c) AMBER ff03ws; and (d) CHARMM36m.

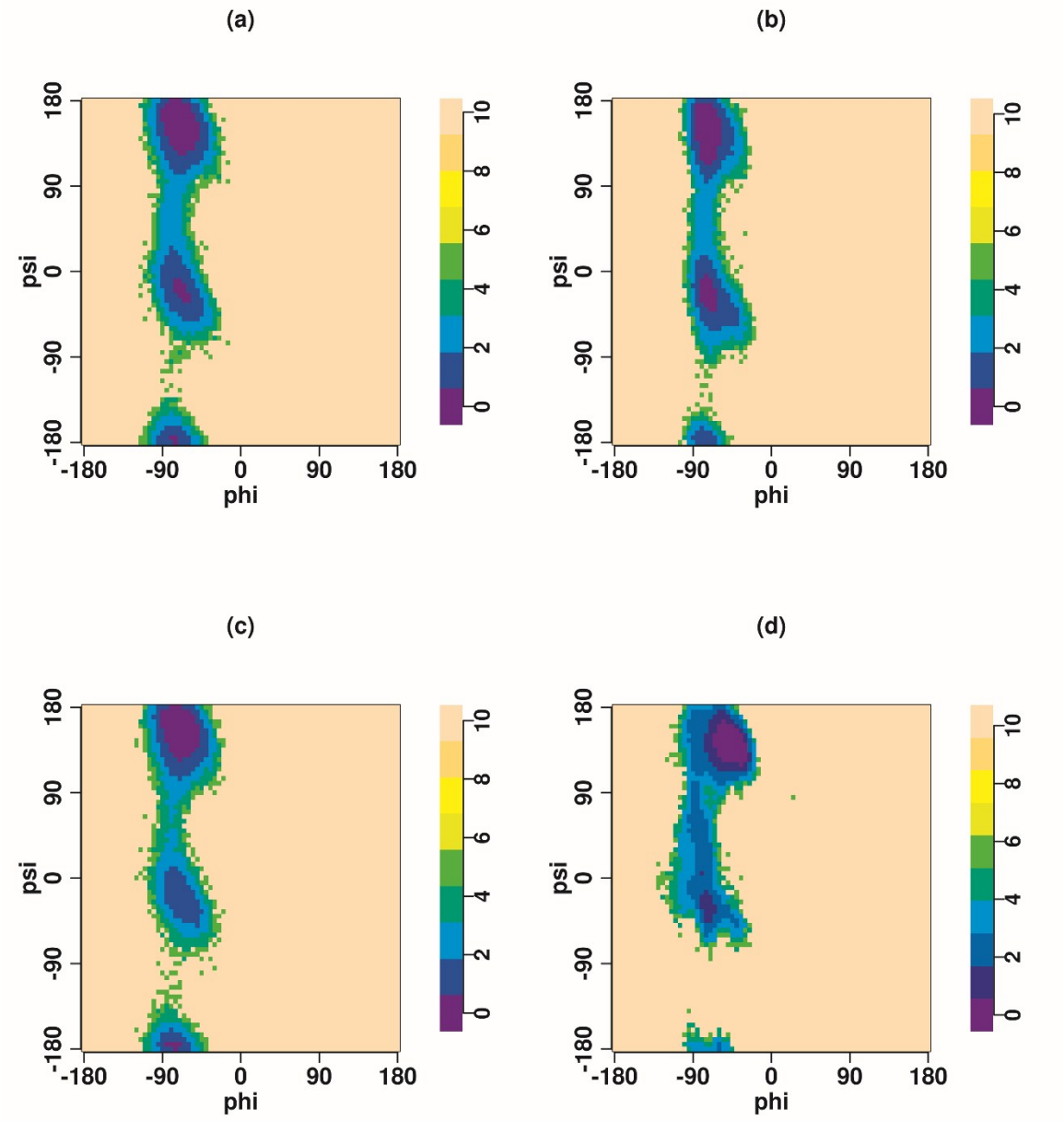

Figure S36. Free energy landscape (in kcal/mole) in ϕ, Ψ dihedral space for proline at position 11 for the third replicate. (a) AMBER ff99SB*-ILDNP; (b) OPLS-AA; (c) AMBER ff03ws; and (d) CHARMM36m.

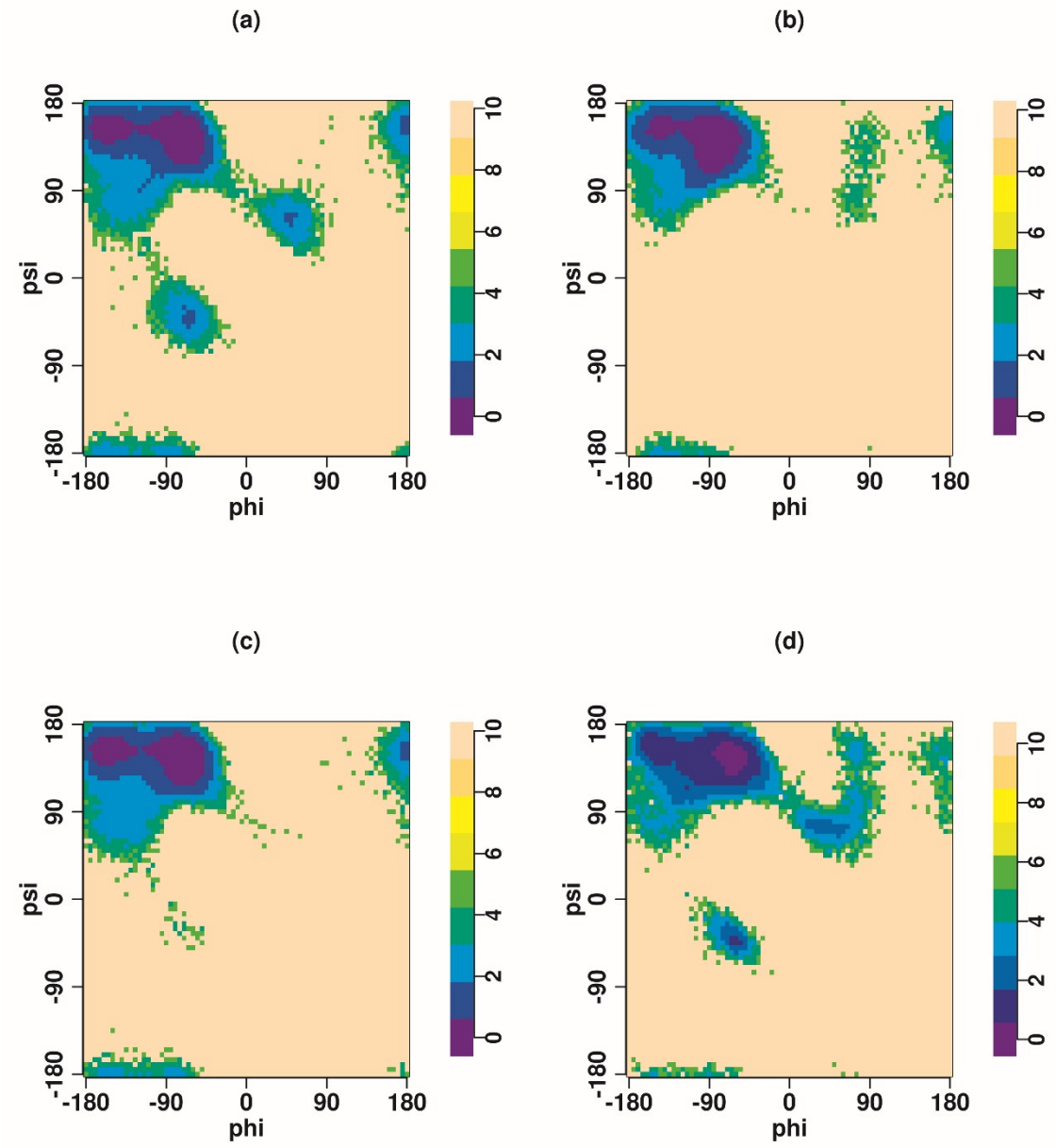

Figure S37. Free energy landscape (in kcal/mole) in ϕ, ψ dihedral space for alanine at position 12 for the third replicate. (a) AMBER ff99SB*-ILDNP; (b) OPLS-AA; (c) AMBER ff03ws; and (d) CHARMM36m.

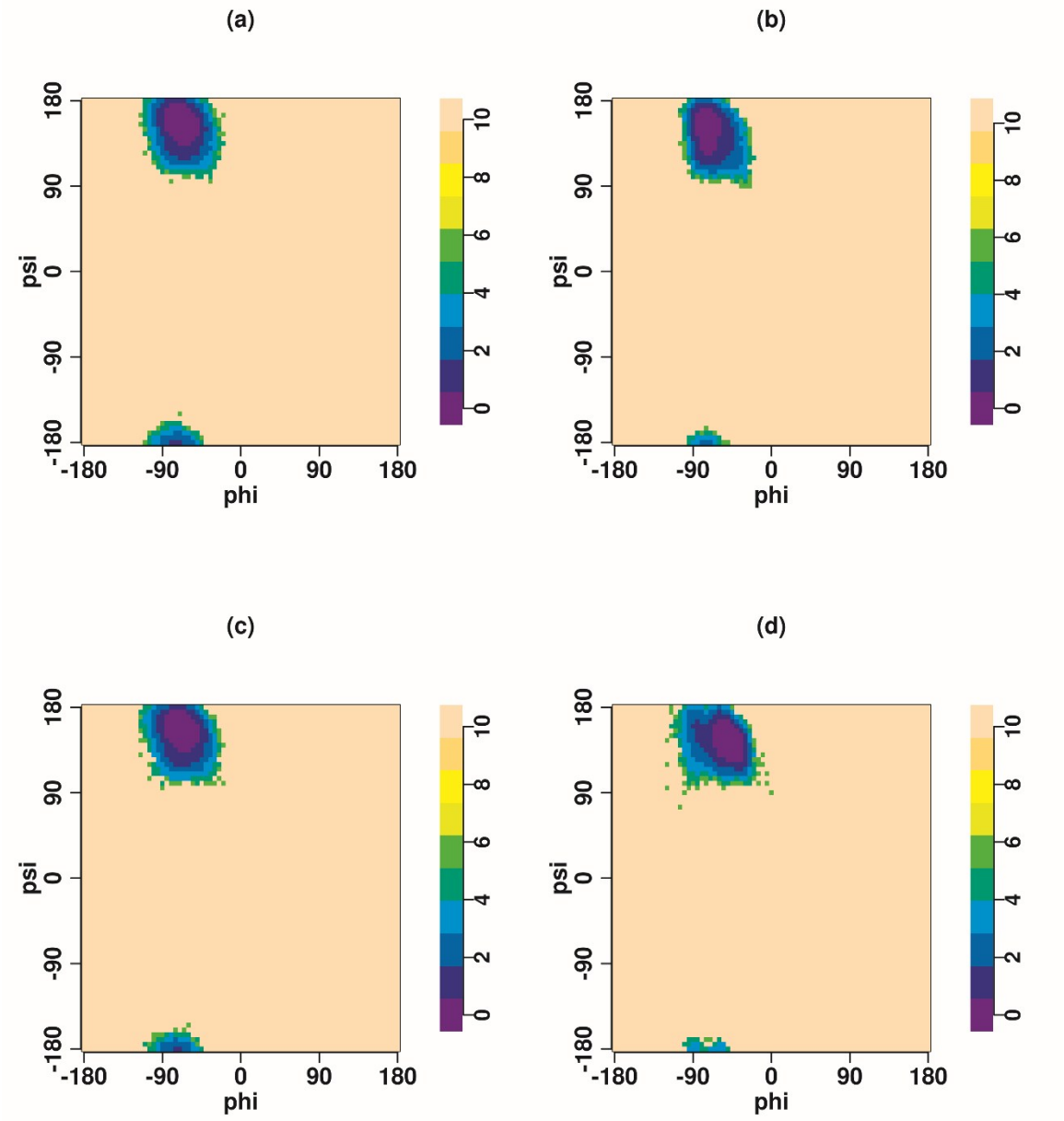

Figure S38. Free energy landscape (in kcal/mole) in ϕ, Ψ dihedral space for proline at position 13 for the third replicate. (a) AMBER ff99SB*-ILDNP; (b) OPLS-AA; (c) AMBER ff03ws; and (d) CHARMM36m.

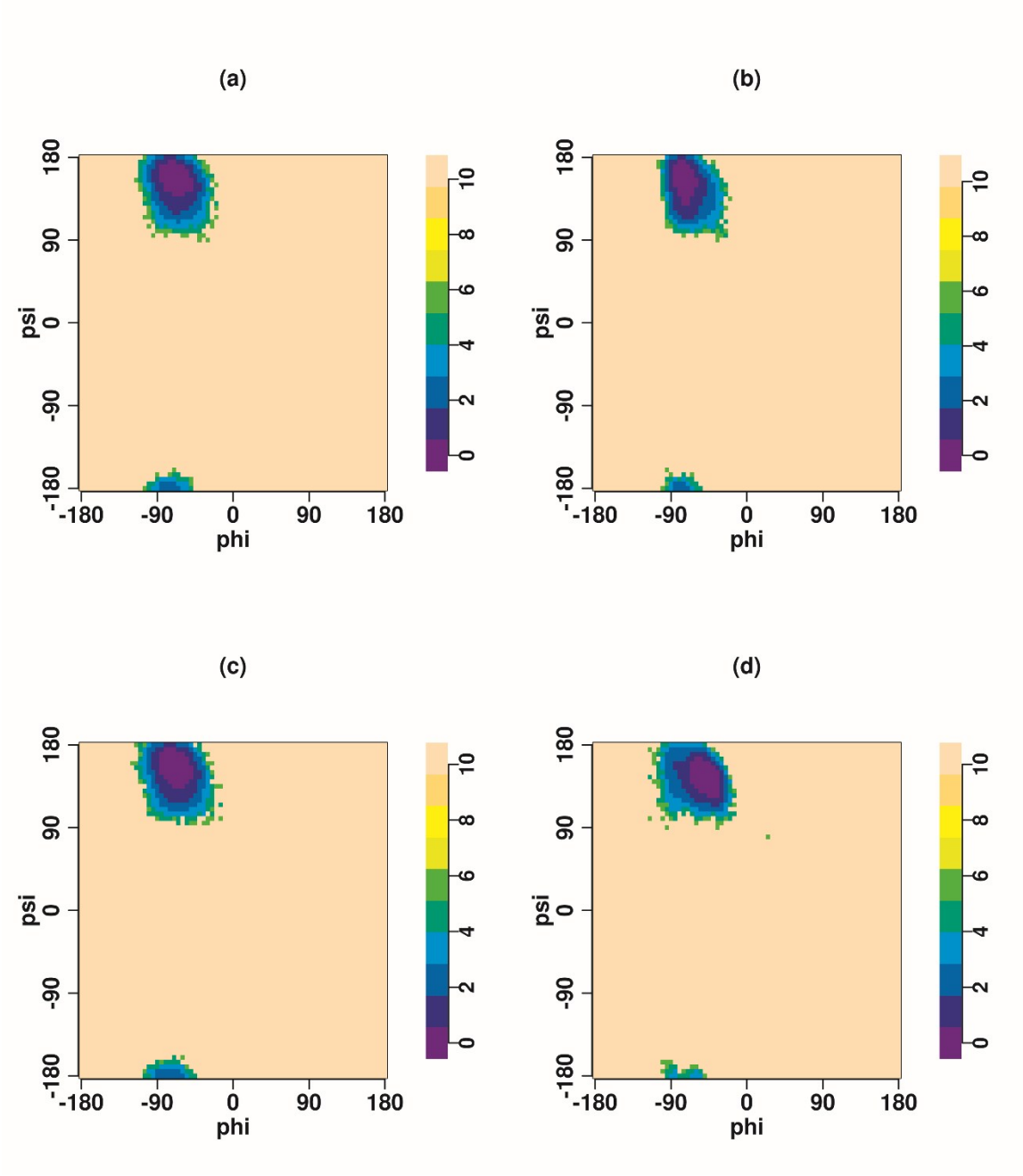

Figure S39. Free energy landscape (in kcal/mole) in ϕ, ψ dihedral space for proline at position 14 for the third replicate. (a) AMBER ff99SB*-ILDNP; (b) OPLS-AA; (c) AMBER ff03ws; and (d) CHARMM36m.

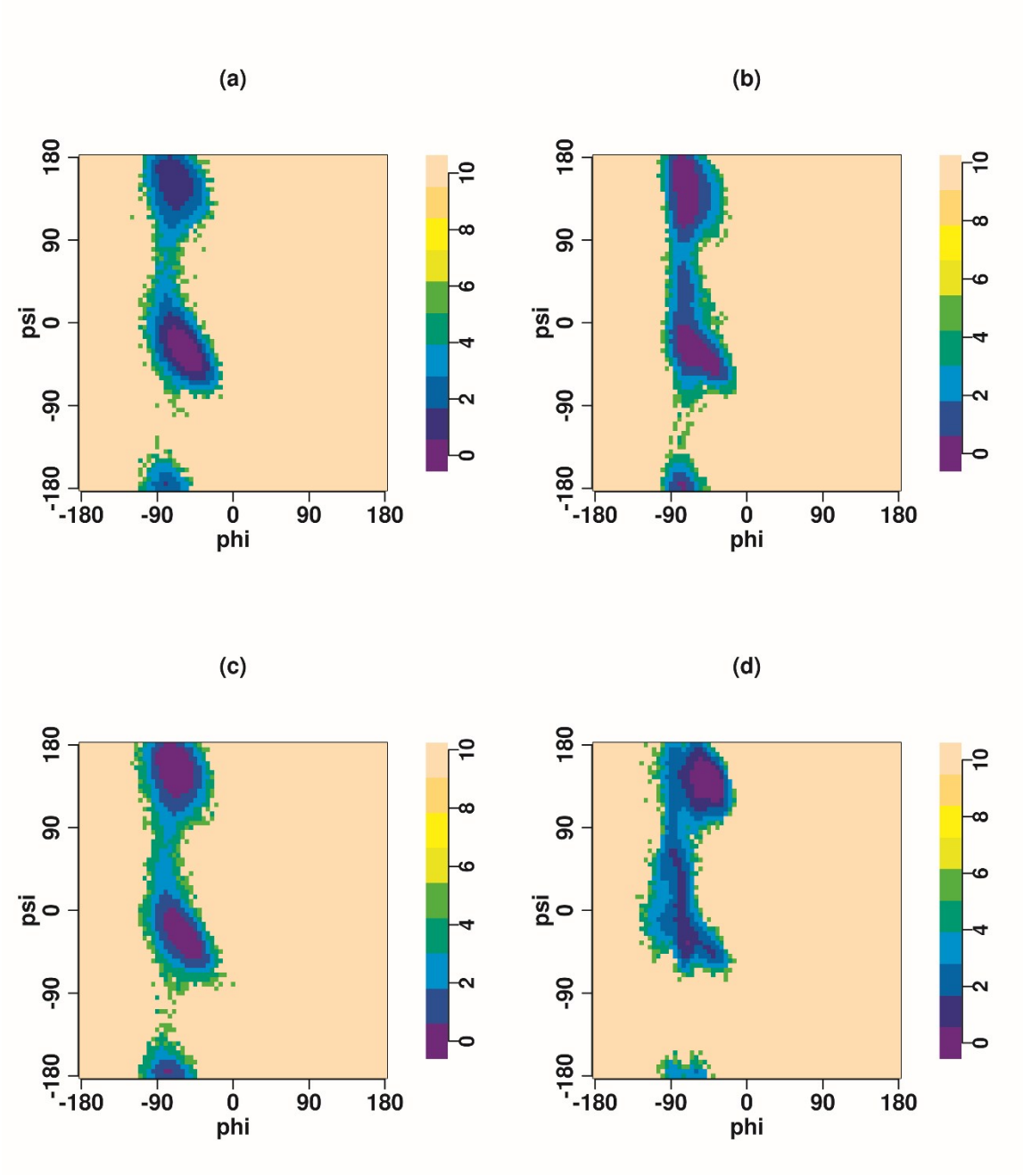

Figure S40. Free energy landscape (in kcal/mole) in ϕ, ψ dihedral space for proline at position 15 for the third replicate. (a) AMBER ff99SB*-ILDNP; (b) OPLS-AA; (c) AMBER ff03ws; and (d) CHARMM36m.

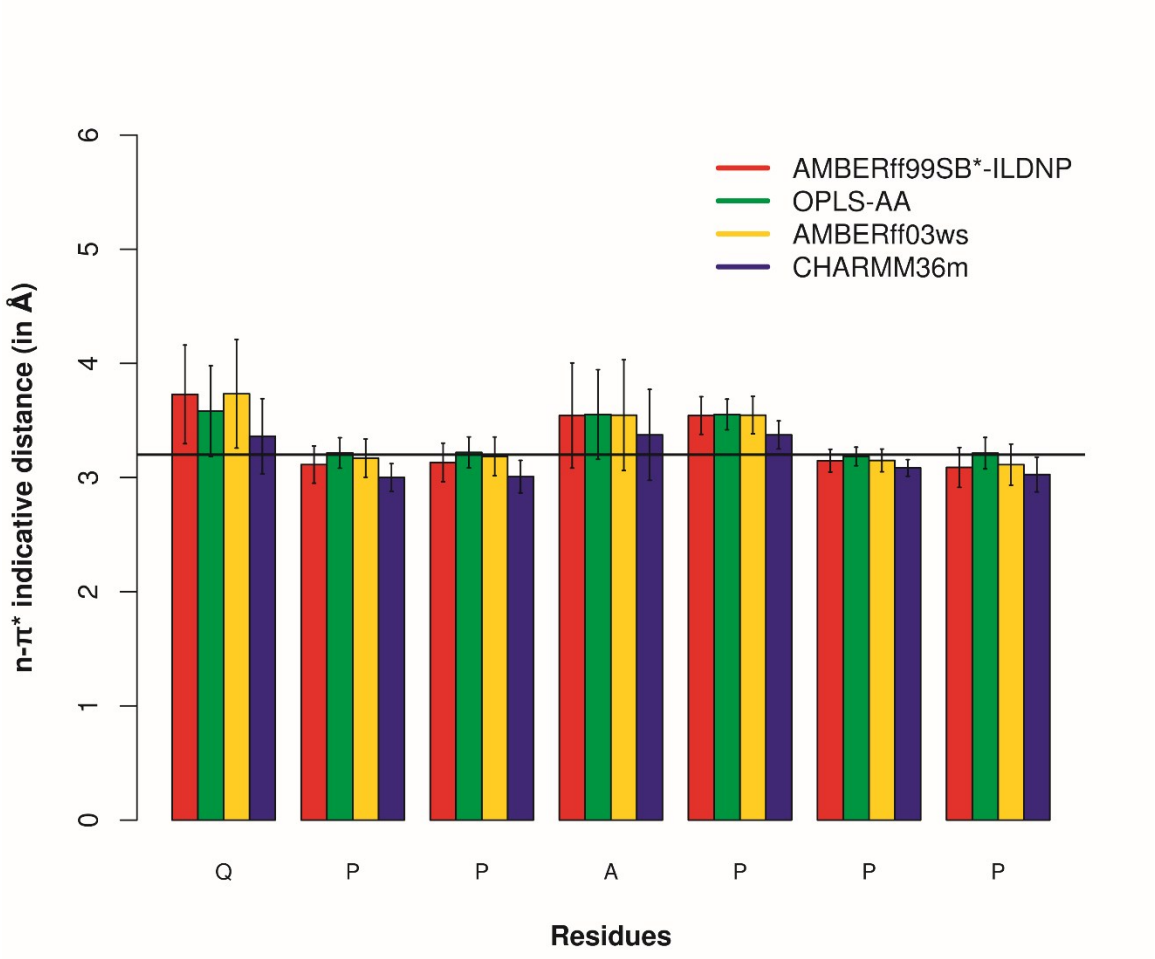

Figure S41. The residue-wise bar plot of the n-π* indicative distance (in Å) for the Q9-P15 region of the p15 FAST peptide for the second replicate corresponding to the force fields AMBER ff99SB*-ILDNP, OPLS-AA, AMBER ff03ws and CHARMM36m. The black line indicates the criterion that distance < 3.22 Å for n-π* interaction.

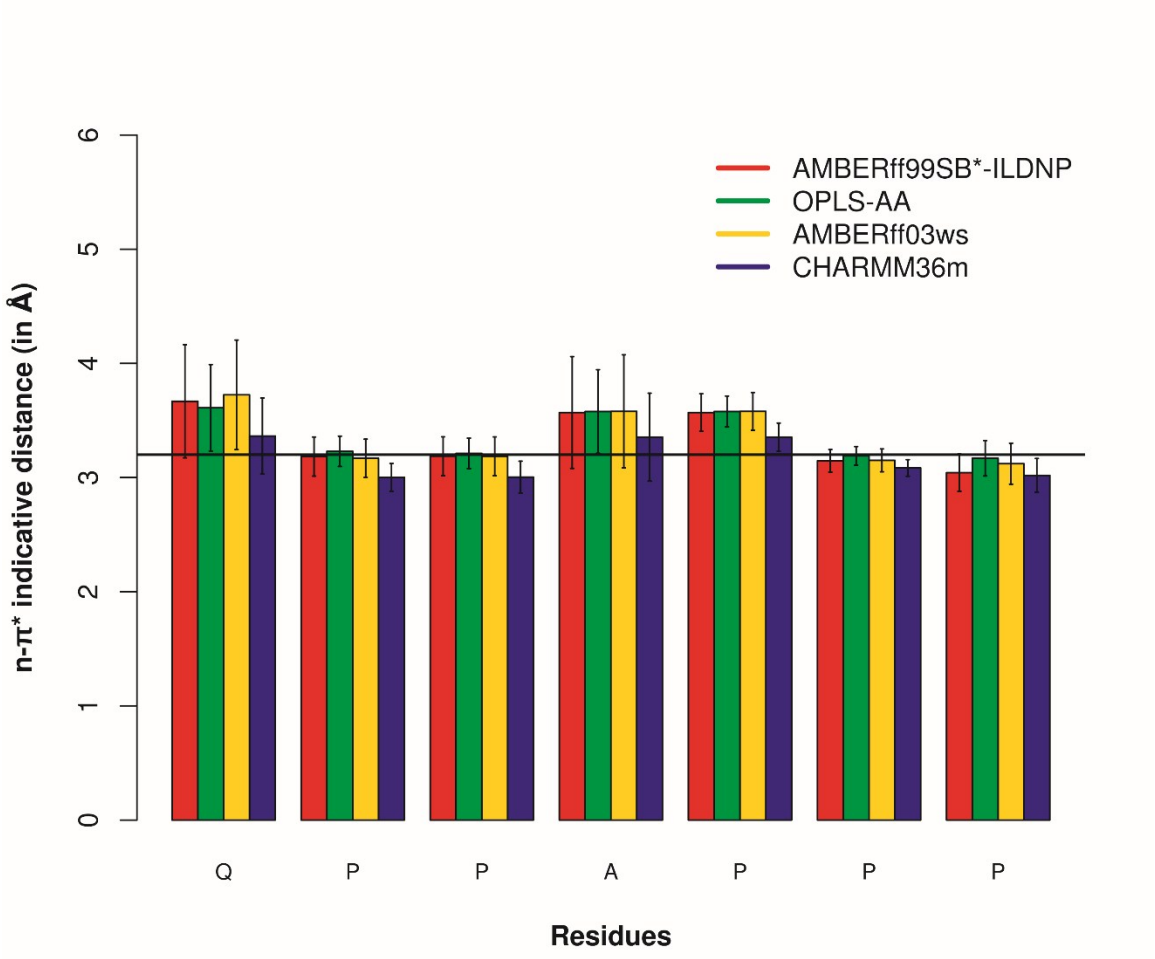

Figure S42. The residue-wise bar plot of the n-π* indicative distance (in Å) for the Q9-P15 region of the p15 FAST peptide for the third replicate corresponding to the force fields AMBER ff99SB*-ILDNP, OPLS-AA, AMBER ff03ws and CHARMM36m. The black line indicates the criterion that distance < 3.22 Å for n-π* interaction.

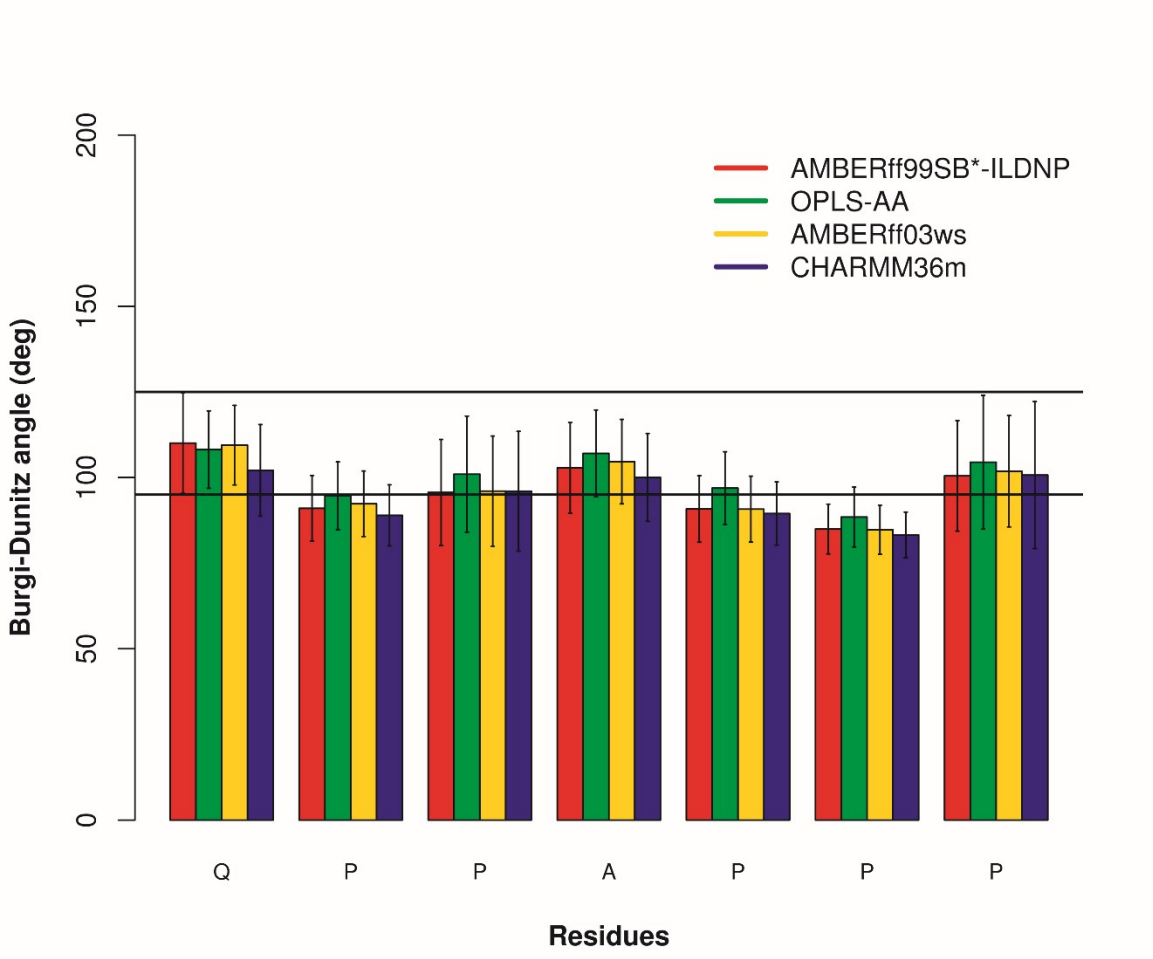

Figure S43. The residue-wise bar plot of the Bùrgi-Dunitz angle (in degrees) for the Q9-P15 region of the p15 FAST peptide for the second replicate corresponding to the force fields AMBER ff99SB*-ILDNP, OPLS-AA, AMBER ff03ws and CHARMM36m. The range of values of Bùrgi-Dunitz angle for n-π* interaction (95° < θ < 125°) is indicated by the lower (95°) and the upper (125°) black lines.

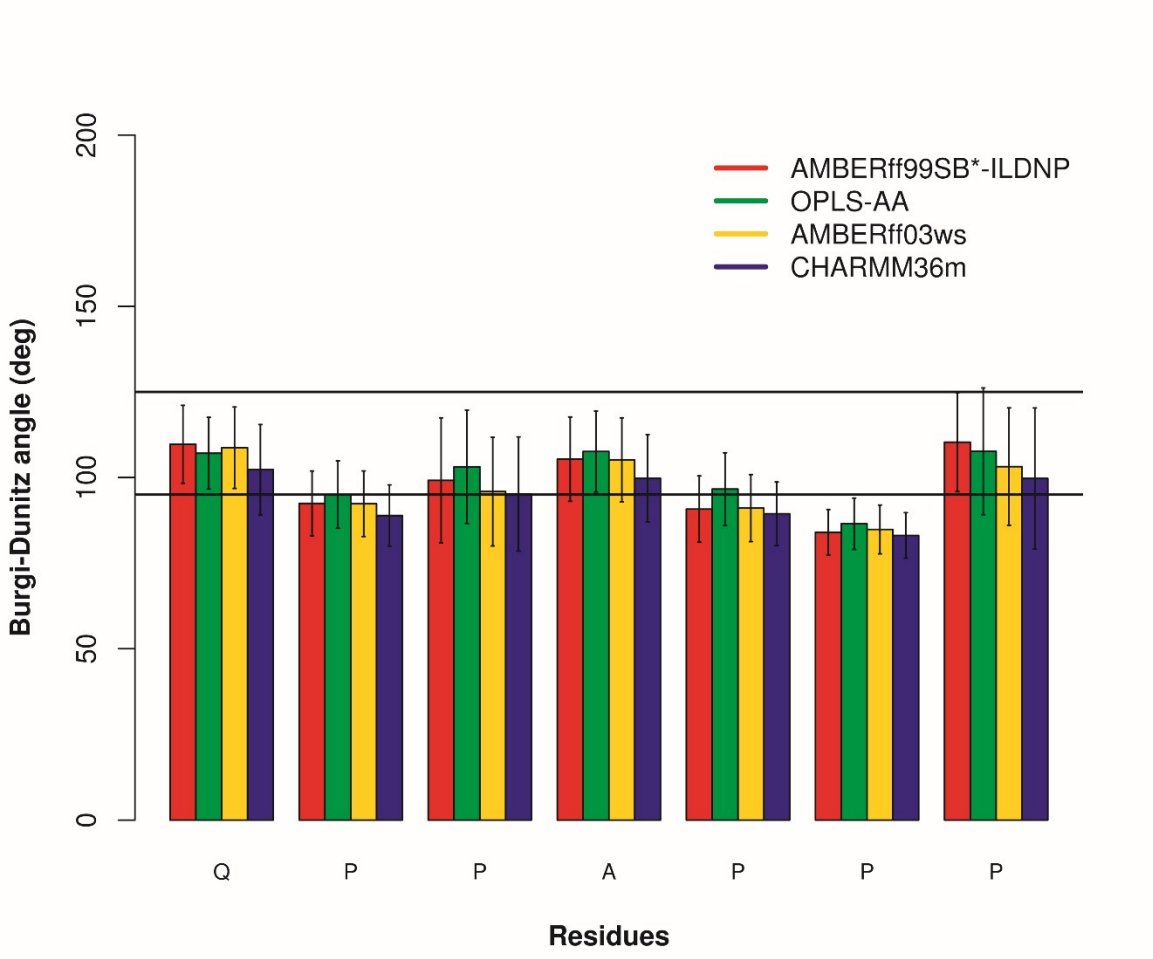

Figure S44. The residue-wise bar plot of the Bùrgi-Dunitz angle (in degrees) for the Q9-P15 region of the p15 FAST peptide for the third replicate corresponding to the force fields AMBER ff99SB*-ILDNP, OPLS-AA, AMBER ff03ws and CHARMM36m. The range of values of Bùrgi-Dunitz angle for n-π* interaction (95° < θ < 125°) is indicated by the lower (95°) and the upper (125°) black lines.

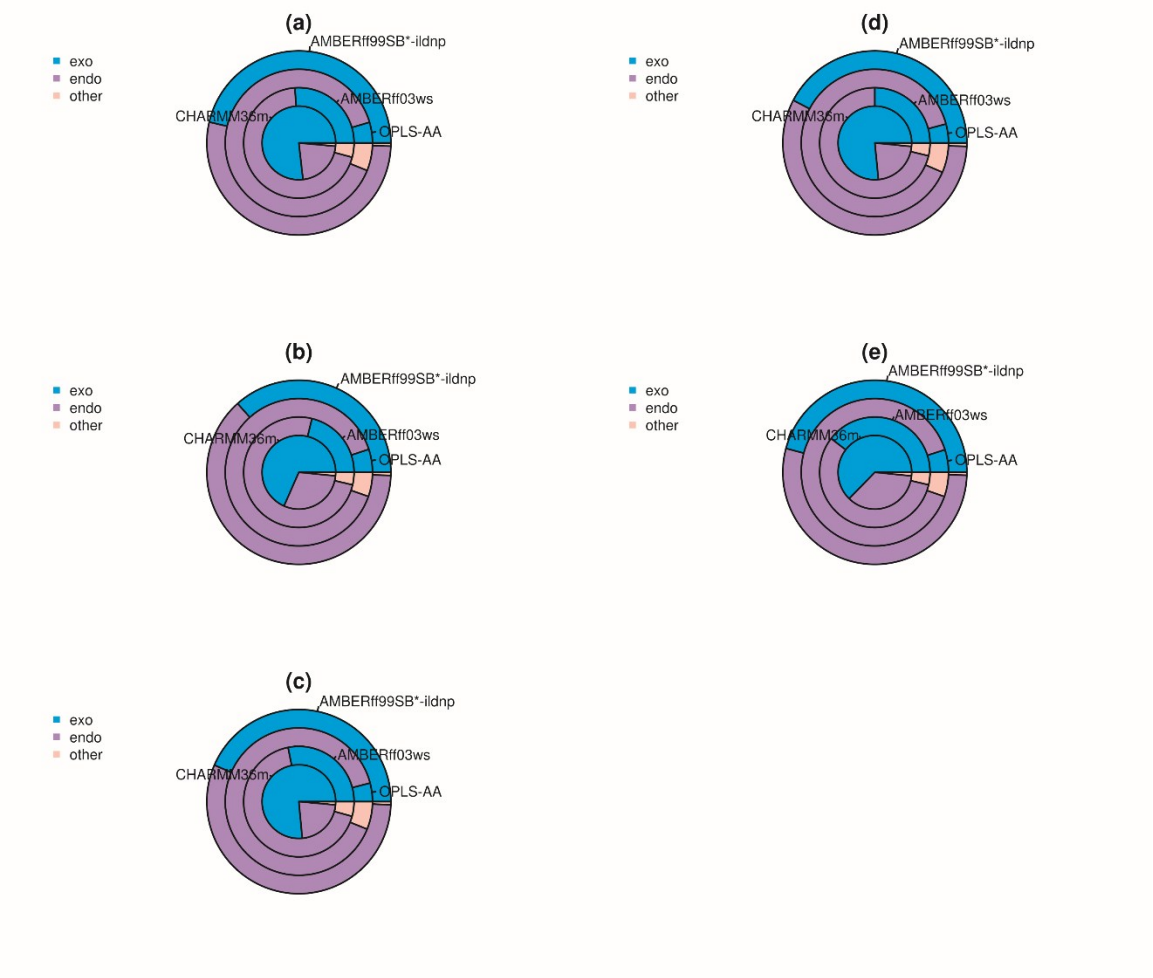

Figure S45. Pie-chart of the exo and endo pucker of the proline residues at positions (a) 10, (b) 11, (c) 13, (d) 14 and (e) 15 for the second replicate corresponding to the force fields AMBER ff99SB*-ILDNP; OPLS-AA; AMBER ff03ws; CHARMM36m (indicated by arrows).

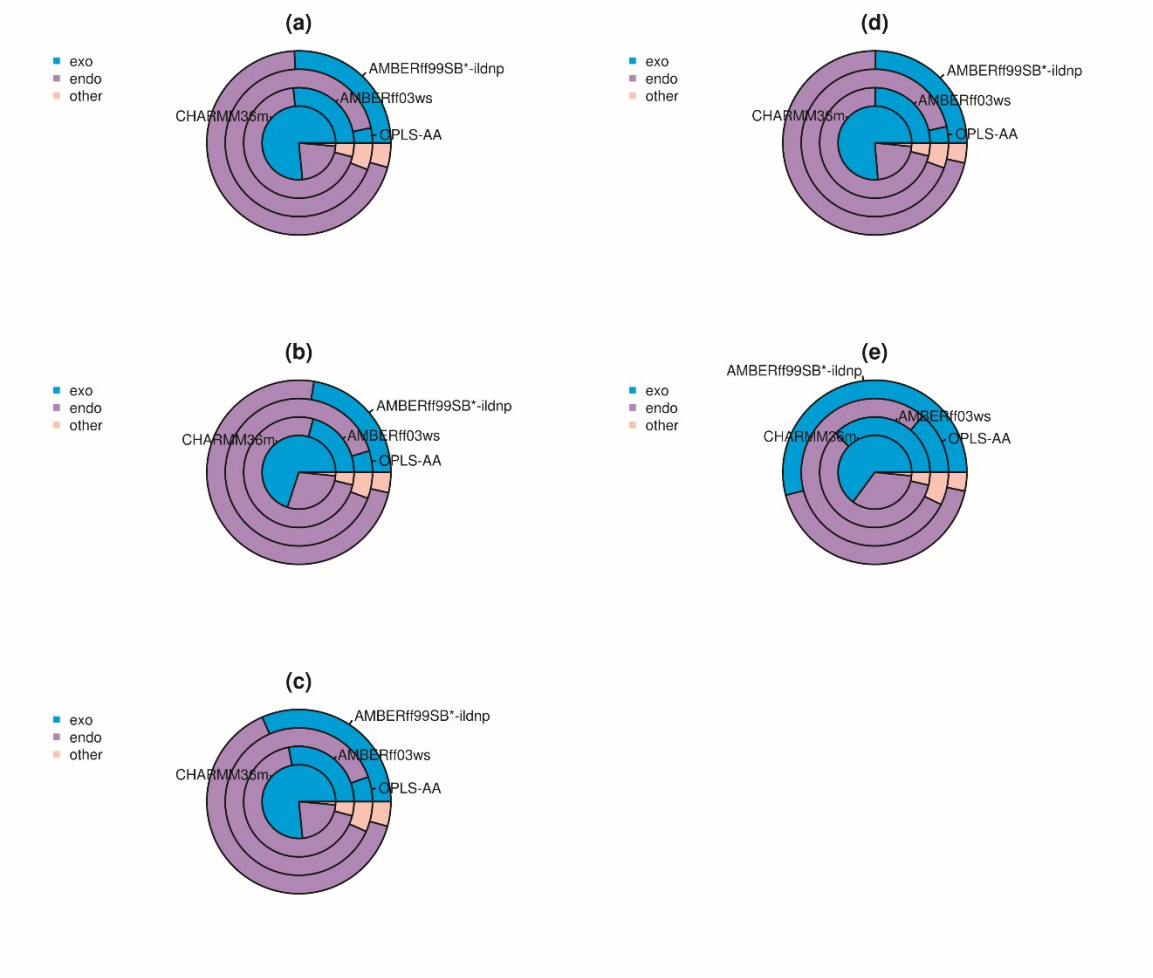

Figure S46. Pie-chart of the exo and endo pucker of the proline residues at positions (a) 10, (b) 11, (c) 13, (d) 14 and (e) 15 for the third replicate corresponding to the force fields AMBER ff99SB*-ILDNP; OPLS-AA; AMBER ff03ws; CHARMM36m (indicated by arrows).

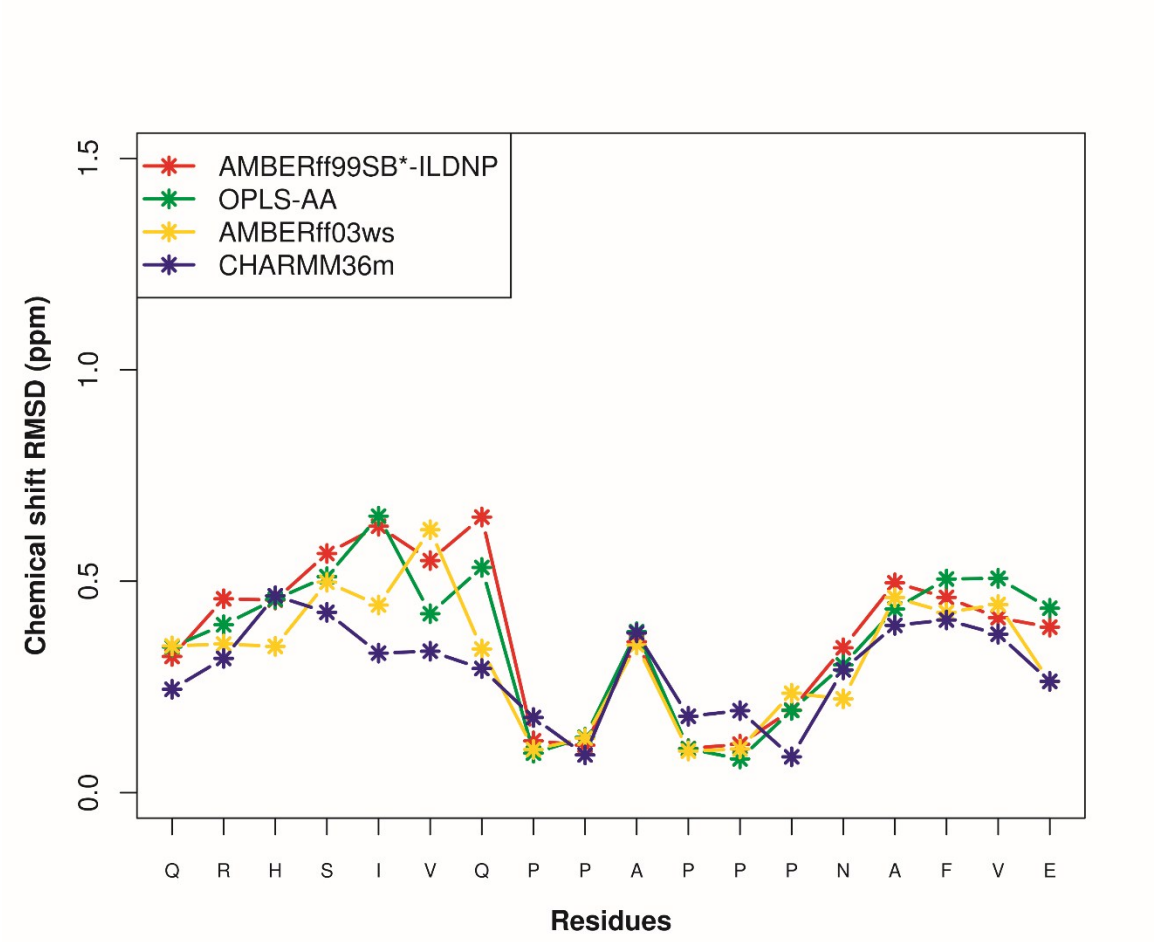

Figure S47. Residue-wise plot of the chemical shift RMSDs (in ppm) of residues Q3 to E20, calculated by SPARTA+ for the second replicate corresponding to the four different force-fields AMBER ff99SB*-ILDNP, OPLS-AA, AMBER ff03ws and CHARMM36m.

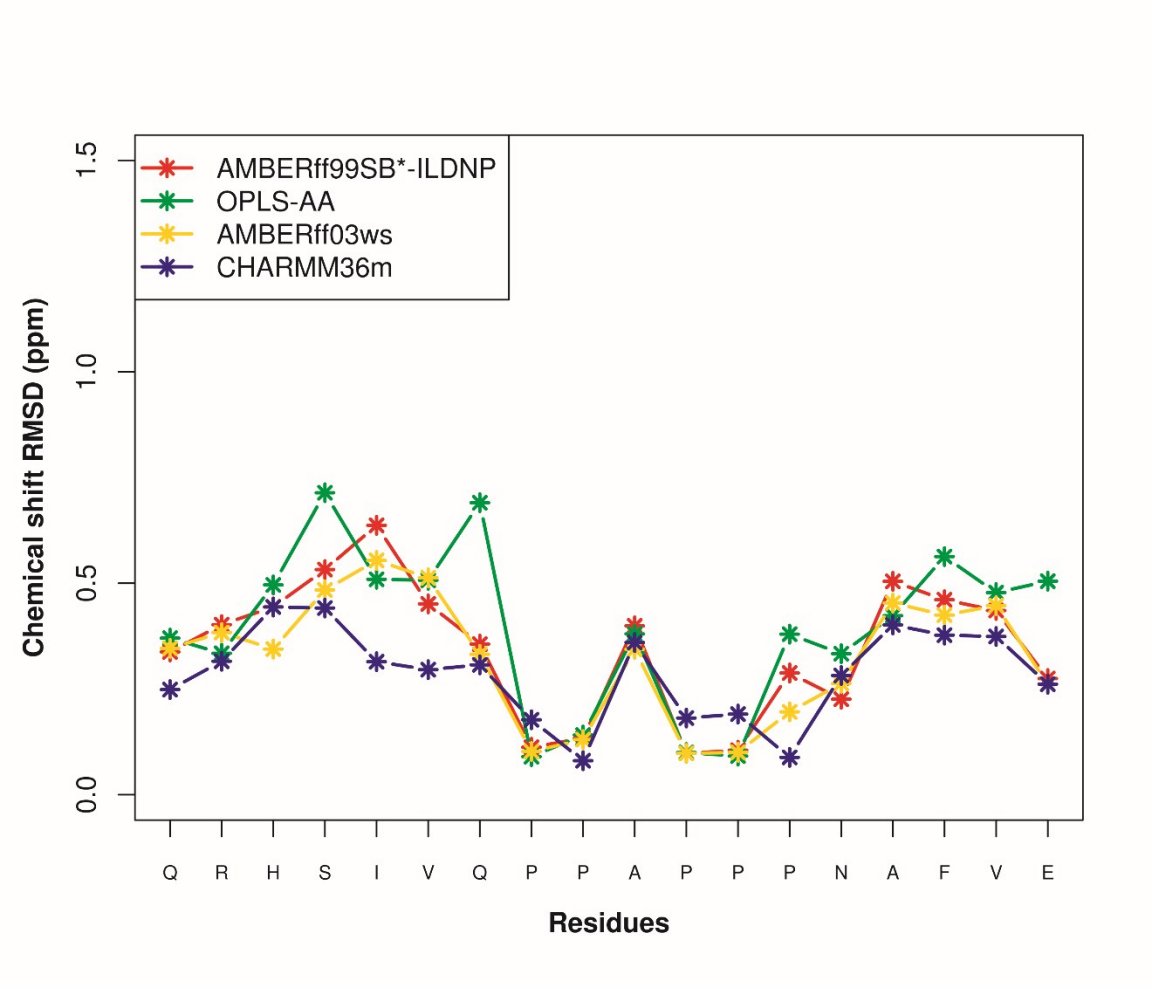

Figure S48. Residue-wise plot of the chemical shift RMSDs (in ppm) of residues Q3 to E20, calculated by SPARTA+ for the third replicate corresponding to the four different force-fields AMBER ff99SB*-ILDNP, OPLS-AA, AMBER ff03ws and CHARMM36m.

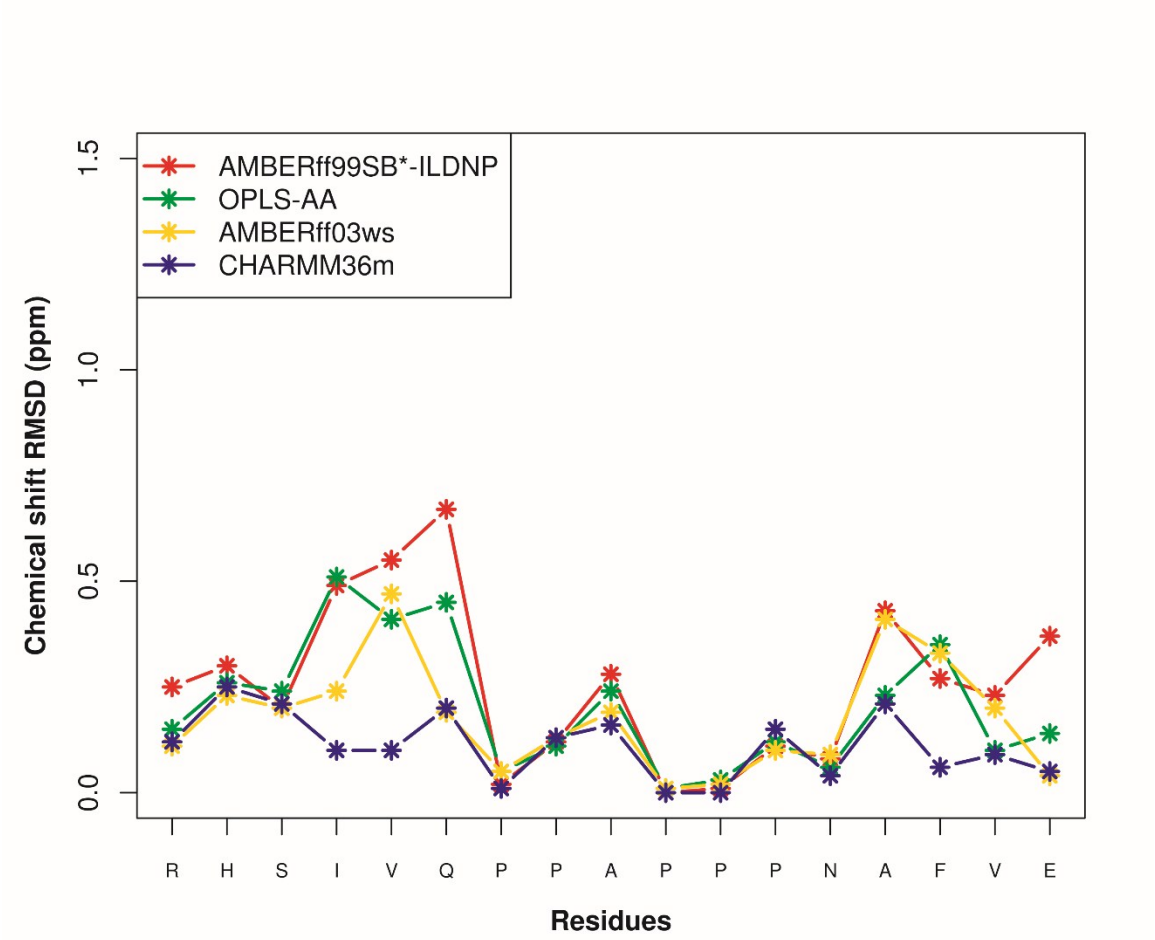

Figure S49. Residue-wise plot of the chemical shift RMSDs (in ppm) of residues R4 to E20, calculated by PPM for the second replicate corresponding to the four different force-fields AMBER ff99SB*-ILDNP, OPLS-AA, AMBER ff03ws and CHARMM36m.

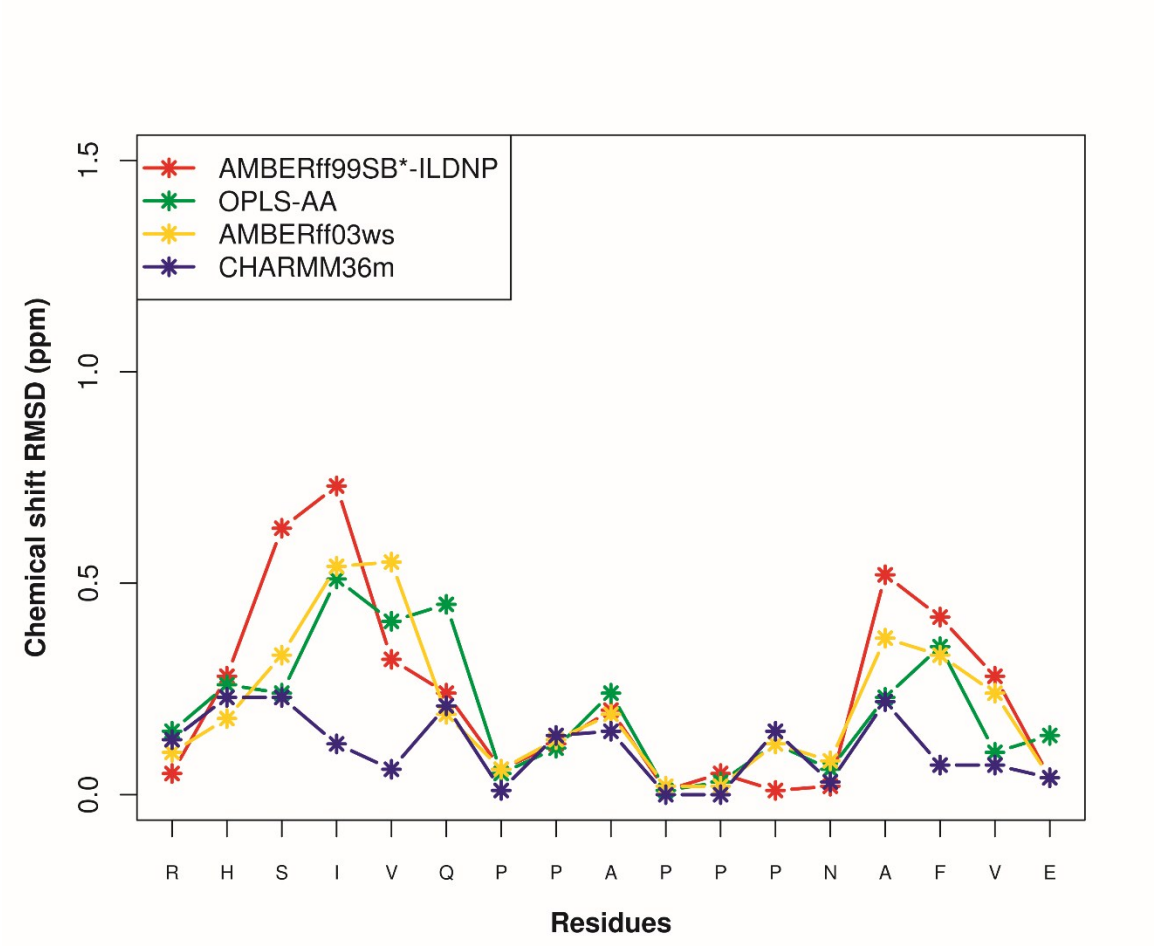

Figure S50. Residue-wise plot of the chemical shift RMSDs (in ppm) of residues R4 to E20, calculated by PPM for the third replicate corresponding to the four different force-fields AMBER ff99SB*-ILDNP, OPLS-AA, AMBER ff03ws and CHARMM36m.

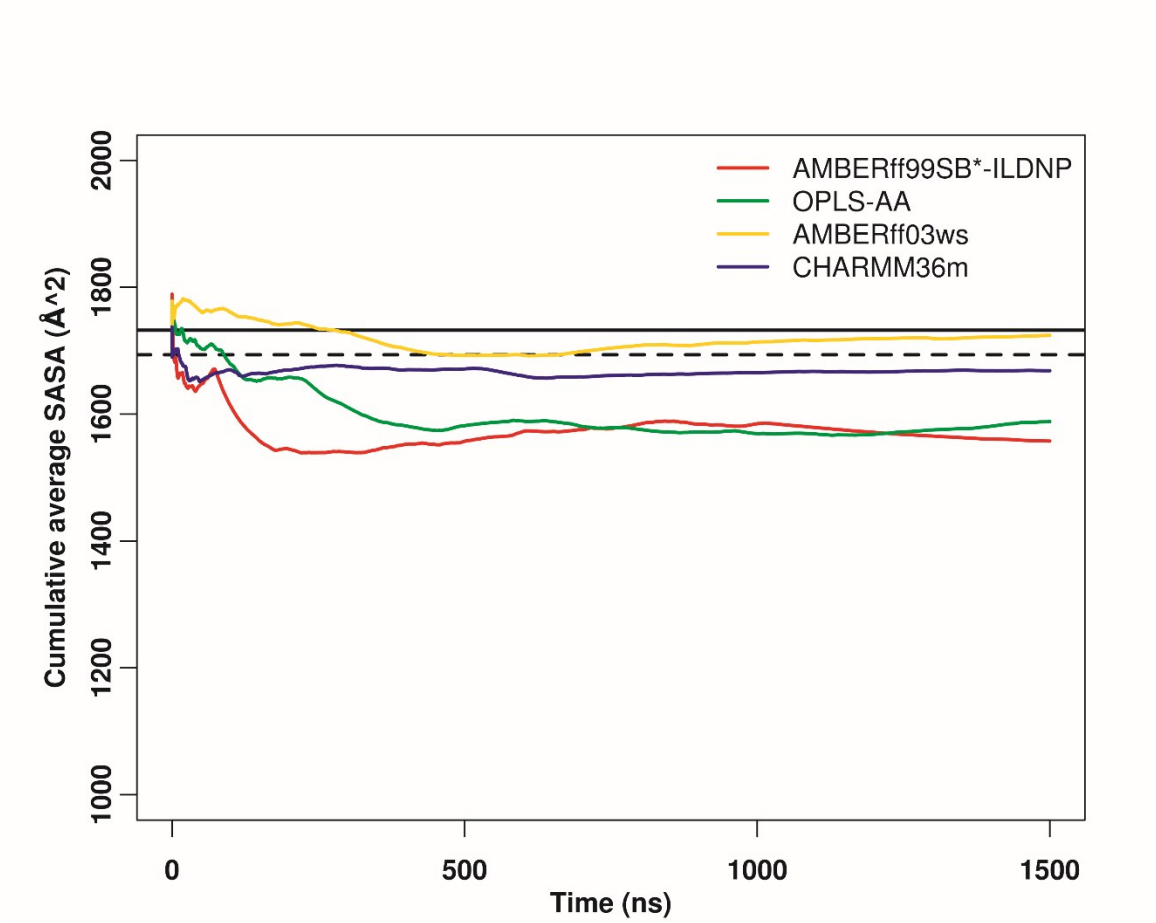

Figure S51. Time evolution of the cumulative average of the solvent accessible surface area (SASA) (in $Å^2$) of the main chain atoms of the p15 FAST peptide for the first replicate corresponding to the force fields AMBER ff99SB*-ILDNP; OPLS-AA; AMBER ff03ws; CHARMM36m. The solid black line indicates the SASA of the main chain atoms of the initial conformation (model 1 reported in the NMR experiment[1]) and the dashed black line indicates the experimental SASA of the main chain atoms of the experimental structure (average SASA of the 10 conformers reported in the NMR experiment[1]).

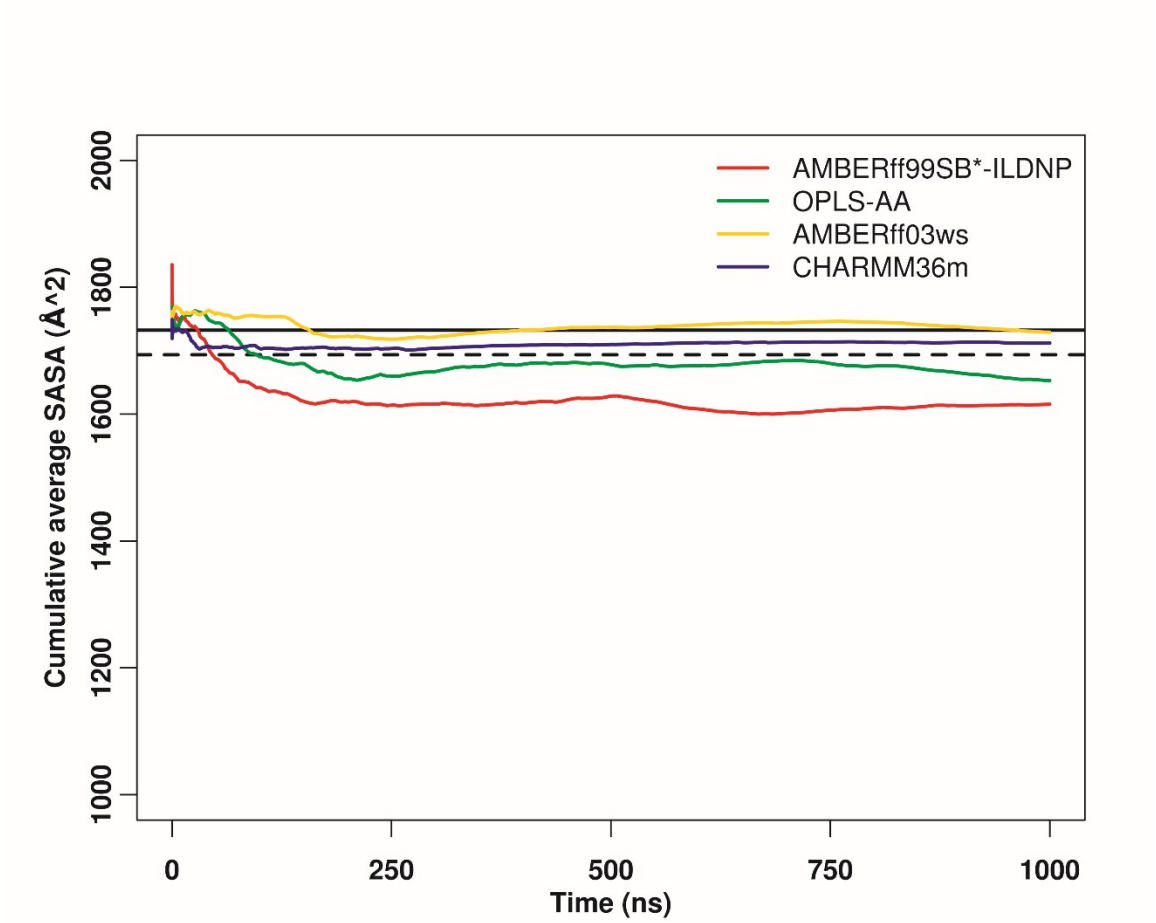

Figure S52. Time evolution of the cumulative average of the solvent accessible surface area (SASA) (in $Å^2$) of the main chain atoms of the p15 FAST peptide for the second replicate corresponding to the force fields AMBER ff99SB*-ILDNP; OPLS-AA; AMBER ff03ws; CHARMM36m. The solid black line indicates the SASA of the main chain atoms of the initial conformation (model 1 reported in the NMR experiment[1]) and the dashed black line indicates the experimental SASA of the main chain atoms of the experimental structure (average SASA of the 10 conformers reported in the NMR experiment[1]).

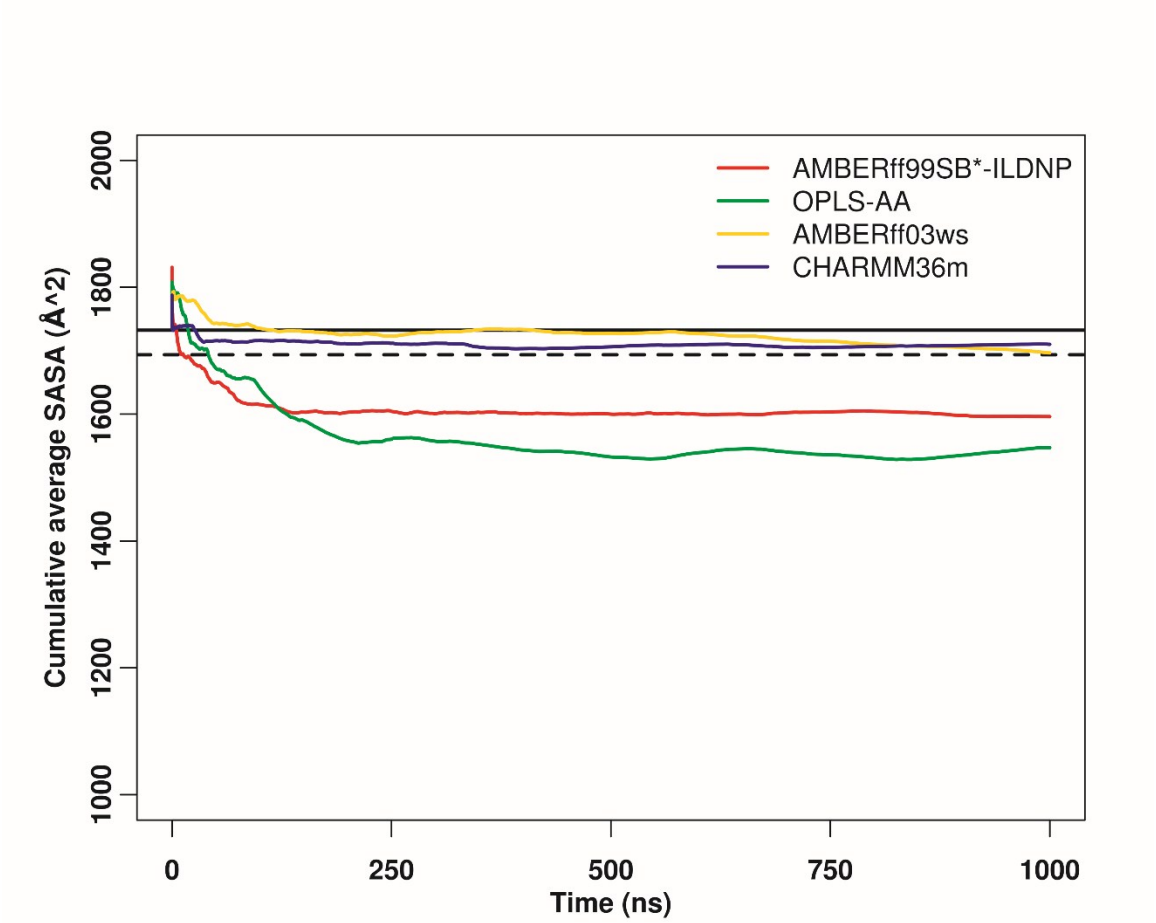

Figure S53. Time evolution of the cumulative average of the solvent accessible surface area (SASA) (in $Å^2$) of the main chain atoms (N, CA, C, O) of the p15 FAST peptide for the third replicate corresponding to the force fields AMBER ff99SB*-ILDNP; OPLS-AA; AMBER ff03ws; CHARMM36m. The solid black line indicates the SASA of the main chain atoms of the initial conformation (model 1 reported in the NMR experiment[1]) and the dashed black line indicates the SASA of the main chain atoms of the experimental structure (average SASA of the 10 conformers reported in the NMR experiment[1]).

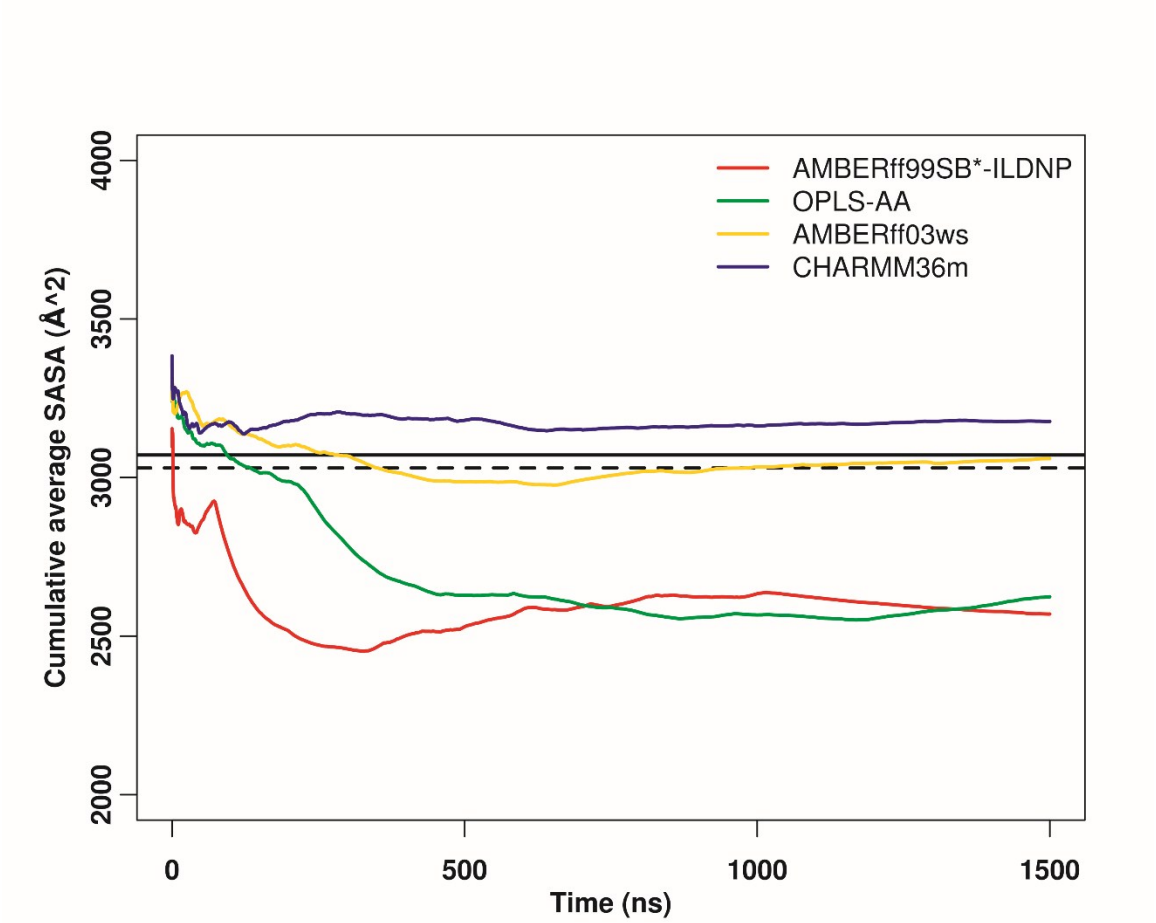

Figure S54. Time evolution of the cumulative average of the solvent accessible surface area (SASA) (in $Å^2$) of the side chain atoms of the p15 FAST peptide for the first replicate corresponding to the force fields AMBER ff99SB*-ILDNP; OPLS-AA; AMBER ff03ws; CHARMM36m. The solid black line indicates the SASA of the side chain atoms of the initial conformation (model 1 reported in the NMR experiment[1]) and the dashed black line indicates the experimental SASA of the side chain atoms of the experimental structure (average SASA of the 10 conformers reported in the NMR experiment[1]).

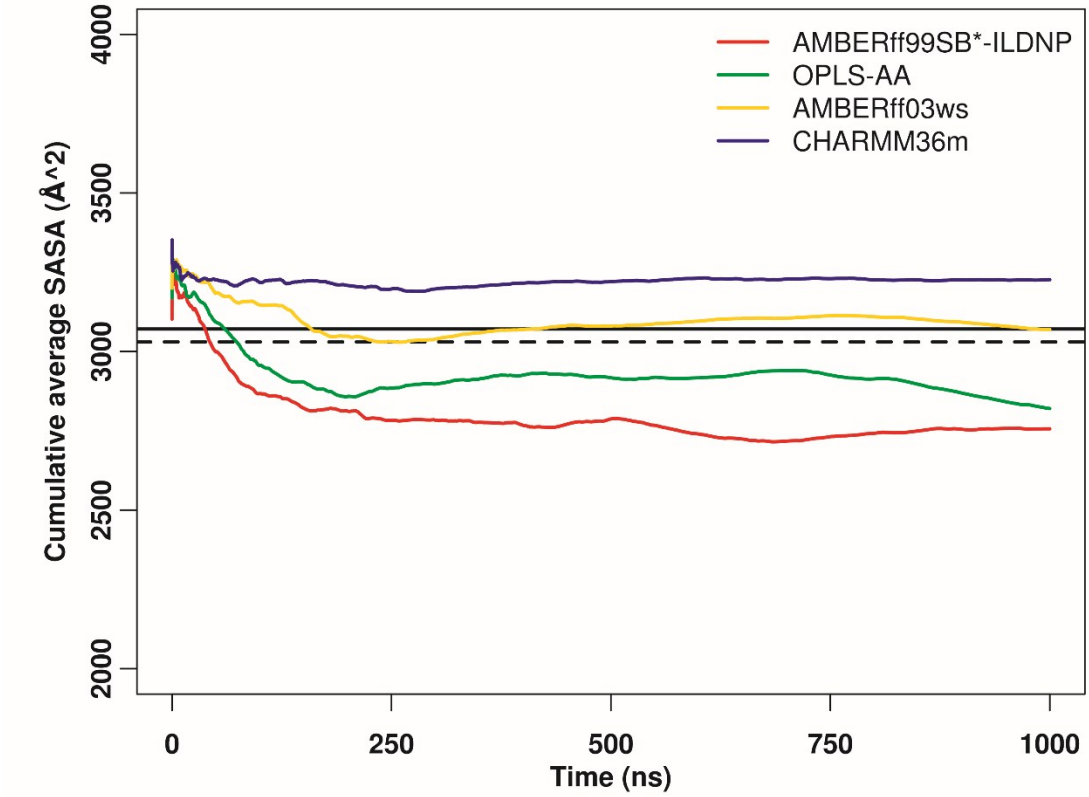

Figure

Figure S55. Time evolution of the cumulative average of the solvent accessible surface area (SASA) (in $Å^2$) of the side chain atoms of the p15 FAST peptide for the second replicate corresponding to the force fields AMBER ff99SB*-ILDNP; OPLS-AA; AMBER ff03ws; CHARMM36m. The solid black line indicates the SASA of the side chain atoms of the initial conformation (model 1 reported in the NMR experiment[1]) and the dashed black line indicates the experimental SASA of the side chain atoms of the experimental structure (average SASA of the 10 conformers reported in the NMR experiment[1]).

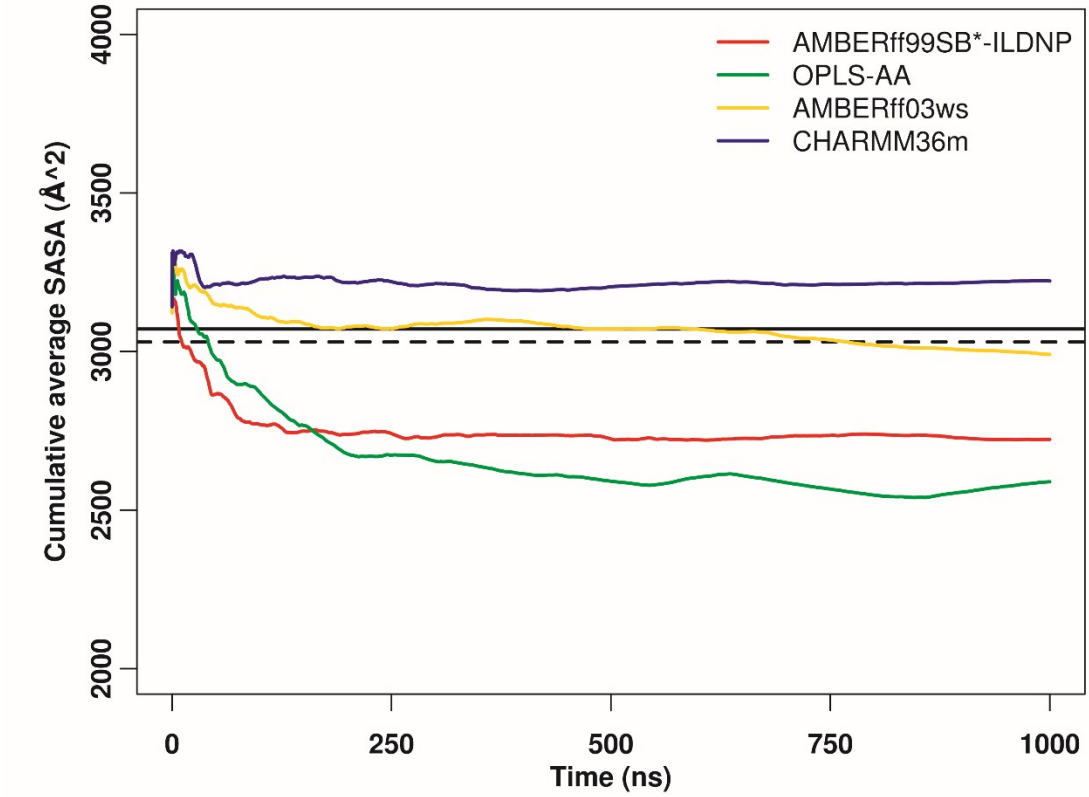

Figure

Figure S56. Time evolution of the cumulative average of the solvent accessible surface area (SASA) (in $Å^2$) of the side chain atoms of the p15 FAST peptide for the third replicate corresponding to the force fields AMBER ff99SB*-ILDNP; OPLS-AA; AMBER ff03ws; CHARMM36m. The solid black line indicates the SASA of the side chain atoms of the initial conformation (model 1 reported in the NMR experiment[1]) and the dashed black line indicates the experimental SASA of the side chain atoms of the experimental structure (average SASA of the 10 conformers reported in the NMR experiment[1]).

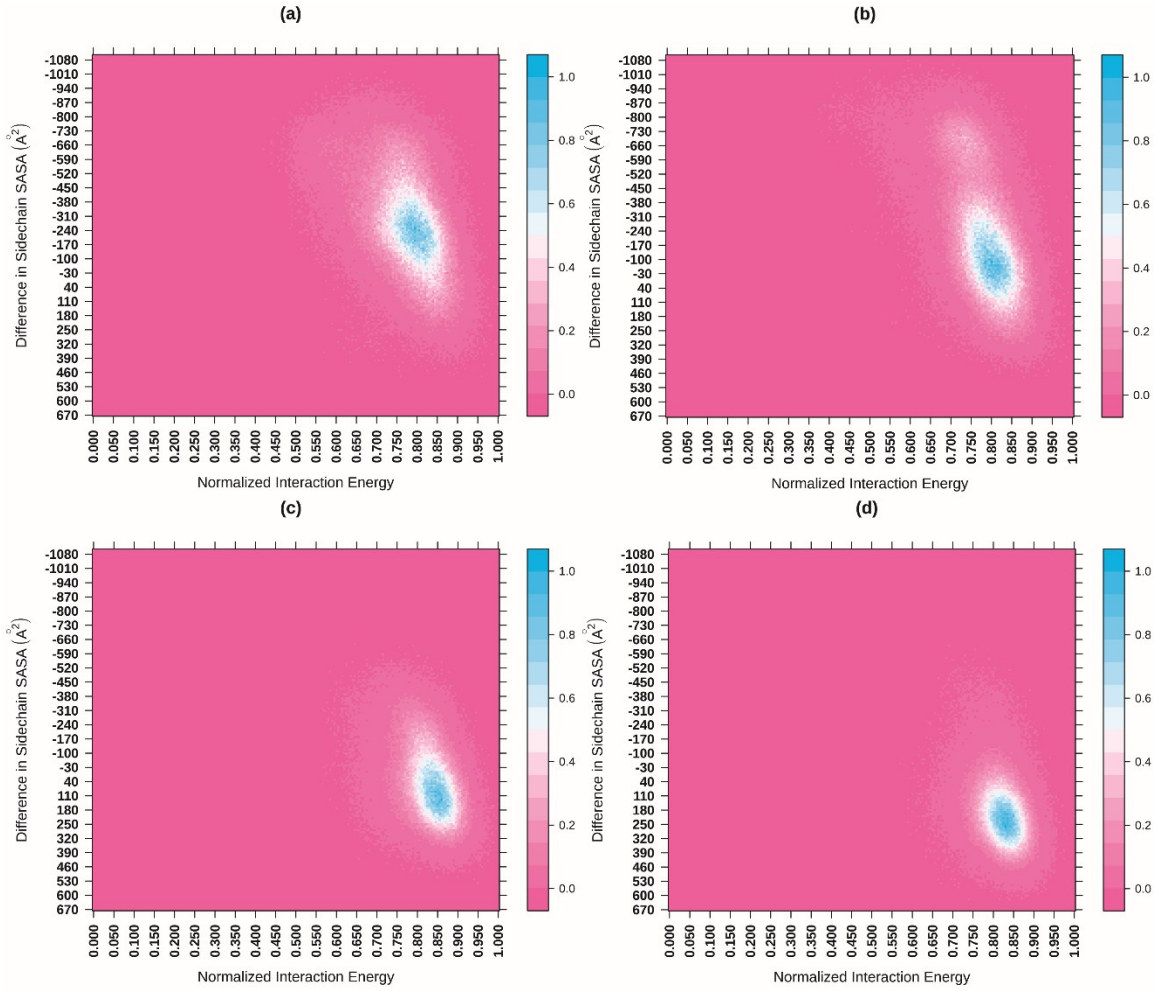

Figure S57. Probability distribution in the normalized interaction energy and the difference in the side chain SASA space of p15 FAST peptide for the second replicate corresponding to the force-fields respectively (a) AMBER ff99SB*-ILDNP; (b) OPLS-AA; (c) AMBER ff03ws; and (d) CHARMM36m.

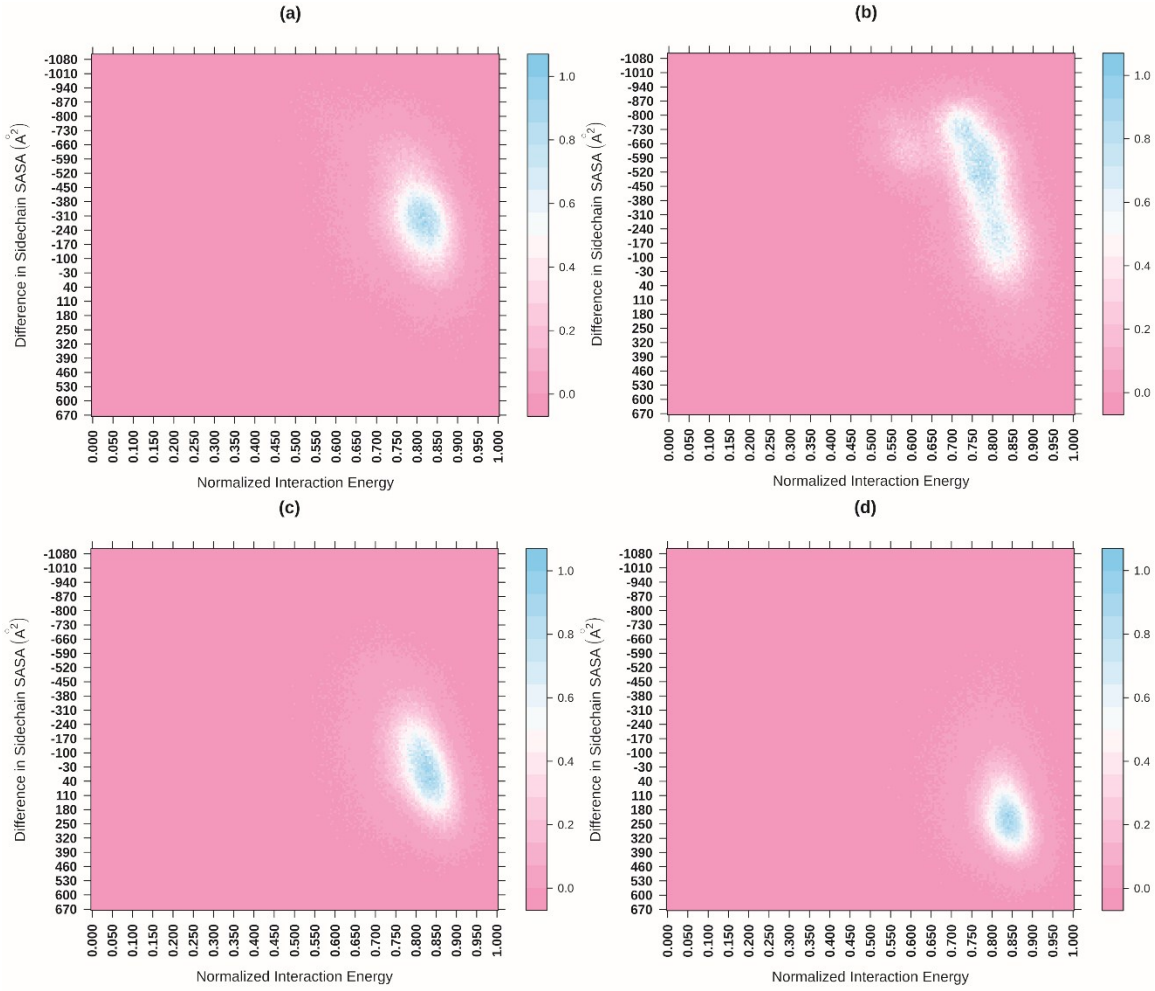

Figure S58. Probability distribution in the normalized interaction energy and the difference in the side chain SASA space of p15 FAST peptide for the third replicate corresponding to the force-fields respectively (a) AMBER ff99SB*-ILDNP; (b) OPLS-AA; (c) AMBER ff03ws; and (d) CHARMM36m.

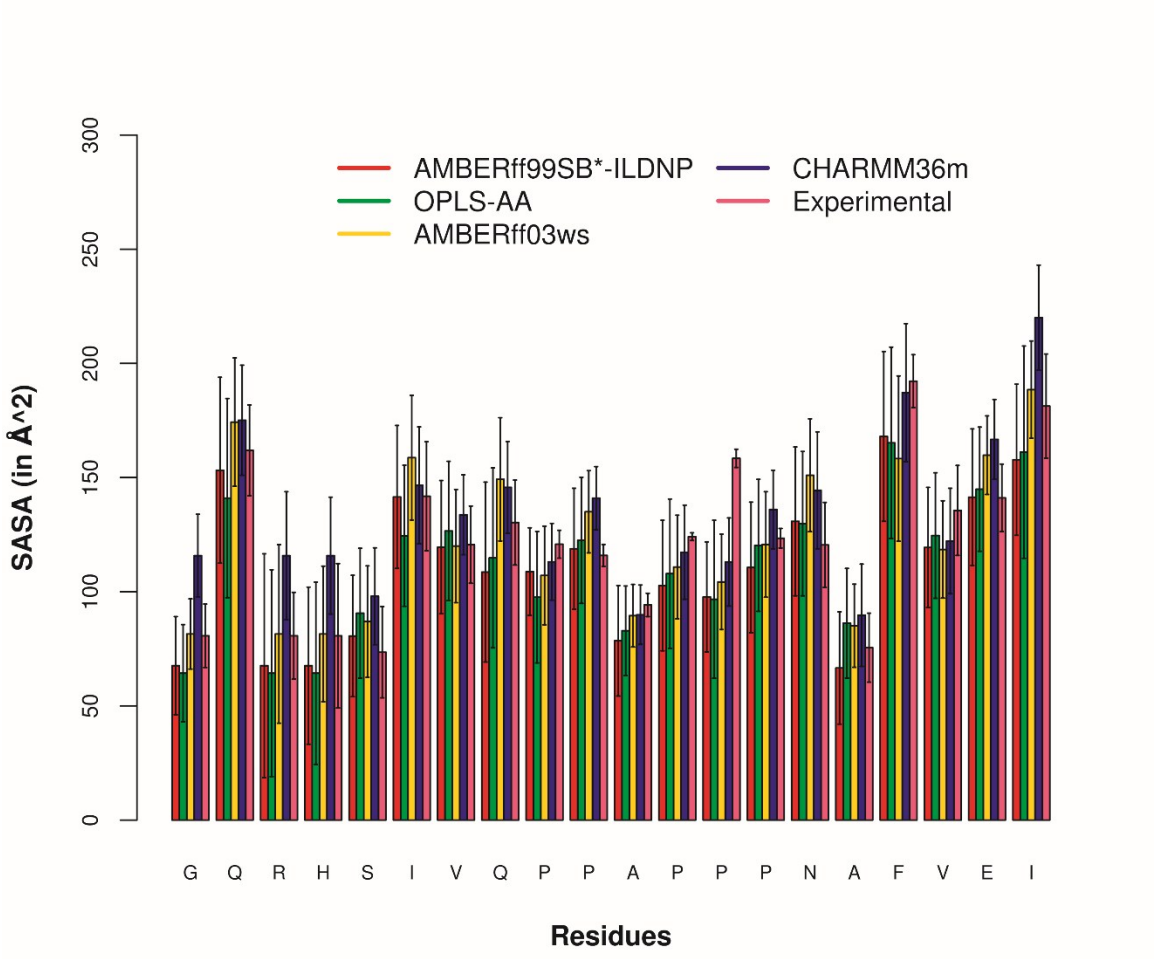

Figure S59. The residue-wise bar plot of the solvent accessible surface area (SASA) (in $Å^2$) of the p15 FAST peptide for the second replicate corresponding to the force fields AMBER ff99SB*-ILDNP, OPLS-AA, AMBER ff03ws, CHARMM36m and the experimental data.

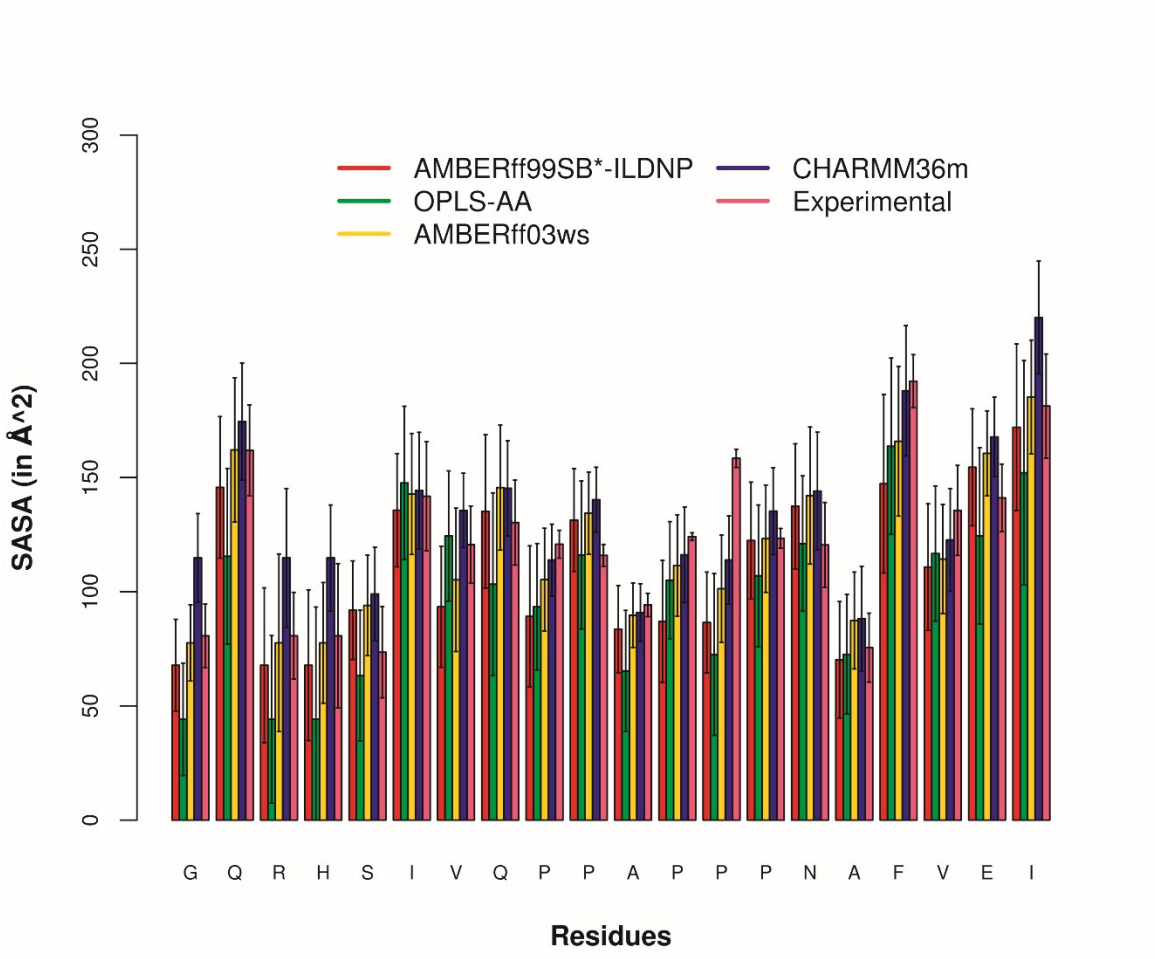

Figure S60. The residue-wise bar plot of the solvent accessible surface area (SASA) (in $Å^2$) of the p15 FAST peptide for the third replicate corresponding to the force fields AMBER ff99SB*-ILDNP, OPLS-AA, AMBER ff03ws, CHARMM36m and the experimental data.

Table S1. Average RMSD values of main chain atoms of the Q9-P15 residues

Force field	Average RMSD of main chain atoms in nm (first replicate)	RMSD of main chain atoms in nm (second replicate)	RMSD of main chain atoms in nm (third replicate)
AMBER ff99SB*-ILDNP	0.193±0.080	0.150± 0.048	0.163± 0.060
OPLS-AA	0.207±0.096	0.153±0.075	0.164±0.086
AMBER ff03ws	0.153± 0.050	0.176±0.050	0.172±0.049
CHARMM36m	0.153±0.046	0.175± 0.043	0.175±0.042

Table S2. Radius of Gyration and End-to-end distance for the second replicate

	AMBER ff99SB*-ILDNP	OPLS-AA	AMBER ff03ws	CHARMM36m	Experimental
Average R_g (nm)	1.157±0.185	1.240±0.261	1.344±0.174	1.465±0.175	1.60±0.06
Average R_{ee} (nm)	2.412±0.839	2.556±0.954	3.088±0.685	3.278±0.663	4.4±0.3
Average $R_{d(Q9\text{-}P15)}$ (nm)	1.703±0.186	1.702±0.244	1.724±0.166	1.638±0.165	1.887±0.006

Table S3. Radius of Gyration and End-to-end distance for the third replicate

	AMBER ff99SB*-ILDNP	OPLS-AA	AMBER ff03ws	CHARMM36m	Experimental
Average R_g (nm)	1.134±0.906	1.054±0.223	1.339±0.165	1.474±0.175	1.60±0.06
Average R_{ee} (nm)	2.508±0.843	1.911±0.908	3.182±0.660	3.289±0.649	4.4±0.3
Average $R_{d(Q9\text{-}P15)}$ (nm)	1.671±0.214	1.647±0.273	1.723±0.165	1.640±0.162	1.887±0.006

Table S4. Percentage of proline ring puckers for the first replicate

Residue	AMBERff99SB*-ILDNP		OPLS-AA		AMBERff03ws		CHARMM36m	
	exo	endo	exo	endo	exo	endo	exo	endo
PRO10	54.90	44.63	3.12	91.19	27.16	68.60	76.28	22.31
PRO11	50.46	49.02	5.04	89.53	20.65	75.66	68.30	30.19
PRO13	45.07	54.45	10.08	82.71	26.37	69.58	77.06	21.54
PRO14	43.53	55.92	3.49	91.42	25.04	71.05	77.44	21.06
PRO15	47.07	52.35	6.63,	88.11	29.88	66.41	65.95	32.51

Table S5. Percentage of proline ring puckers for the second replicate

Residue	AMBERff99SB*-ILDNP		OPLS-AA		AMBERff03ws		CHARMM36m	
	exo	endo	exo	endo	exo	endo	exo	endo
PRO10	46.36	53.09	4.53	89.36	26.17	69.65	76.80	21.80
PRO11	36.60	62.84	5.05	89.63	21.20	75.14	68.40	30.04
PRO13	43.52	55.94	4.07	89.83	28.17	67.63	76.49	22.09
PRO14	42.34	57.05	4.15	89.33	25.02	71.23	76.56	21.92
PRO15	45.83	53.65	4.96	89.69	39.56	56.79	62.71	35.70

Table S6. Percentage of proline ring puckers for the third replicate

Residue	AMBERff99SB*-ILDNP		OPLS-AA		AMBERff03ws		CHARMM36m	
	exo	endo	exo	endo	exo	endo	exo	endo
PRO10	25.78	69.95	3.29	90.82	26.62	69.30	76.57	22.02
PRO11	22.35	74.07	4.71	89.54	20.81	75.50	69.96	28.46
PRO13	31.52	64.15	5.44	87.92	27.97	67.87	76.63	21.93
PRO14	24.88	71.61	3.60	90.88	24.90	71.31	76.35	22.13
PRO15	54.02	42.69	13.78	79.01	37.58	58.64	64.89	33.55

Table S7. Average frame-wise chemical shift RMSD values for alpha and amide protons calculated using SPARTA+ for the second replicate

Force field	Average chemical shift RMSD (alpha protons) in ppm	Average chemical shift RMSD (amide protons) in ppm
AMBER ff99SB*-ILDNP	0.290±0.063	0.474±0.091
OPLS-AA	0.294±0.076	0.438±0.089
AMBER ff03ws	0.269±0.060	0.382±0.081
CHARMM36m	0.242±0.061	0.328±0.082

Table S8. Average frame-wise chemical shift RMSD values for alpha and amide protons calculated using SPARTA+ for the third replicate

Force field	Average chemical shift RMSD (alpha protons) in ppm	Average chemical shift RMSD (amide protons) in ppm
AMBER ff99SB*-ILDNP	0.283±0.063	0.417±0.075
OPLS-AA	0.319±0.082	0.486±0.089
AMBER ff03ws	0.268±0.060	0.380±0.085
CHARMM36m	0.240±0.057	0.318±0.081

Table S9. Chemical shift RMSD values for alpha, amide and side chain protons calculated using PPM for the first replicate

Force field	Chemical shift RMSD (alpha protons) in ppm	Chemical shift RMSD (amide protons) in ppm	Chemical shift RMSD (Side chain protons) in ppm
AMBER ff99SB*-ILDNP	0.097	0.555	0.1
OPLS-AA	0.092	0.413	0.108
AMBER ff03ws	0.099	0.375	0.083
CHARMM36m	0.070	0.227	0.082

Table S10. Chemical shift RMSD values for alpha, amide and side chain protons calculated using PPM for the second replicate

Force field	Chemical shift RMSD (alpha protons) in ppm	Chemical shift RMSD (amide protons) in ppm	Chemical shift RMSD (Side chain protons) in ppm
AMBER ff99SB*-ILDNP	0.097	0.524	0.077
OPLS-AA	0.090	0.407	0.070
AMBER ff03ws	0.093	0.345	0.066
CHARMM36m	0.071	0.202	0.060

Table S11. Chemical shift RMSD values for alpha, amide and side chain protons calculated using PPM for the third replicate

Force field	Chemical shift RMSD (alpha protons) in ppm	Chemical shift RMSD (amide protons) in ppm	Chemical shift RMSD (Side chain protons) in ppm
AMBER ff99SB*-ILDNP	0.096	0.528	0.070
OPLS-AA	0.081	0.568	0.083
AMBER ff03ws	0.099	0.419	0.064
CHARMM36m	0.071	0.204	0.061

Table S12. Frequency of Residue-wise solute-solvent ($C'_i{=}O_i \ldots H$) hydrogen bond for the first replicate

Residue	AMBERff99SB*-ILDNP	OPLS-AA	AMBERff03ws	CHARMM36m
GLN9	0.629	0.707	1.102	0.919
PRO10	0.974	0.752	0.776	1.049
PRO11	1.105	0.959	0.944	1.085
ALA12	0.684	0.707	1.096	1.007
PRO13	0.795	0.849	0.766	1.008
PRO14	0.911	0.673	0.699	0.808
PRO15	0.839	0.799	0.708	0.877

Table S13. Frequency of Residue-wise solute-solvent ($C'_i=O_i \ldots H$) hydrogen bond for the second replicate

Residue	AMBERff99SB*-ILDNP	OPLS-AA	AMBERff03ws	CHARMM36m
GLN9	0.7456	0.6479	1.1871	0.9376
PRO10	0.9854	0.7724	0.8016	1.0724
PRO11	1.1524	1.0425	0.9797	1.0992
ALA12	0.9819	0.7806	1.1016	1.0149
PRO13	0.9953	0.8490	0.7598	1.0029
PRO14	0.7278	0.6918	0.5484	0.8545
PRO15	0.7344	0.8213	0.6271	0.8704

Table S14. Frequency of Residue-wise solute-solvent ($C'_i=O_i \ldots H$) hydrogen bond for the second replicate

Residue	AMBERff99SB*-ILDNP	OPLS-AA	AMBERff03ws	CHARMM36m
GLN9	0.7456	0.6269	1.0908	0.9294
PRO10	0.9854	0.6096	0.7671	1.0642
PRO11	1.1524	1.0342	0.9420	1.0874
ALA12	0.9819	0.6795	1.0494	1.0143
PRO13	0.9953	0.8370	0.7200	1.0103
PRO14	0.7278	0.5089	0.5252	0.8543
PRO15	0.7344	0.6402	0.6036	0.8841